FORSTERITE DISSOLUTION KINETICS: APPLICATIONS AND IMPLICATIONS FOR CHEMICAL WEATHERING

Amanda Albright Olsen

Dissertation submitted to the faculty of the Virginia Polytechnic Institute and State University in partial fulfillment of the requirements for the degree of

DOCTOR OF PHILOSOPHY
In
GEOSCIENCES

J. Donald Rimstidt, *Chair*
Robert Bodnar
Patricia Dove
Madeline Schreiber

Keywords: forsterite dissolution, olivine, mineral dissolution kinetics, chemical weathering, ligand-promoted dissolution, ionic strength

June 21, 2007
Blacksburg, Virginia

FORSTERITE DISSOLUTION KINETICS: APPLICATIONS AND IMPLICATIONS FOR CHEMICAL WEATHERING

Amanda Albright Olsen

ABSTRACT

Silicate minerals are the most common mineral group in the earth's crust so it is not surprising that their weathering reactions dominate the chemistry of many earth surface processes. This project used forsterite as a model system to identify the important factors that affect silicate mineral dissolution rates and grain lifetimes in the weathering environment.

I determined an empirical rate law for forsterite dissolution of forsterite in oxalic acid solutions:

$$r_{fo} = 10^{-7.05+I^{0.5}} a_{H^+}^{0.46} + 10^{-5.51} m_{Ox^{2-}}^{0.36} a_{H^+}^{0.46}$$

based on a series of 124 semi-batch reactor experiments over a *pH* range of 0 to 7 and total oxalate concentrations between 0 and 0.35 m at 25°C. These experiments show that oxalate-promoted dissolution rates depend upon both oxalate concentration and pH. I propose a reaction mechanism in which a hydrogen ion and an oxalate ion are simultaneously present in the activated complex for the reaction that releases H_4SiO_4 into solution. By analogy, I propose that water acts as a ligand in the absence of oxalate.

I also ran 82 batch reactor experiments in magnesium and sodium sulfate and magnesium and potassium nitrate solutions. These experiments show that ionic strength up to 12 m, log m_{Mg} up to 4 m, and log m_{SO4} up to 3 m have no effect on forsterite dissolution rates. However, decreasing a_{H2O} slows forsterite dissolution rates. The effect of decreasing dissolution rates with decreasing a_{H2O} is consistent with the idea that water acts as a ligand that participates in the dissolution process.

Forsterite dissolution rate data from previously published studies were combined with results from my experiments and regressed to produce rate laws at low and high pH. For pH < 5.05

$$r_{BET} = 1.00 \times 10^{5} \left(e^{\frac{-68550}{RT}} \right) a_{H^+}^{0.48} \quad \text{or} \quad r_{geo} = 1.10 \times 10^{6} \left(e^{\frac{-69715}{RT}} \right) a_{H^+}^{0.50}$$

and for pH > 5.05

$$r_{BET} = 32.36 \left(e^{\frac{-55084}{RT}} \right) a_{H^+}^{0.22} \quad \text{or} \quad r_{geo} = 759 \left(e^{\frac{-58924}{RT}} \right) a_{H^+}^{0.24}$$

I then developed a diagram that shows the effect rate-determining variables on the lifetime of olivine grains in weathering environments using these rate laws.

ACKNOWLEDGEMENTS

This work was supported by the U.S. Department of Energy Basic Energy Sciences grant DE-FG02-03ER14751. I would like to thank Martha Griffith and Heather Shannon for laboratory assistance. Much of the previous data used in Chapters 3 and 4 were compiled by Jodi Rosso. Michael A. Velbel, Alian Wang, and one anonymous reviewer provided helpful reviews of Chapter 3. I'd like to thank Danielle Huminicki, Ari Mitra, and other graduate students at Virginia Tech for helpful conversations relating to this dissertation. I am indebted to my committee members, Robert Bodnar, Patricia Dove, and Madeline Schreiber, for helpful suggestions and advice, as well as my advisor, J. Donald Rimstidt, for help and support over the past five years. Finally, I'd like to thank my family, and in particular my husband, Brian Olsen.

TABLE OF CONTENTS

TABLE OF FIGURES

TABLE OF TABLES

CHAPTER 1: INTRODUCTION

Silicate minerals make up 92 weight percent of the earth's crust so it is not surprising that their weathering reactions dominate the chemistry of the earth's hydrosphere, atmosphere, and pedosphere. Dissolving silicate minerals consume hydrogen ions produced when CO_2 dissolves into surface and groundwaters. Forsterite dissolves in natural waters via the reaction

$$Mg_2SiO_4+4H_2CO_3 = 2Mg_2{+}{+}H_4SiO_4+4HCO_{3-} \qquad (1)$$

The balance between CO_2 input into the atmosphere by volcanic eruptions and CO_2 consumption by mineral weathering controls atmospheric carbon dioxide levels on timescales of a million years (WHITE and BRANTLEY, 1995). Although mineral dissolution kinetics and weathering reactions have been extensively studied, some fundamental questions regarding how minerals dissolve remain unanswered. The impact of these dissolution reactions depends on the details of each mineral's reaction kinetics.

This project used forsterite as a model system to identify the important factors that affect silicate mineral dissolution rates and grain lifetimes in the weathering environment. Silicate minerals with Si-O-Si bonding dissolve slowly and incongruently, often forming leached layers on the mineral surface. Olivine is an orthosilicate that has no Si-O-Si bonds so that it dissolves quickly and congruently, making it an ideal model system to investigate the fundamental processes that affect dissolution rates. Olivine dissolution rates have been measured by several investigators over a wide range of geologically relevant conditions (BAILEY, 1976; BLUM and LASAGA, 1988; CHEN and BRANTLEY, 2000; GIAMMAR et al., 2005; GOLUBEV et al., 2005; GRANDSTAFF, 1978; GRANDSTAFF, 1980; GRANDSTAFF, 1986; HÄNCHEN et al., 2006; JONCKBLOEDT, 1998; LUCE et al., 1972a; OELKERS, 2001; OLSEN and RIMSTIDT, 2007; POKROVSKY and SCHOTT, 2000b; ROSSO and RIMSTIDT, 2000; SANEMASA et al., 1972; SIEGEL and PFANNKUCH, 1984; VAN HERK et al., 1989; WOGELIUS and WALTHER, 1991b; WOGELIUS and WALTHER, 1992). These studies provide many valuable data; however, they are generally run over a narrow range of conditions.

This dissertation reports the results of three related projects that aim to address the following issues:

1. What is the effect of organic ligands on forsterite dissolution rates? How can this be expressed in a rate law? What does this effect tell us about the reaction mechanism?
2. How can we summarize our knowledge of all the factors that affect the rate of forsterite dissolution into a diagram that allows us to predict weathering rates in terms of grain lifetimes?
3. What is the effect of ionic strength, magnesium concentration, sulfate concentration, and activity of water on forsterite dissolution rates? What do these effects tell us about the dissolution reaction mechanism? How can we use this knowledge to create a highly reliable rate law that summarizes all existing dissolution rate data?

The second chapter of this dissertation reports the effect of oxalic acid on forsterite dissolution rates. Oxalic acid is a common and important organic acid that is present in concentrations up to 0.001 M in the weathering environment (FOX and COMERFORD, 1990). Previous studies of the effect of organic acids on forsterite dissolution rates (GRANDSTAFF, 1986; WOGELIUS and WALTHER, 1991a) did not simultaneously vary both pH and organic acid concentration in a systematic manner and reported results from a very limited number of experiments. Therefore, until now it was not possible to develop a rate law for forsterite dissolution that shows how organic acids affect rates. This dissertation reports rates from 124 semi-batch reactor experiments over a *pH* range of 0 to 7 and an m_{ox} range of 0 to 0.35 m at 25°C. I found that oxalate at these concentrations can increase dissolution rates by over an order of magnitude. Additionally, the rate law developed from these rate data clarifies the relationship between proton-promoted dissolution and ligand-promoted dissolution (FURRER and STUMM, 1986; STUMM and WOLLAST, 1990). This information was combined with ab initio quantum mechanics modeling done by Yun Liu to describe the reaction mechanism for forsterite; these results are not included in my dissertation but were published in LIU et al. (2006b).

In the third chapter of this dissertation, I developed a method to estimate olivine grain lifetime as a function of factors known to affect the dissolution rate. This mineral lifetime diagram considers olivine composition, pH, hydrodynamics, temperature, grain size, and the discrepancy between dissolution rates measured in

laboratories versus in the field. Application of this model to Martian conditions allows us to estimate the duration of liquid water on that planet (OLSEN and RIMSTIDT, 2007), which gives researchers who are interested in possible life on Mars a timeframe during which water would have been present. This diagram could also be applied to terrestrial weathering environments that contain olivine such as weathering basalt.

The final chapter of my dissertation examines the effect of salinity on forsterite dissolution rates. High ionic strength solutions are important in arid environments as well as in many industrial applications. I combined the results of a series of 47 experiments in $MgSO_4$, Na_2SO_4, and $Mg(NO_3)_2$ solutions with 35 experiments conducted in KNO_3 solutions as part of the oxalic acid experiments. The experiments were run over a pH range of 1 to 4 and with ionic strengths up to 12 m. Multiple linear regression of the data from these experiments showed that ionic strength, aqueous magnesium, and aqueous sulfate do not affect dissolution rates. However, the lower activity of water at high ionic strength causes a decrease in dissolution rates. In addition, I also compiled forsterite dissolution rate data from fourteen previous experimental studies and used these data to develop a very robust rate law for forsterite dissolution as a function of pH and temperature. Analysis of this data set showed that the activation energy and H^+ reaction order change near pH 5.05, indicating that the reaction mechanism at $pH < 5.05$ is different from that at $pH > 5.05$. I also compare rates calculated using BET surface areas with rates calculated using geometric surface areas and find that models based on either surface area determination predict forsterite dissolution rates with equal accuracy.

By choosing forsterite as a model system, I have created reliable rate laws by combining new experimental data with previously published data. I have also determined that ionic strength, aqueous magnesium, and aqueous sulfate do not affect forsterite dissolution rates, while decreasing water activity decreases dissolution rates, and increasing organic acid concentration accelerates dissolution rates. I have also created a clearer picture of the activated complex of forsterite dissolution by showing that water acts as a ligand in the dissolution process. Using this information, I created a mineral lifetime diagram that allows us to visualize the effect of many rate determining variables on the chemical weathering of forsterite.

1.1 REFERENCES

Bailey, A., 1976. Effects of temperature on the reaction of silicates with aqueous solutions in the low temperature range. In: Cadek, J. and Paces, T. Eds.)*Proceed. Internat. Symp. on Water-Rock Interaction*. Geological Survey Prague, Prague.

Blum, A. E. and Lasaga, A. C., 1988. Role of surface speciation in the low-temperature dissolution of minerals. *Nature* **331**, 431-433.

Chen, Y. and Brantley, S. L., 2000. Forsterite dissolution at 65°C and 2<pH<5. *Chem. Geol.* **165**, 267-281.

Fox, T. R. and Comerford, N. B., 1990. Low-molecular-weight organic acids in selected forest soils of the southeastern USA. *Soil Science Society of America Journal* **54**, 1139-1144.

Furrer, C. and Stumm, W., 1986. The coordination chemistry of weathering: I. Dissolution kinetics of gamma-Al2O3 and BeO. *Geochimica et Cosmochimica Acta* **50**, 1847-1860.

Giammar, D. E., Bruant, R. G., and Peters, C. A., 2005. Forsterite dissolution and magnesite precipitation at conditions relevant for deep saline aquifer storage and sequestration of carbon dioxide. *Chemical Geology* **217**, 257-276.

Golubev, S. V., Pokrovsky, O. S., and Schott, J., 2005. Experimental determination of the effect of dissolved CO_2 on the dissolution kinetics of Mg and Ca silicates at 25 C. *Chemical Geology*, 227-238.

Grandstaff, D. E., 1978. Changes in surface area and morphology and the mechanism of forsterite dissolution. *Geochimica et Cosmochimica Acta* **42**, 1899-1901.

Grandstaff, D. E., 1980. The dissolution rate of forsteritic olivine from Hawaiian beach sand. In: Grandstaff, D. E. (Ed.),*International Symposium on Water-Rock Interaction, 3rd*, Edmonton, Alberta.

Grandstaff, D. E., 1986. The dissolution rate of forsteritic olivine from Hawaiian beach sand. In: Colman, S. M. and Dethier, D. P. Eds.), *Rates of Chemical Weathering of Rocks and Minerals*. Academic Press, Orlando, Florida.

Hänchen, M., Prigiobbe, V., Storti, G., Seward, T. M., and Mazzotti, M., 2006. Dissolution kinetics of forsteritic olivine at 90-150°C including effects of presence of CO_2. *Geochimica et Cosmochimica Acta* **70**, 4403-4416.

Jonckbloedt, R. C. L., 1998. Olivine dissolution in sulfuric acid at elevated temperatures-implications for the olivine process, an alternative waste acid neutralizing process. *Journal of Geochemical Exploration* **62**, 337-346.

Liu, Y., Olsen, A. A., and Rimstidt, J. D., 2006. Mechanism for the dissolution of olivine series minerals in acidic solutions. *American Mineralogist* **91**, 455-458.

Luce, R. W., Bartlett, R. W., and Parks, G. W., 1972. Dissolution kinetics of magnesium silicates. *Geochimica et Cosmochimica Acta* **36**, 35-50.

Oelkers, E. H., 2001. An experimental study of forsterite dissolution rates as a function of temperature and aqueous Mg and Si concentrations. *Chemical Geology* **175**, 485-494.

Olsen, A. A. and Rimstidt, J. D., 2007. Using a mineral lifetime diagram to evaluate the persistence of olivine on Mars. *American Mineralogist* **92**.

Pokrovsky, O. S. and Schott, J., 2000. Kinetics and mechanism of forsterite dissolution at 25 C and pH from 1 to 12. *Geochimica et Cosmochimica Acta* **64**, 3313-3325.

Rosso, J. J. and Rimstidt, J. D., 2000. A high resolution study of forsterite dissolution rates. *Geochimica et Cosmochimica Acta* **64**, 797-811.

Sanemasa, I., Yoshida, M., and Ozawa, T., 1972. The dissolution of olivine in aqueous solutions of inorganic acids. *Bulletin of the Chemical Society of Japan* **45**, 1741-1746.

Siegel, D. I. and Pfannkuch, H. O., 1984. Silicate mineral dissolution at pH 4 and near standard temperature and pressure. *Geochimica et Cosmochimica Acta* **48**, 197-201.

Stumm, W. and Wollast, R., 1990. Coordination of chemistry of weathering: kinetics of the surface-controlled dissolution of oxide minerals. *Reviews of Geophysics* **28**, 53-69.

Van Herk, J., Pietersen, H. S., and Schuiling, R. D., 1989. Neutralization of industrial waste acids with olivine- The dissolution of forsteritic olivine at 40-70°C. *Chemical Geology* **76**, 341-352.

White, A. F. and Brantley, S. L., 1995. *Chemical weathering rates of silicate minerals*. Mineralogical Society of America, Washington, D.C.

Wogelius, R. and Walther, J., 1991a. Olivine dissolution at 25C: Effects of pH, CO2, and organic acids. *Geochimica et Cosmochimica Acta* **55**, 943-954.

Wogelius, R. A. and Walther, J. V., 1991b. Olivine dissolution at 25C: Effects of pH, CO2, and organic acids. *Geochimica et Cosmochimica Acta* **55**, 943-954.

Wogelius, R. A. and Walther, J. V., 1992. Olivine dissolution kinetics at near-surface conditions. *Chemical Geology* **97**, 101-112.

CHAPTER 2: OXALATE-PROMOTED FORSTERITE DISSOLUTION AT LOW PH

2.1 ABSTRACT

We ran a series of 124 semi-batch reactor experiments to measure the dissolution rate of forsterite in solutions of nitric and oxalic acid solutions over a *pH* range of 0 to 7 and total oxalate concentrations between 0 and 0.35 m at 25°C. We found that the empirical rate law for the dissolution of forsterite in these solutions is

$$r_{fo} = 10^{-7.05+I^{0.5}} a_{H^+}^{0.46} + 10^{-5.51} m_{Ox^{2-}}^{0.36} a_{H^+}^{0.46}.$$

The first term of the rate law expresses the dissolution rate for solutions with no oxalate and the second term expresses the additional rate produced by the presence of oxalate ions.

Our experiments show that oxalate-promoted dissolution rates depend upon both oxalate concentration and pH. Based on this, we propose a reaction mechanism in which a hydrogen ion and an oxalate ion are simultaneously present in the activated complex for the reaction that releases H_4SiO_4 into solution. By analogy, we propose that water acts as a ligand in the absence of oxalate, so the first term of our rate law has $a_{H_2O}^{m}$ (=1) as a hidden term. Thus our results confirm that both a proton and a ligand (either an anion or a water molecule) must be present in the activated complex for forsterite dissolution, suggesting that proton-promoted and ligand-promoted dissolution are simply two aspects of the same process, and that the distinction between the two is artificial.

The increased dissolution rate of forsterite produced by oxalate ions at a concentration of 0.001 m, a concentration comparable to the amount of organic acids in typical soils, translates into an approximately a 6-fold increase in forsterite dissolution rates at pH > 4.2. This suggests that organic acids have a measurable, but not profound, effect on chemical weathering.

2.2 INTRODUCTION

Table of Notation 2

a_{H^+}	activity of hydrogen ions
A	surface area (m^2)
I	stoichiometric ionic strength (molal)
I_T	"true" ionic strength (molal)
K_1'	apparent first dissociation constant for oxalic acid hydrolysis
K_2'	apparent second dissociation constant for oxalic acid hydrolysis
k_i	rate constant for reaction i
M	mass of solution at sample time (g)
M_0	initial mass of solution (g)
M_{fo}	mass of forsterite grains (g)
Δm	change in Mg concentration over a time interval (molal)
$m_{i,c}$	corrected concentration for species i (molal)
m_i	concentration of species i (molal)
r'	apparent rate (molal/sec)
r	total rate of olivine destruction (mol/m^2sec)
r_w	rate of olivine destruction as a function of pH and water activity (mol/m^2sec)
r_{ox}	rate of olivine destruction as a function of pH and oxalate concentration (mol/m^2sec)
T_{ox}	total concentration of oxalate species (molal)

The role of organic acids in enhancing chemical weathering rates has been recognized for at least three decades (HUANG and KIANG, 1972). Researchers have documented the effect of a variety of organic acids on the dissolution rate of various silicate minerals. Stumm and collaborators (FURRER and STUMM, 1986; STUMM and WOLLAST, 1990) proposed the term "ligand-promoted" dissolution to explain how organic ligands enhance dissolution rates and developed a model of the reaction mechanism based on the formation of a cation-ligand surface species. However, CASEY (2001) points out that that hydrogen ions are also involved in the ligand-promoted reaction mechanism. The objective of this study is to investigate the simultaneous effect of hydrogen ions and the oxalate ligand on forsterite dissolution rate and to express these effects in terms of an empirical rate law. We then discuss the implications of this rate law with regard to reaction mechanism.

Organic acids are present in all soils. They are produced by the decomposition of organic detritus as well as by plant roots, which secrete them in order to mobilize

nutrients from nearby soil. Although concentrations of organic acids in soils vary greatly depending on environment and soil type, average organic acid concentrations in soil solutions are generally less than 0.001 M (DREVER and VANCE, 1994). However, concentrations can be much higher in areas with large amounts of decomposing organic matter or immediately adjacent to plant roots.

Several previous studies of the effect of organic acids on the dissolution rate of oxides and silicates show that polyfunctional acids such as oxalate and citrate enhance dissolution to a greater degree than monofunctional acids such as acetate (FRANKLIN et al., 1994; HUANG and KIANG, 1972; WELCH and ULLMAN, 1993). Because oxalate is present in soils at concentrations up to 0.001 M (FOX and COMERFORD, 1990), we surmise that oxalate is one of the most important organic ligands in soil solution. Oxalate significantly enhances feldspar dissolution rates with Ca-rich plagioclases showing the greatest effect (AMRHEIN and SUAREZ, 1988; BLUM and STILLINGS, 1995; FRANKLIN et al., 1994; MANLEY and EVANS, 1986; MAST and DREVER, 1987; STILLINGS et al., 1996; WELCH and ULLMAN, 1993; WELCH and ULLMAN, 1996). Bennett et al. (1988) reported that oxalate and citrate enhance quartz dissolution rates by almost an order of magnitude, but Franklin et al. (1994) found little effect, and Poulson et al. (1997) attributed any increase in quartz dissolution rates in previous studies to the presence of Na^+ in solution. Cama and Ganor (2006) showed that oxalate can increase kaolinite dissolution rates by up to 30 times.

The purpose of this study was to determine a rate law that expresses the effect of oxalate ions on the dissolution rate of forsterite. A second goal was to use oxalate as a chemical probe of the reaction mechanism. We chose olivine for this study because it is structurally simple and dissolves stoichiometrically, which allows us to obtain a clearer idea of the reaction mechanism. We chose oxalate for our studies in order to make our experiments comparable to those from previous studies, and because oxalate is an important ligand in soil solutions. Because we performed our experiments for short time periods (2 hours), we were able to run a large number of experiments (124), which allowed us to investigate a much wider range of pH and oxalate concentrations than was considered in previous studies.

2.3 MATERIALS AND METHODS

2.3.1 Materials

We used forsteritic (Fo92) olivine from Aimcor Mine, Green Mountain, NC, USA, for all experiments. For a detailed description of this material, see Rosso and Rimstidt (2000). The olivine was crushed and sieved and the 45-60 mesh size (250-350 μm) was retained. Because the olivine grains were coated with a small amount of talc, they were pretreated by sonicating in 1 m HNO_3 10 times for 1 minute each time, followed by soaking in 6 m HNO_3 overnight to remove as much talc as possible prior to the experiments. In addition to removing the talc, this pretreatment provided a silica-rich surface on which to conduct our experiments, which meant that initial dissolution was stoichiometric. A similar pre-treatment was used for pyroxene and amphibole surfaces (SCHOTT et al., 1981). Because grains of this size are near the limit for reliable BET surface area analysis, we chose to normalize our reaction rates using a surface area of 0.0528 m^2/g based on the empirical equation from Brantley and Mellott (2000), which is comparable to surface areas for grains of this diameter in other olivine studies.

2.3.2 Experimental Methods

One hundred and twenty four batch reactor experiments were run over the pH range of 0 to 7. Each experiment consisted of 5 grams of forsterite and 100 mL of solution in a 250 mL Erlenmeyer flask immersed in a shaker bath set at 25ºC. Solutions were made using nitric acid and potassium hydroxide to adjust pH, potassium nitrate to adjust ionic strength, and oxalic acid ($C_2H_2O_4$) to vary total oxalic acid concentrations from 0 to 0.35 m. Approximately 6 mL of solution was collected every 20 minutes over the 2 hour duration of each experiment. Magnesium concentrations were determined by Atomic Absorbance spectrometry (AA). Silica concentrations were determined using the molybdate blue colorimetric method (GOVETT, 1961).

2.3.3 Correction for sample withdrawal

Because approximately 6 mL of solution was sampled six times over the course of each experiment, it was necessary to perform a correction for the changing surface area to mass ratio so that the data could be analyzed as an ideal batch reactor experiment. Removing a solution sample caused the surface area to mass of solution ratio to increase as the experiment progressed, thereby making the concentration of magnesium and silica present in subsequent samples higher than would occur in an unsampled reactor. In order to adjust for this, we calculated the amount of magnesium or silica that would have been present under ideal unsampled batch reactor conditions. To find the corrected concentration, we summed the change in Mg concentration over each time interval multiplied by the mass of solution present at the time of sampling and then divided this product by the mass of solution present at the beginning of the experiment.

$$m_{i,c} = \frac{\sum_{i=1}^{n} \Delta m(i) M(i)}{M_0} \qquad (2.1)$$

This adjusted the sample concentration downward by 2 to 30 percent.

2.3.4 Data Filtering/Data Selection

Six concentration versus time data were collected for both magnesium and silica from each of the 124 experiments. These data were filtered to remove values that were potentially affected by non-random errors. First, all negative concentrations were eliminated. Then, 12 release rates with a Si/Mg ratio of less than 0.2 or greater than 5 were eliminated because this is indicative of highly non-stoichiometric dissolution. Additionally, five experiments that were conducted at pH values of less than 0.5 were discarded due to inaccurate pH measurements.

2.3.5 Initial Rate Method

Data were analyzed using the initial rate method where the concentration versus time data were fit by linear regression and the apparent rate (r', molal/sec) was taken as the slope of the regression line. The apparent rate was converted to the rate of forsterite destruction using the relationship:

$$r = \frac{r'M}{A}. \quad (2.2)$$

Additionally, Mg release rates were standardized to Si release rates by dividing by 1.84, the stoichiometric ratio of silica to magnesium in the olivine sample. Thus our reported rates are the rate of forsterite destruction in mol/m^2sec. Mg and Si release rates for each experiment were averaged and these average rates were used in subsequent regression models.

2.3.6 Calculation of oxalic acid speciation

It was necessary to account for oxalate speciation in order to quantify the amount of each oxalate species present at each pH. Using the total oxalic acid concentration, as well as the amounts of HNO_3 and KOH used to adjust the pH, we calculated the stoichiometric ionic strength (I). We used I along with the following equations to calculate the apparent equilibrium constants for the first and second dissociation of oxalic acid. For the first dissociation,

$$H_2C_2O_4 = H^+ + HC_2O_4^- \quad (2.3)$$

the apparent hydrolysis constant was calculated using the equation

$$\log K_1' = -0.3001I^2 + 0.7538I - 1.3816 \quad (2.4)$$

(KETTLER et al., 1998). For the second dissociation reaction,

$$HC_2O_4^- = H^+ + C_2O_4^{2-} \quad (2.5)$$

the apparent hydrolysis constant was calculated using the equation

$$\log K_1' = -0.4206I^2 + 1.1486I - 4.2105 \quad (2.6)$$

(KETTLER et al., 1998). Then the concentration of oxalate ion was found from the relationship

$$m_{C_2O_4^{2-}} = \frac{T_{ox}}{\left(\frac{a_{H^+}^2}{K_1' K_2'} + \frac{a_{H^+}}{K_2'} + 1\right)} \quad (2.7)$$

and the concentration of bioxalate ion and oxalic acid were calculated from

$$m_{HC_2O_4^-} = \frac{a_{H^+} m_{C_2O_4^{2-}}}{K_2'} \quad (2.8)$$

$$m_{H_2C_2O_4} = \frac{a_{H^+} m_{HC_2O_4^-}}{K_1'} \quad (2.9).$$

We used these concentrations to calculate a true ionic strength based on the oxalic acid speciation using the equation

$$I_T = \frac{1}{2}\left(m_{H^+} + m_{K^+} + m_{NO_3^-} + m_{HC_2O_4} + 4m_{C_2O_4^{2-}}\right) \quad (2.10).$$

This "true" ionic strength, rather than the stoichiometric ionic strength, was used in later regression models.

2.4 RESULTS

The results of all rate experiments are tabulated in Appendix 2.1 along with the variables (a_{H+} and $I^{0.5}$) that were used in the regression model. In order to calculate the portion of the rate due to the presence of oxalate, we first determined forsterite dissolution rates as a function of *pH* in solutions that contained no organic ligands (Appendix 2.1; Figure 2.1). These experiments involved an array of 36 oxalic acid-free experiments over an ionic strength range of 0.1 to 2.4 m for *pH* ranging from 1 to 4.

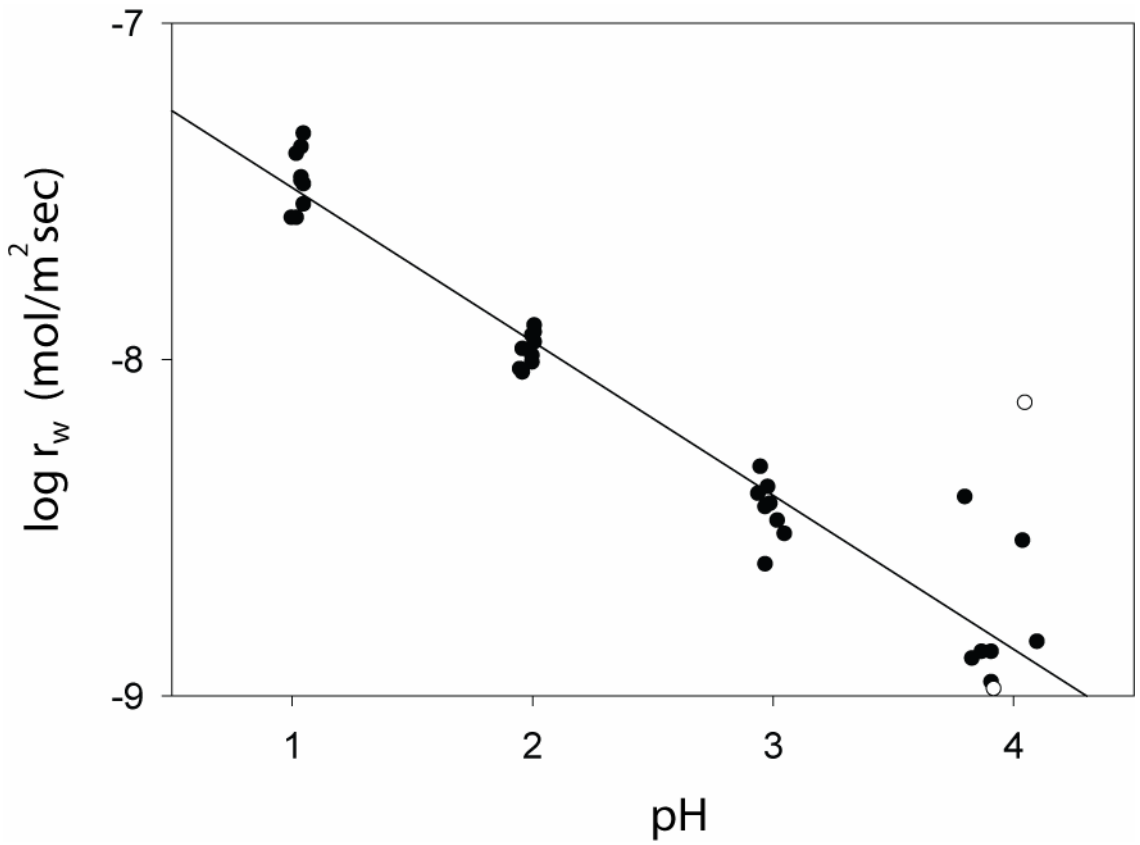

Figure 2.1. Log r versus pH for experiments that did not contain oxalic acid. The line is result of regression analysis. Open dots are data that were rejected from the data set and were not used in the regression model.

We developed a rate law for these data by fitting log r_w versus pH and $I^{0.5}$ using multiple linear regression. Figure 2.2 shows leverage plots for this regression model. Both $I^{0.5}$ and pH were found to be significant predictors of log r_w; however, the effect of $I^{0.5}$ was very small and had no practical effect, so it was not included in the rate model. Simple linear regression of log r_w versus pH produced the rate model

$$\log r_w = -7.03(0.05) - 0.46(0.02)pH \quad (2.11)$$

where the numbers in parenthesis are one standard error of the regression coefficient (R^2=0.94). Equation 2.11 can be transformed to the rate law

$$r_w = 10^{-7.03} a_{H^+}^{0.46} \qquad (2.12)$$

where 1<*pH*<4 and 0<*I*<2.4. This fit is consistent with the rate law reported by (OLSEN and RIMSTIDT, 2007)

$$r = 10^{-6.90} a_{H^+}^{0.48} \quad (2.13)$$

which is based on data from six previous studies at *pH*<6 (BLUM and LASAGA, 1988; LUCE et al., 1972b; OELKERS, 2001; POKROVSKY and SCHOTT, 2000b; ROSSO and RIMSTIDT, 2000; WOGELIUS and WALTHER, 1991a).

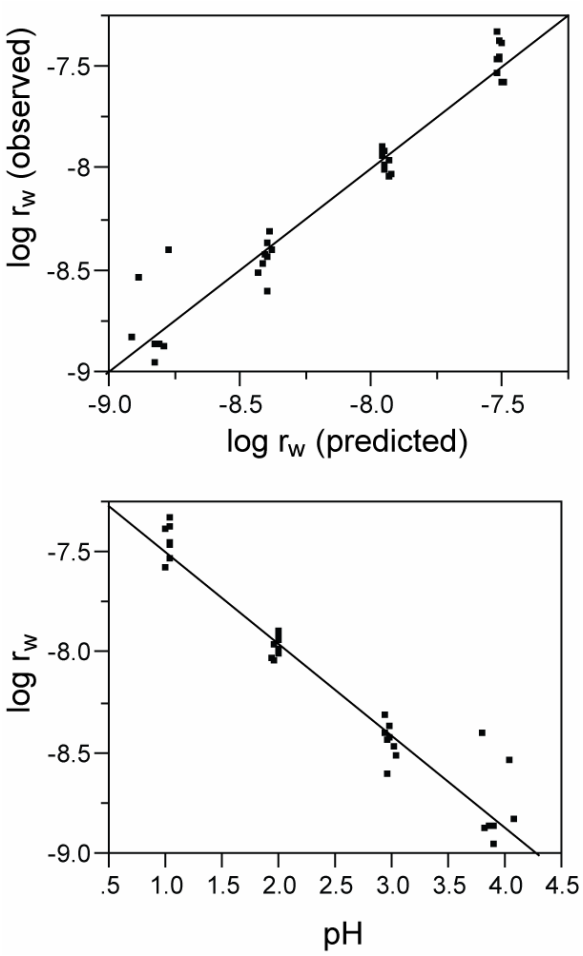

Figure 2.2. Results of the multiple linear regression model for the oxalate-free experiments for 34 data points. The top graph shows predicted log r_w versus observed log r_w, $R^2 = 0.94$; The bottom graph shows the effect of *pH* on log r_w, $P < 0.0001$.

The mathematical form of the rate law describing the effect of oxalate on forsterite dissolution is constrained by the requirement that as the oxalate concentration approaches zero the predicted rate must approach the rate of dissolution in oxalate-free solution as predicted by Equation 2.12. This means that the contribution of oxalate to the overall rate must be expressed by a term that is added to r_w so the overall rate is

$$r = r_w + r_{ox} \qquad (2.14)$$

This general form for a rate law for ligand-promoted dissolution has been applied to other olivine data (GRANDSTAFF, 1986; WOGELIUS and WALTHER, 1992) and plagioclase feldspar (STILLINGS et al., 1996).

This two-term rate law required us to analyze our data in two steps. Because the reaction rates are additive, we first calculated the rate for the oxalate-free reaction using Equation (12) and then subtracted that rate from the observed rate for oxalate-containing experiments. This gave us the dissolution rate that is due only to the oxalate reaction.

The oxalate dissolution rates were regressed versus *pH*, m_{ox}, and $I^{0.5}$ using multiple linear regression. Figure 2.3 shows leverage plots for this regression model. Both *pH* and m_{ox} are significant predictors of log rate but $I^{0.5}$ is not. The regression model produced by this fit is

$$\log r_{ox} = -5.44(0.15) + 0.40(0.03)\log m_{Ox^{2-}} - 0.47(0.02)pH \quad (2.15)$$

where the numbers in parenthesis are one standard error of the regression coefficients. This can be transformed to the rate law

$$r_{ox} = 10^{-5.44} m_{Ox^{2-}}^{0.40} a_{H^+}^{0.47} \quad (2.16)$$

Because the concentrations of bioxalate and oxalic acid are highly correlated with the oxalate concentration, it is not possible statistically to separate out their effect on the rate. However, because the effect seems to be greater at higher *pH*, where oxalate ion is the dominant species, we infer that oxalate is the dominant rate-enhancing ligand. Because total rate is equal to the sum of the oxalate-free reaction and the oxalate-enhanced reaction (Equation 14), the overall rate law is

$$r = \left(10^{-7.03} a_{H^+}^{0.46}\right) + \left(10^{-5.44} m_{Ox^{2-}}^{0.40} a_{H^+}^{0.47}\right) \qquad (2.17).$$

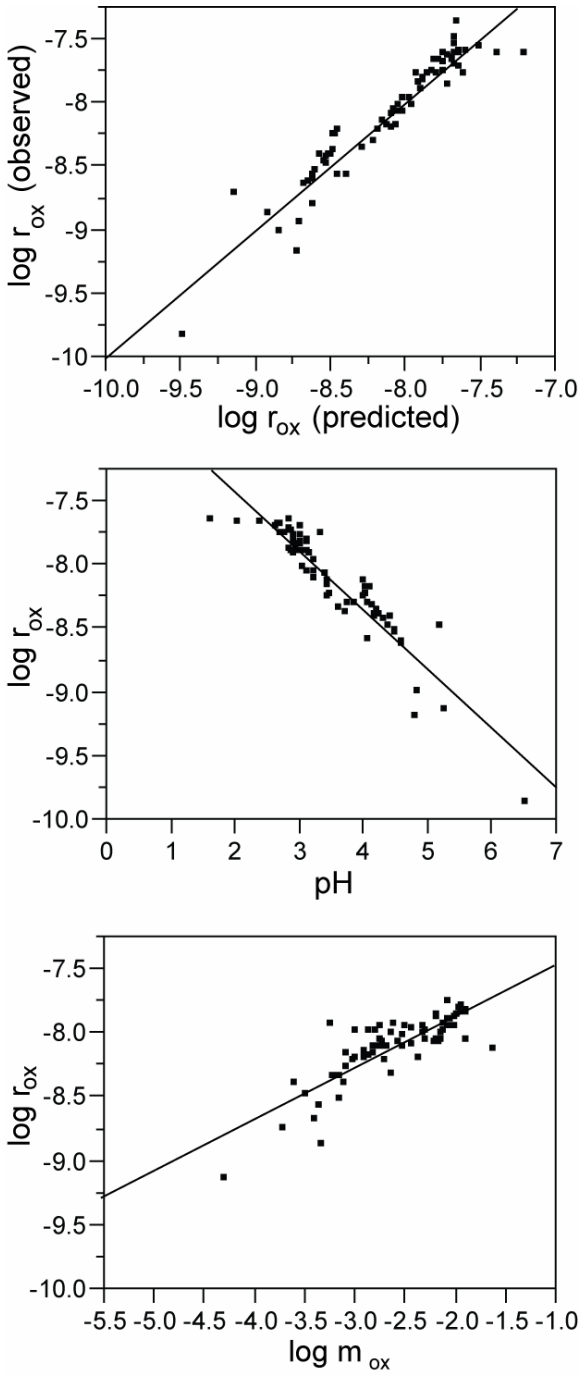

Figure 2.3. Results of the multiple linear regression model for the oxalic acid-containing experiments for 73 data points. The top graph shows predicted log r_{ox} versus observed log r_{ox}, R^2=0.90; The middle graph shows the effect of *pH* on log r_{ox}, $P < 0.0001$; The bottom graph shows the effect of log m_{ox} on log r_{ox}, $P < 0.0001$.

2.5 DISCUSSION AND CONCLUSIONS

Two previous studies examined the effect of organic ligands on forsterite dissolution. Grandstaff (1986) found that concentrations of EDTA up to 0.1 M and potassium hydrogen phthalate (KHP) up to 0.01 M increases forsterite dissolution rates by up to two orders of magnitude. Grandstaff suggests a rate law of the form

$$r = r_w + k_{KHP} a_{KHP}^{0.53} \qquad (2.18)$$

but does not give values for r_w or k_{KHP}. Wogelius and Walther (1991a; 1992) found an increase in rate of 0.75 log units at *pH* 4 in the presence of 10^{-3} m ascorbic acid or 0.05 m KHP. They proposed a rate law of the form

$$r = r_w + 0.8 \times 10^{-9} m_{KHP}^{0.45} \qquad (2.19).$$

They suggest that rates in the presence of organic ligands are "roughly *pH* independent." Both studies found that rate enhancement is greater at high *pH* and that rates approach proton-promoted dissolution rates at low *pH* values. However, both studies completed only a few experiments over a narrow range of conditions.

Choosing an appropriate form for a rate law requires consideration of how previous rate laws have been written. Dissolution rates are sometimes described as the product of the near equilibrium and far from equilibrium dissolution rates (NAGY et al., 1991).

$$R_{net} = -k_+ \prod_j a_j^{m_j} \left(1 - e^{\frac{n\Delta G_r}{RT}} \right) \qquad (2.20)$$

Although dissolution rates are sometimes written to include departure from equilibrium, we chose not to use this term because when reactions are run under conditions where $\Delta G_r > 5RT$, the $\left(1 - e^{\frac{n\Delta G_r}{RT}} \right)$ collapses to 1 and no longer has an effect on dissolution rate.

Thus, the dissolution rate is simply expressed by the product of the activities of rate-controlling variables in solution. Forsterite dissolution experiments run at low to neutral *pH* are always very far from equilibrium; in fact, the chemical potential driving the reaction at then end of a typical experiment (Experiment SB80: $m_{Mg} = 5.73 \times 10^{-4}$ m, $m_{Si} = 2.72 \times 10^{-4}$ m, *pH* = 3.95) is -284 kJ/mol, or 114 *RT,* which is dramatically greater than

the $5RT$ value where the term in parenthesis in Equation 2.20 collapses to 1. This conclusion is consistent with reports that aqueous silica and magnesium concentrations have little or no effect on dissolution rates (OELKERS, 2001; POKROVSKY and SCHOTT, 2000b; ROSSO and RIMSTIDT, 2000). Because departure from equilibrium is not important in this rate law, the rate is only a function of pH, m_{ox}, and $I^{0.5}$, so we have included only those variables in our regression model (Equation 2.17).

In our experiments, we found that the rate enhancement due to the addition of oxalic acid is greatest when the pH is above 4.2, the second dissociation constant for oxalic acid; see Figure 1 in Liu et al. (2006b). However, for a constant total oxalate concentration, the effect of oxalate species on the dissolution rate decreases with decreasing pH below pH = 4.2 (= pK_2) until the contribution of r_{ox} to the overall rate becomes insignificant. This suggests that bioxalate ion and oxalic acid, which become predominant at low pH, do not play an important role in the dissolution process. We would not expect oxalic acid to participate in a ligand exchange reaction because it is uncharged. Bioxalate might participate, but its effect would likely be smaller than that of the more highly charged oxalate (STILLINGS et al., 1996).

The most striking feature of the oxalate term in the rate law (Equation 2.17) is that it contains a term for hydrogen ions that is comparable to that found for oxalate-free solutions. We interpret this to mean that H^+ participates in the rate-determining step for oxalate-promoted dissolution in the same way it participates in the oxalate-free reaction. This, combined with the form of Equation 2.16, which is dictated by the requirement that as the concentration of oxalate becomes zero, the rate becomes equal to r_w (STILLINGS et al., 1996) gives us insight into the mechanism of olivine dissolution. Although previous studies (see White and Brantley (1995) and references therein) of silicate and oxide dissolution have discussed the effects of pH and of organic acids on the rates in terms of proton-promoted and ligand-promoted mechanisms, our results confirm that both H^+ and ligands must be simultaneously present in the activated complex in order to account for the rate dependence on both H^+ and oxalate found in the second term of Equation 2.17. Both terms of Equation 2.17 have the same format; therefore, based on analogy we propose that H_2O acts as a ligand in the oxalate-free reaction. These results provide solid evidence that the activated complex for olivine dissolution contains both a H^+ and a

ligand. This model is applicable for systems where a ligand such as oxalate has been added, or in organic-free systems where water acts as the ligand. This result was anticipated by Casey and Westrich (1992) who showed that orthosilicate group dissolution rates are proportional to the rate of exchange of water molecules around a dissolved cation (CASEY and WESTRICH, 1992).

Based on this information, we can propose a mechanism for the rate-determining step for forsterite dissolution. Previous studies have shown that, in the initial stages of forsterite dissolution experiments at low *pH*, magnesium is released to solution faster than silica (POKROVSKY and SCHOTT, 2000b; WOGELIUS and WALTHER, 1991a). This incongruent dissolution behavior is confirmed by XPS studies that show that acid-leached forsterite surfaces have a higher Si/Mg ratio than unreacted surfaces (POKROVSKY and SCHOTT, 2000b; SEYAMA et al., 1996). By acid-leaching our forsterite grains prior to our experiments, we created such a Si-enriched surface, allowing us to achieve stoichiometric dissolution at the beginning of our experiments rather than waiting for long periods of time. The Si/Mg ratios of our solution samples showed that most attained congruency within the first 20 minutes of reaction. Because we know that upon initial contact with an acidic solution, precursor reactions quickly release Mg^{2+}, enriching the surface in silica, we can infer that Si release is the rate-determining step in the overall forsterite dissolution process. Based on our rate law and the observed pH-dependence of oxalate-promoted dissolution, we believe that the release of H_4SiO_4 into solution requires simultaneous hydrogen ion attachment to the underbonded Mg-O-Si oxygen atom and oxalate attachment to the Mg site. This results in the transfer of electronic charge from the Mg-O bond into the O-H bond (Figure 2.4) and results in the dissociation of the Mg-O, which releases H_4SiO_4 into solution. Because protonation of the Mg-O-Si oxygen is necessary for this ligand-exchange reaction to occur, this elementary reaction step has a strong pH dependence. A similar argument was made in Liu et al. (2006b). This pH dependence is consistent with earlier work by Casey and Ludwig (1996) who suggested that ligand-promoted dissolution is dependent on adsorbed protons.

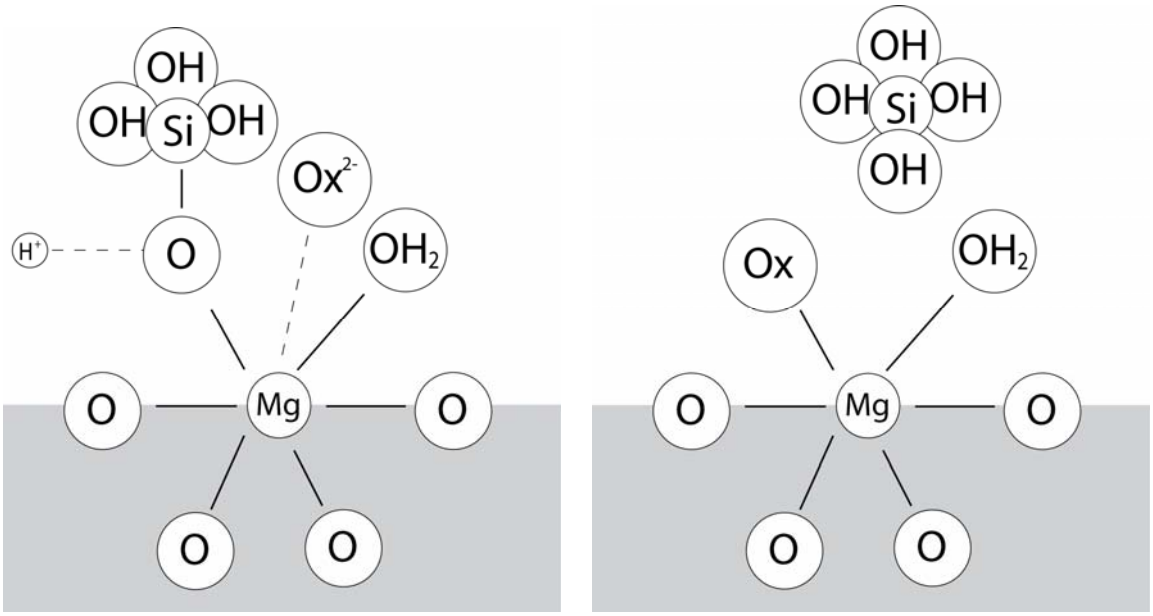

Figure 2.4. Proposed activated complex for the rate-determining step of forsterite dissolution. As H^+ approaches the connecting oxygen atom and oxalate approaches the Mg atom, electronic charge transfers from the Mg-O bond to form OH and Mg-oxalate bonds. This releases H_4SiO_4 into solution.

The same reaction mechanism can be used to explain what has been called proton-promoted dissolution, where only water acts as a ligand. Thus it seems that the distinction between proton-promoted dissolution and ligand-promoted dissolution in the literature is largely artificial. Rates are enhanced with the addition of ligands because the ligands are more effective than water in mounting a nucleophilic attack on the Mg site to produce a ligand exchange reaction. Oxalate is more highly charged than water; therefore, dissolution rates in the presence of oxalate are higher. However, because the concentration of water is 55.5 mol/L, water plays an important role in the overall dissolution mechanism due to its high concentration.

Our experimental results and analysis show that oxalate concentrations that are reported for some soils (0.001 m) can enhance forsterite dissolution by up to almost one order of magnitude (Figure 2.5). This translates to a 0.8 log unit decrease in olivine grain lifetimes (OLSEN and RIMSTIDT, 2007). This effect would be strongest at pH above 4, which is expected for most natural waters. Additionally, the effect of organic ligands

could be greatly enhanced in areas that have abnormally high levels of organic acids, such as in the vicinity of plant roots or in exceptionally organic-rich soils. It has also been suggested that organic ligands may lower the pH of soil solutions, synergistically accelerating proton-promoted dissolution in addition to the accelerating effect of the organic acids (DREVER and VANCE, 1994); however, this may be offset by the decreased concentration of the oxalate ions due to oxalic acid hydrolysis at low pH.

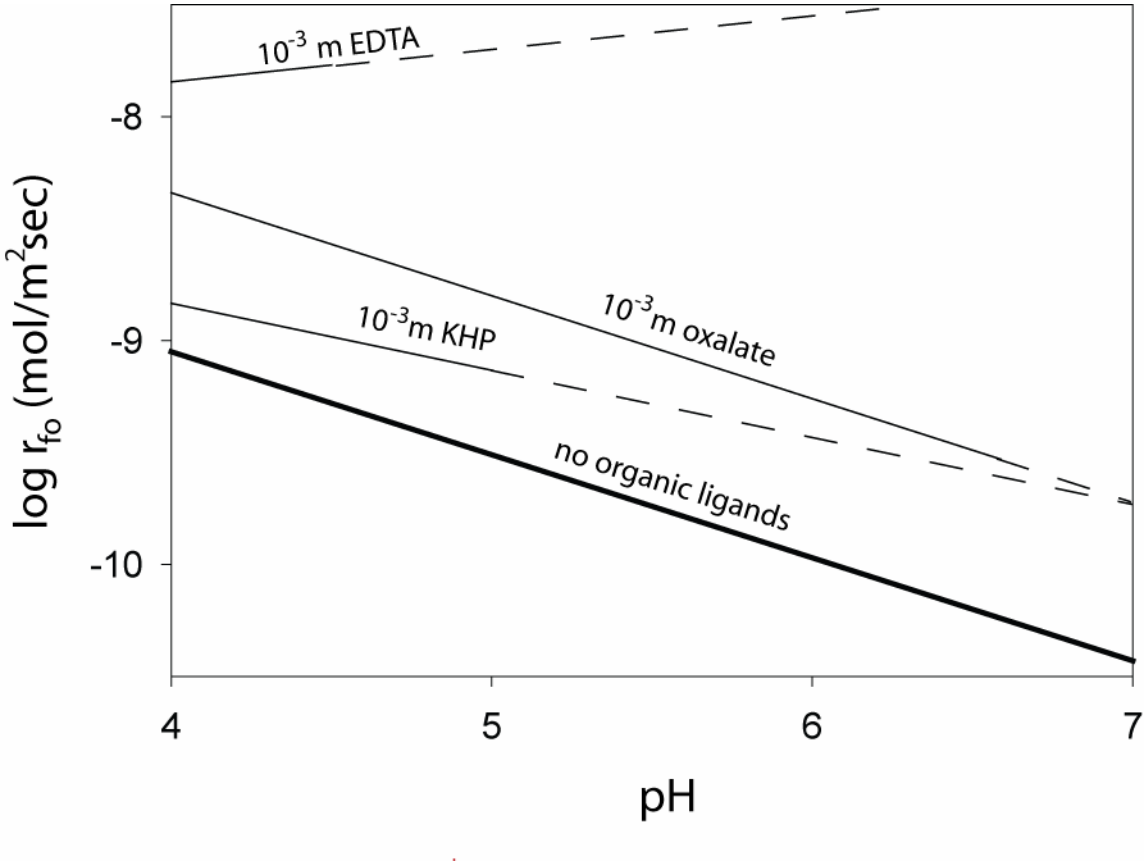

Figure 2.5. Log r versus pH for some organic acids at 0.001 m. The bold line shows the model for dissolution rate when no organic acids are present, line for oxalate comes from this study, line for EDTA is based on data from Wogelius and Walther (1991a; 1992), and line for EDTA is based on data from Grandstaff (1986).

2.6 REFERENCES

Amrhein, C. and Suarez, D. L., 1988. The use of a surface complexation model to describe the kinetics of ligand-promoted dissolution of Anorthite. *Geochimica et Cosmochimica Acta* **52**, 2785-2793.

Bennett, P. C., Melcer, M. E., Siegel, D. I., and Hassett, J. P., 1988. The dissolution of quartz in dilute aqueous solutions of organic acids at 25°C *Geochimica et Cosmochimica Acta* **52**, 1521-1530.

Blum, A. E. and Lasaga, A. C., 1988. Role of surface speciation in the low-temperature dissolution of minerals. *Nature* **331**, 431-433.

Blum, A. E. and Stillings, L. L., 1995. Feldspar Dissolution Kinetics. In: White, A. F. and Brantley, S. L. Eds.), *Chemical weathering rates of silicate minerals*. Mineralogical Society of America, Washington, D.C.

Brantley, S. L. and Mellott, N. P., 2000. Surface area and porosity of primary silicate minerals. *American Mineralogist* **85**, 1767-1783.

Cama, J. and Ganor, J., 2006. The effects of organic acid on the dissolution of silicate minerals: A case study of oxalate catalysis of kaolinite dissolution. *Geochimica et Cosmochimica Acta* **70**, 2191-2209.

Casey, W. and Westrich, H., 1992. Control of dissolution rates of orthosilicate minerals by divalent metal-oxygen bonds. *Nature* **355**, 157-159.

Casey, W. H., 2001. A view of reactions at mineral surfaces from the aqueous phase. *Mineralogical Magazine* **65**, 323-337.

Casey, W. H. and Ludwig, C., 1996. The mechanism of dissolution of oxide minerals. *Nature* **381**, 506-509.

Drever, J. I. and Vance, G. F., 1994. Role of Soil Organic Acids in Mineral Weathering Processes. In: Pittman, E. D. and Lewan, M. D. Eds.), *Organic Acids in Geological Processes*. Springer-Verlag, New York.

Fox, T. R. and Comerford, N. B., 1990. Low-molecular-weight organic acids in selected forest soils of the southeastern USA. *Soil Science Society of America Journal* **54**, 1139-1144.

Franklin, S. P., Hajash, A. J., Dewers, T. A., and Tieh, T. T., 1994. The role of carboxylic acids in albite and quartz dissolutions: An experimental study under diagenetic conditions. *Geochimica et Cosmochimica Acta* **58**, 4259-4279.

Furrer, C. and Stumm, W., 1986. The coordination chemistry of weathering: I. Dissolution kinetics of gamma-Al2O3 and BeO. *Geochimica et Cosmochimica Acta* **50**, 1847-1860.

Govett, G. J. S., 1961. Critical factors in the colorimetric determination of silica. *Analytica Chimica Acta* **25**, 69-80.

Grandstaff, D. E., 1986. The dissolution rate of forsteritic olivine from Hawaiian beach sand. In: Colman, S. M. and Dethier, D. P. Eds.), *Rates of Chemical Weathering of Rocks and Minerals*. Academic Press, Orlando, FL.

Huang, W. H. and Kiang, W. C., 1972. Laboratory dissolution of plagioclase feldspars in water and organic acids at room temperature. **57**, 1849-1859.

Kettler, R. M., Wesolowski, D. J., and Palmer, D. A., 1998. Dissociation Constants of Oxalic Acid in Aqueous Sodium Chloride and Sodium Trifluoromethanesulfonate Media to 175 C. *Journal of Chemical Engineering Data* **43**, 337-350.

Liu, Y., Olsen, A. A., and Rimstidt, J. D., 2006. Mechanism for the dissolution of olivine series minerals in acidic solutions. *American Mineralogist* **91**, 455-458.

Luce, R. W., Bartlett, R. W., and Parks, G. W., 1972. Dissolution kinetics of magnesium silicates. *Geochimica et Cosmochimica Acta* **36**, 35-50.

Manley, E. P. and Evans, L. J., 1986. Dissolution of feldspars by low-molecular-weight aliphatic and aromatic acids. *Soil Science*, 106-112.

Mast, A. M. and Drever, J. I., 1987. The effect of oxalate on the dissolution rates of oligoclase and tremolite. *Geochimica et Cosmochimica Acta* **51**, 2559-2568.

Nagy, K., Blum, A., and Lasaga, A., 1991. Dissolution and precipitation kinetics of kaolinite at 80C and pH 3: the dependance on solution saturation state. *American Journal of Science* **291**, 649-686.

Oelkers, E. H., 2001. An experimental study of forsterite dissolution rates as a function of temperature and aqueous Mg and Si concentrations. *Chemical Geology* **175**, 485-494.

Olsen, A. A. and Rimstidt, J. D., 2007. Using a mineral lifetime diagram to evaluate the persistence of olivine on Mars. *American Mineralogist* **92**.

Pokrovsky, O. S. and Schott, J., 2000. Kinetics and mechanism of forsterite dissolution at 25 C and pH from 1 to 12. *Geochimica et Cosmochimica Acta* **64**, 3313-3325.

Poulson, S. R., Drever, J. I., and Stillings, L. L., 1997. Aqueous Si-oxalate complexing, oxalate adsorption onto quartz, and the effect of oxalate upon quartz dissolution rates. *Chemical Geology* **140**, 1-7.

Rosso, J. J. and Rimstidt, J. D., 2000. A high resolution study of forsterite dissolution rates. *Geochimica et Cosmochimica Acta* **64**, 797-811.

Schott, J., Berner, R. A., and Sjoberg, E. L., 1981. Mechanism of pyroxene and amphibole weathering- I. Experimental studies of iron-free minerals. *Geochimica et Cosmochimica Acta* **45**, 2123-2135.

Seyama, H., Soma, M., and Tanaka, A., 1996. Surface characterization of acid-leached olivines by X-ray photoelectron spectroscopy. *Chemical Geology* **129**, 209-216.

Stillings, L. L., Drever, J. I., Brantley, S. L., Sun, Y., and Oxburgh, R., 1996. Rates of feldspar dissolution at pH 3-7 with 0-8 mM oxalic acid. *Chemical Geology* **132**, 79-89.

Stumm, W. and Wollast, R., 1990. Coordination of chemistry of weathering: kinetics of the surface-controlled dissolution of oxide minerals. *Reviews of Geophysics* **28**, 53-69.

Welch, S. A. and Ullman, W. J., 1993. The effect of organic acids on plagioclase dissolution rates and stoichiometry. *Geochimica et Cosmochimica Acta* **57**, 2725-2736.

Welch, S. A. and Ullman, W. J., 1996. Feldspar dissolution in acidic and organic solutions: Compositional and pH dependence of dissolution rate. *Geochimica et Cosmochimica Acta* **60**, 2939-2948.

White, A. F. and Brantley, S. L., 1995. *Chemical weathering rates of silicate minerals*. Mineralogical Society of America, Washington, D.C.

Wogelius, R. and Walther, J., 1991. Olivine dissolution at 25C: Effects of pH, CO2, and organic acids. *Geochimica et Cosmochimica Acta* **55**, 943-954.
Wogelius, R. A. and Walther, J. V., 1992. Olivine dissolution kinetics at near-surface conditions. *Chemical Geology* **97**, 101-112.

APPENDIX 2.1

Magnesium and silica release rates for all experiments in mol/m^2sec. All rates were standardized to a surface area of 0.0528 m^2/g, and Mg release rates (r_{mg}) have been standardized to Si release rates (r_{si}) by dividing by 1.84. Entries at the end of the table marked with an asterisk were not included in regression model due to anomalous Si/Mg ratio.

Sample	pH	log r_{Mg} (mol/m^2 sec)	log r_{Si} (mol/m^2 sec)	T_{ox}	I
OX1	2.26	-7.52	-7.53	0.070	0.168
OX2	1.79	-7.38	-7.38	0.140	0.313
OX3	1.68	-7.35	-7.44	0.210	0.456
OX5	1.44	-7.26	-7.46	0.350	0.743
OX6	4.01	-8.24	-8.23	0.010	0.026
OX7	4.02	-8.14	-8.12	0.017	0.046
OX8	4.01	-8.14	-8.07	0.023	0.061
OX9	4	-8.10	-8.14	0.027	0.074
OX10	4.01	-8.09	-8.13	0.031	0.084
OX11	4.06	-7.93	-8.14	0.034	0.092
OX12	4.01	-7.92	-8.15	0.037	0.100
OX13	4.00	-7.93	-8.12	0.039	0.106
OX14	4.01	-7.91	-8.12	0.041	0.112
OX22	5.65	-8.87	-8.44	0.033	0.097
OX26	6.26	-9.49	-9.65	0.002	0.004
OX33	4.6	-9.00	-8.63	0.001	0.003
OX34	4.58	-8.83	-8.65	0.002	0.006
OX35	4.52	-8.53	-8.44	0.003	0.009
OX36	4.52	-8.44	-8.26	0.004	0.012
OX37	4.58	-8.54	-8.27	0.006	0.015
OX38	4.53	-8.53	-8.20	0.007	0.017
OX39	4.56	-8.24	-8.15	0.008	0.020
OX40	4.57	-8.25	-8.17	0.009	0.023
OX41	4.58	-8.19	-8.14	0.010	0.026
OX42	4.71	-8.90	-8.87	0.003	0.007
OX43	4.69	-8.68	-8.40	0.004	0.010
OX44	4.73	-8.63	-8.38	0.005	0.013
OX45	4.77	-8.56	-8.38	0.006	0.016
OX46	4.68	-8.45	-8.34	0.007	0.019
OX47	4.73	-8.44	-8.38	0.008	0.022
OX48	4.77	-8.43	-8.31	0.009	0.025
OX49	4.77	-8.43	-8.30	0.011	0.027
OX50	4.74	-8.36	-8.29	0.012	0.030
SB44	1.71	-7.25	-7.42	0.074	0.171
SB45	2.14	-7.50	-7.54	0.054	0.135
SB46	2.62	-7.63	-7.66	0.048	0.123
SB47	3.10	-7.65	-7.74	0.043	0.115
SB48	3.58	-7.79	-7.66	0.040	0.109

Sample	pH	log r_{Mg} (mol/m^2sec)	log r_{Si} (mol/m^2sec)	T_{ox}	I
SB49	4.05	-7.97	-7.98	0.035	0.103
SB51	4.50	-8.24	-8.25	0.032	0.098
SB52	4.96	-8.50	-8.49	0.031	0.096
SB53	5.47	-8.71	-8.75	0.030	0.094
SB55	6.59	-8.98	-8.52	0.029	0.093
SB61	0.62	-7.16	-7.33	0.033	0.520
SB62	1.02	-7.07	-7.21	0.083	0.299
SB63	1.45	-7.30	-7.33	0.082	0.190
SB64	1.94	-7.39	-7.49	0.053	0.136
SB65	2.30	-7.49	-7.55	0.047	0.124
SB66	2.75	-7.60	-7.70	0.044	0.117
SB67	3.20	-7.72	-7.73	0.040	0.111
SB68	3.60	-7.88	-8.02	0.035	0.103
SB71	0.59	-7.17	-7.26	0.053	0.471
SB72	0.68	-7.23	-7.29	0.069	0.398
SB73	1.21	-7.25	-7.32	0.096	0.242
SB74	1.86	-7.46	-7.50	0.073	0.166
SB75	3.72	-7.81	-7.86	0.055	0.133
SB76	4.00	-7.88	-7.94	0.052	0.128
SB77	4.29	-7.98	-8.03	0.045	0.118
SB78	3.58	-7.74	-7.81	0.051	0.127
SB79	3.75	-7.75	-7.86	0.050	0.124
SB80	3.95	-7.88	-7.95	0.047	0.121
SB81	4.13	-7.87	-7.96	0.046	0.119
SB82	4.33	-8.04	-8.05	0.044	0.116
SB83	4.50	-8.09	-8.11	0.043	0.114
SB84	5.54	-8.56	-8.52	0.095	0.192
SB85	6.55	-9.08	-8.68	0.094	0.191
SB89	0.49	-7.09	-7.19	0.096	0.670
SB90	0.54	-7.14	-7.19	0.097	0.586
SB91	0.76	-7.19	-7.25	0.099	0.383
SB92	1.10	-7.25	-7.30	0.100	0.253
SB93	1.50	-7.31	-7.43	0.078	0.183
SB94	1.82	-7.40	-7.49	0.068	0.160
SB95	2.15	-7.46	-7.52	0.063	0.147
SB 96	2.97	-8.61	-8.61	0	0.119
SB 97	3.02	-8.49	-8.47	0	0.313
SB 98	3.02	-8.48	-8.47	0	0.610
SB 99	2.99	-8.42	-8.45	0	0.907
SB100	2.98	-8.36	-8.40	0	1.205
SB101	2.95	-8.34	-8.30	0	1.502
SB102	2.94	-8.44	-8.37	0	1.801
SB103	2.97	-8.39	-8.50	0	2.096
SB104	3.05	-8.49	-8.55	0	2.387
SB105	1.96	-8.07	-8.02	0	0.120
SB106	1.95	-8.04	-8.02	0	0.308
SB107	1.96	-7.97	-7.97	0	0.609

Sample	pH	log r_{Mg} (mol/m^2sec)	log r_{Si} (mol/m^2sec)	T_{ox}	I
SB108	2	-8.03	-8.00	0	0.903
SB109	2.01	-7.92	-7.98	0	1.198
SB110	2.01	-7.91	-7.94	0	1.496
SB111	2	-8.03	-7.95	0	1.795
SB112	2.01	-7.92	-7.89	0	2.090
SB113	2	-7.94	-7.91	0	2.385
SB114	3.83	-9.22	-8.70	0	0.101
SB115	3.91	-8.97	-8.79	0	0.301
SB118	3.87	-9.13	-8.71	0	1.189
SB119	3.91	-8.86	-9.08	0	1.486
SB120	3.8	-8.41	N/A	0	1.784
SB121	4.1	-8.75	-8.94	0	2.081
SB122	4.04	-8.53	-8.56	0	2.376
SB123	1	-7.63	-7.54	0	0.218
SB124	1.02	-7.59	-7.58	0	0.406
SB125	1.05	-7.58	-7.50	0	0.690
SB126	1.05	-7.55	-7.41	0	0.990
SB127	1.04	-7.55	-7.38	0	1.291
SB128	1.02	-7.54	-7.28	0	1.593
SB129	1.04	-7.45	-7.31	0	1.883
SB130	1.05	-7.48	-7.22	0	2.167
SB131	1.04	-7.49	-7.46	0	2.467
OX4*	1.55	-7.17	-7.81	0.280	0.599
OX23*	6.16	-9.69	-8.51	0.035	0.103
OX24*	6.94	-9.28	-8.60	0.000	0.001
OX25*	6.52	-9.84	-8.95	0.001	0.003
OX27*	6.20	-10.01	-8.69	0.002	0.006
OX28*	6.37	-9.67	-8.65	0.003	0.007
OX30*	5.83	-9.74	-8.70	0.004	0.010
OX31*	6.31	-10.26	-8.51	0.004	0.011
OX32*	6.47	-9.73	-8.58	0.005	0.013
SB54*	6.07	-9.07	-10.54	0.029	0.094
SB116*	4.05	-7.86	-8.99	0	0.595
SB117*	3.92	-9.84	-8.71	0	0.892

CHAPTER 3. USING A MINERAL LIFETIME DIAGRAM TO EVALUATE THE PERSISTENCE OF OLIVINE ON MARS

3.1 ABSTRACT

We present a diagram that shows the effect of pH, temperature, grain size, composition, hydrodynamics, and the laboratory/field discrepancy on the lifetime of olivine grains in weathering environments. This diagram has wide applicability. For example, because the persistence of olivine grains on Mars can be used to constrain the duration of liquid water, we can use this diagram to predict a range of possible maximum contact times for olivine grains with liquid water before they dissolve away completely. Depending upon the physicochemical conditions, this contact time could range between a few thousand and several million years.

3.2 INTRODUCTION

We have available a large database of laboratory-determined mineral dissolution rates that were collected with the intention of applying this information to understand chemical weathering in the field. However, application of these experimental results to predict weathering patterns has proved somewhat elusive. In this note we show how to present these laboratory rate measurements in a way that allows visualization of the effect of pertinent rate-controlling variables on the lifetime of mineral grains in the weathering environment. Because of the current interest in olivine weathering and its implication for the duration of liquid water on Mars, we use this as an example of how this mineral lifetime diagram can be applied to investigate an interesting scientific question.

One of the most compelling scientific questions of space exploration is whether we can find evidence of living organisms at other places in the solar system. Because its surface composition and climate overlap with terrestrial conditions, Mars provides an excellent prospect for finding evidence for the independent development of life (Knoll

and Grotzinger, 2006). However, a key ingredient needed for the development of life is liquid water so the likelihood of finding traces of life depends upon the sustained occurrence of liquid water in Martian history. Numerous observations, including aqueous alteration phases, cross lamination, hematite-rich concretions, thick weathering rinds on basalts, resistant siliciclastic fracture fills, and polygonal crack systems (Christensen et al., 2000; Christensen et al., 2004; Clark et al., 2005; Klingelhofer et al., 2004; Squyres et al., 2004; Squyres and Knoll, 2005; Squyres et al., 2006; Yen et al., 2005) show that liquid water did exist on the Martian surface. However, most studies suggest that the amounts and duration of liquid water were limited (Christensen et al., 2004; Madden et al., 2004; Squyres et al., 2006). An important constraint on the duration of liquid water is the observed presence of olivine crystals on the Martian surface. Because olivine dissolves relatively quickly in the presence of liquid water, its continued presence on the Martian surface suggests that the amount and duration of liquid water were limited. Stopar et al. (Stopar et al., 2006) produced a similar analysis of olivine lifetimes. However, our mineral lifetime diagram show how olivine grain lifetime to rate-controlling variables so that new estimate of grain lifetimes can be made as our knowledge of Martian surface conditions evolves.

Olivine is present on Mars in two distinct environments: within Surface Type 1 basalts consisting of primarily plagioclase and clinopyroxene with small amounts of olivine (Bandfield et al., 2000; McSween Jr. et al., 2003) and in olivine-rich basalts (Bibring et al., 2005; Mustard et al., 2005; Rogers et al., 2005) which are generally present as small outcrops, often inside of impact crators, but are exposed over 30,000 km^2 at Nili Fossae (Hamilton and Christensen, 2005). Although an understanding of Martian mineralogy is incomplete, no terrains containing significant quantities of both olivine and aqueous alteration products have been observed. Because olivine is not in contact with any alteration products, it is difficult to constrain the pH of an aqueous fluid that might have been in contact with olivine on Mars. However, based on the work of Madden et al. (MADDEN et al., 2004) we expect the pH of a solution in contact with jarosite to range approximately from 2.5 to 4.5. Additionally, groundwater in high-olivine basalts in Iceland, a possible Earth analog for Martian basalts, has an average pH of 7.5 at an average temperature of 277 K (Stefansson and Gislason, 2001). We believe that these

two end members reasonably bracket the pH range of solutions in contact with olivine on Mars.

3.3 METHODS

We have used the large body of published information about olivine dissolution rates along with a shrinking particle model for grain lifetimes to predict the maximum time that olivine grains could persist in an aqueous environment. Our goal is to systemically examine the effects of known or suspected rate-controlling variables. We have compiled laboratory dissolution rates and used them to construct a baseline model for the lifetime of a 1 mm grain in dilute solutions with pH between 0 and 12 at 298 K. Then we evaluate how changing other important rate controlling parameters affects this lifetime.

Data from eight olivine dissolution studies (Blum and Lasaga, 1988; Grandstaff, 1986; Luce et al., 1972a; Oelkers, 2001; Pokrovsky and Schott, 2000b; Rosso and Rimstidt, 2000; Siegel and Pfannkuch, 1984; Wogelius and Walther, 1991b) were used to develop empirical dissolution rate expressions for forsteritic olivine over the pH range of 0 to 12 (Figure 3.1). All experiments were conducted at 298 K, at low ionic strength, and at low P_{CO2}. In total, 175 Si release rates and 167 Mg release rates were compiled. Both Si and Mg release rates were used to compute rates of olivine destruction in mol/m^2sec. Mg rate data were adjusted for olivine compositions ranging from Fo91 to Fo100 to account for the fayalite component (Rosso and Rimstidt, 2000). Experiments showing strong incongruent dissolution with Si/Mg release ratios greater than 5 or less than 0.2 were discarded. All data from Siegel and Pfannkuch (Siegel and Pfannkuch, 1984) were discarded due to anomalously high Si/Mg ratios and do not appear on the figure. Results from Grandstaff (Grandstaff, 1986) were excluded from the figure and regression because the rates are anomalously slower than the other studies by 1.5 to 2.5 orders of magnitude. Outliers in the regression models were identified and discarded using Chauvenet's criterion, a procedure which identifies outliers by calculating the number of points that would be expected to fall outside of a given number of standard deviations; if a higher than expected number of data points fall outside of this range, they can then be rejected (Taylor, 1982).

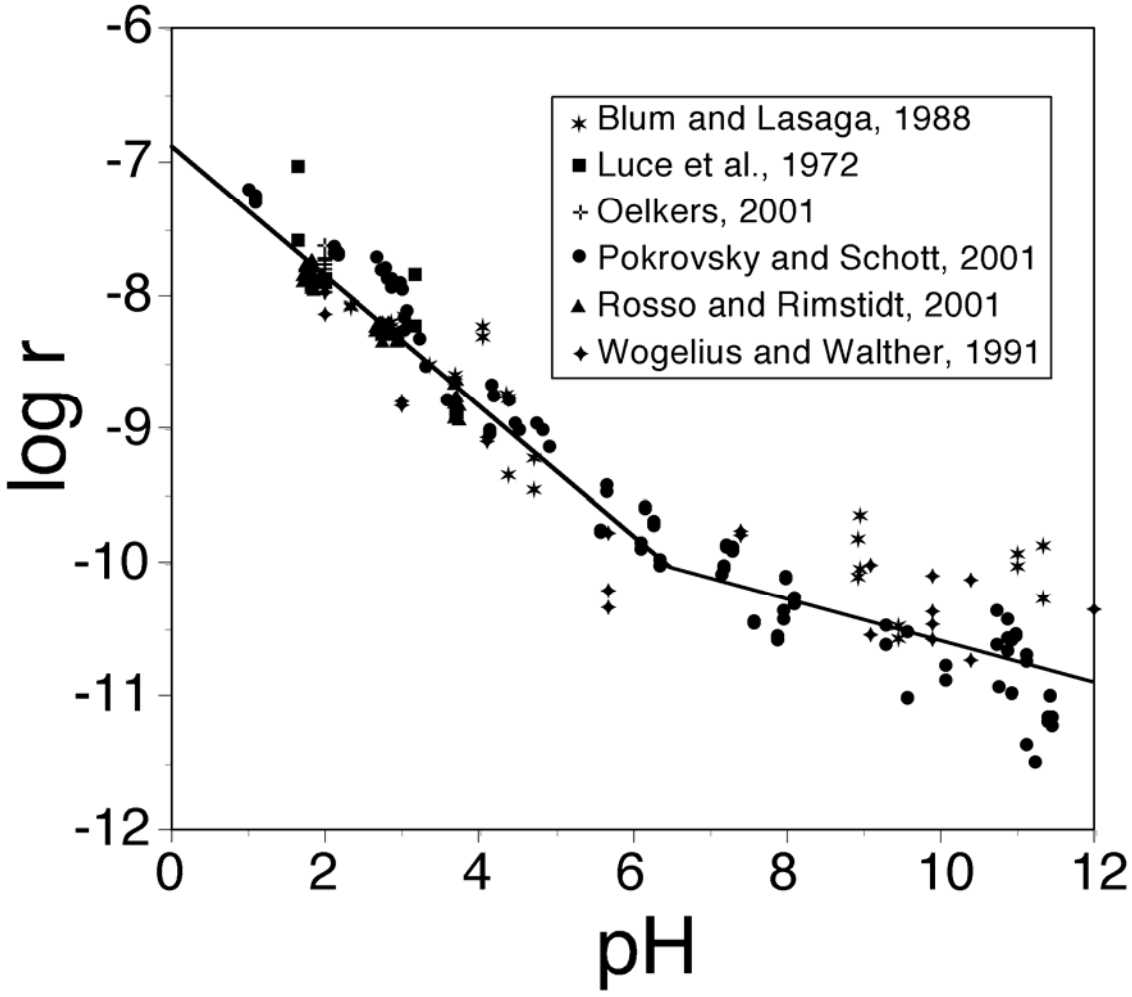

Figure 3.1. Reported rates of forsterite dissolution (Blum and Lasaga, 1988; Luce et al., 1972a; Oelkers, 2001; Pokrovsky and Schott, 2000b; Rosso and Rimstidt, 2000; Siegel and Pfannkuch, 1984; Wogelius and Walther, 1991b) in mol/m^{2}s. Black lines represent results of regression models from Equations 3.1 and 3.2.

3.4 RESULTS AND DISCUSSION

Because the olivine dissolution rates show a clear break in slope near pH 6, we chose to fit them with two separate equations, one for pH<6 and the other for pH>6:

$$\log r_{pH<6} = -0.48(0.01)pH - 6.90(0.03)\ R^2=0.88 \qquad (3.1)$$

$$\log r_{pH>6} = -0.18(0.02)pH - 8.8(0.2)\ R^2=0.49 \qquad (3.2)$$

where the numbers in parentheses represent one standard error of the regression coefficients.

We then used these equations to construct the line in Figure 3.2, which predicts olivine lifetimes in dilute solutions at 298 K as a function of pH. The lifetime (t) of a dissolving spherical olivine grain is related to its rate of dissolution (r) by the expression

$$t = \frac{d}{2V_m r} \qquad (3.3)$$

where d is the grain diameter and V_m is the molar volume of olivine (Lasaga, 1998). This olivine lifetime model constrains the maximum time that an olivine grain could have been in contact with liquid water before dissolving away completely.

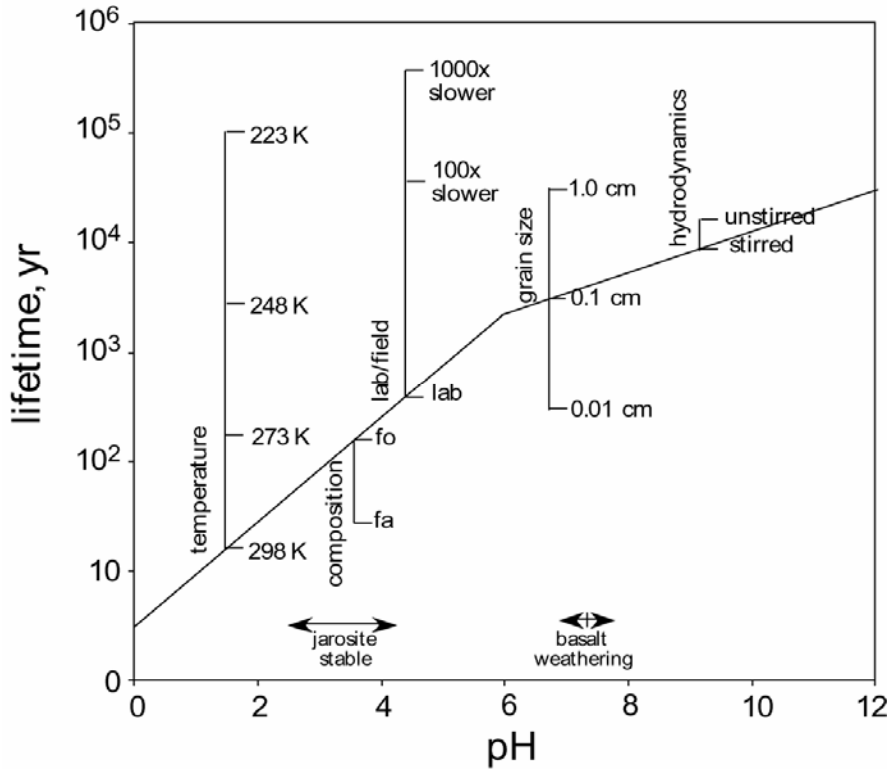

Figure 3.2. Forsterite grain lifetime diagram**.** Forsterite grain lifetimes are given as a function of pH for laboratory conditions at 298 K. Vertical scales show how changing temperature, olivine composition, field conditions, grain size, and hydrodynamics increase (scales above graph) or decrease (scales below graph) olivine grain lifetimes. Scales have been placed at arbitrary pH values and can describe conditions at any pH.

A number of factors could change olivine lifetimes from the reference case shown in Figure 3.2. These factors include dissolved carbonate (Golubev et al., 2005; Pokrovsky and Schott, 2000b; Wogelius and Walther, 1991b), H_4SiO_4 (Oelkers, 2001; Pokrovsky and Schott, 2000b), Mg^{2+} (Oelkers, 2001; Pokrovsky and Schott, 2000b), grain coatings (Weissbart and Rimstidt, 2000), ionic strength, fayalite/forsterite ratio (Westrich et al., 1993), temperature (Jonckbloedt, 1998; Oelkers, 2001; Rosso and Rimstidt, 2000; Van Herk et al., 1989), grain size, hydrodynamics (Rimstidt et al., 1996), and an unexplained discrepancy between field and laboratory dissolution rates (Velbel, 1986; Velbel, 1993; White and Brantley, 2003). The effect of each of these factors on olivine lifetime has been evaluated and the magnitude of each effect is shown by the vertical scales on Figure 3.2. Those scale bars that lie above the lifetime versus pH reference line represent factors that increase grain lifetime and those that lie below this line represent factors that shorten grain lifetime.

Although there have been some reports that P_{CO2} or dissolved carbonate species affect olivine dissolution rates, the most recent results (Golubev et al., 2005) indicate that carbonate ions do not have a significant effect. One early study (Wogelius and Walthur, 1991b) reported that the presence of dissolved CO_2 at atmospheric partial pressures decreased the dissolution rate of forsterite by approximately ten times. However, these dissolution experiments were not stoichiometric, suggesting that the measured rates were influenced by another factor. A similar study (Pokrovsky and Schott, 2000b) showed that as $\log a_{CO_3^{2-}}$ increases from -5 to -2, dissolution rates decreased by 1.5 orders of magnitude at pH>8. However, dissolution rates in that study were calculated using rates of Mg release, which may have been reduced by non-stoichiometric dissolution and the development of a brucite-like leached layer or by the formation of magnesite in the experiments. More recent experiments (Golubev et al., 2005) show no effect on the rate of HCO_3^- up to 0.01 M or of CO_3^{2-} up to 0.005 M. Based on these more recent, carefully-executed experiments we conclude that carbonate ions do not significantly affect olivine dissolution rates.

The olivine dissolution reaction is far from equilibrium so we do not expect that aqueous Mg^{2+} and H_4SiO_4 will reprecipitate as olivine. Oelkers (2001) and Pokrovsky and Schott (2000b) showed that olivine dissolution rates are not affected by aqueous

Mg^{2+} concentrations up to 0.05 M. Olivine dissolution does not seem to be affected by aqueous H_4SiO_4 concentrations up to 0.0005 M at low pH (Oelkers, 2001). However, Pokrovsky and Schott (2000b) report that aqueous Si concentrations of 0.001 M decreased the dissolution rate by approximately five times at pH above 8.8. We have not shown this effect in Figure 3.2 because it is relatively small and because this pH falls outside of the target pH range that we discussed in the Introduction. However, the effect of aqueous silica may be significant at pH above 8.8.

Various coatings could form on weathering olivine. For example, silica-rich leached layers can form on silicate minerals that have Si-O-Si bonds (Weissbart and Rimtidt, 2000). Although olivine has been reported to develop a Si-enriched surface at low pH and a Mg-enriched surface at high pH, this layer is only 10-20 Å in thickness and there is no evidence that it affects dissolution rates (Pokrovsky and Schott, 2000a). Secondary mineral precipitates such as sepiolite or chrysotile could grow as coatings on olivine surfaces in high pH silica- and magnesium-rich solutions. Iddingsite, a poorly defined mixture of hydrous silicates of iron and magnesium, has been observed as an alteration product on iron-rich olivine grains both terrestrially (Kuebler et al., 2003; Wilson, 2004) and on meteorites (Leshin and Vicenzi, 2006). However, because olivine has been detected using remote sensing, we can conclude such coatings must be thin to absent on some Martian olivine or they would obscure the olivine signal. Our analysis applies only to those observable uncoated olivine grains so that the effect of coatings can be neglected.

Increasing the amount of the fayalite component in olivine can increase dissolution rates by up to six times (Wogelius and Walther, 1992). Signatures for Fo_{91}, Fo_{60} and Fo_{68}, and Fo_{53} have all been detected on Mars using the Mars Global Surveyor Thermal Emission Spectrometer (Koeppen and Hamilton, 2006). Although most olivine dissolution studies have been performed at near-endmember forsterite and fayalite compositions, (Westrich et al., 1993) showed that there is an exponential relationship between dissolution rate and composition. Because dissolution rates of both forsterite and fayalite have been determined (Wogelius and Walther, 1992), we can use this relationship (Westrich et al., 1993) to postulate that all Martian olivine dissolution would be bracketed between these two endmember dissolution rates (Figure 3.2).

Lowering the temperature would significantly slow olivine dissolution rates and extend grain lifetimes. Smith et al. (2004) found that Martian soil temperatures ranged from approximately 210 K to 290 K depending on time of day. Also, it is possible that Mars was much warmer early in its history (Carr, 1996), although recent studies suggest that Mars has most likely been at its current temperature for the past 4 billion years (Shuster and Weiss, 2005). Numerous studies have examined the effect of temperature on forsterite dissolution rates and determined activation energy values for forsterite dissolution (Jonckbloedt, 1998; Oelkers, 2001; Rosso and Rimstidt, 2000; Van Herk et al., 1989; Wogelius and Walther, 1992). Although no experiments have been done at temperatures less than 298 K, we can use the Arrhenius equation

$$\ln k_T = \ln k_{T,R} - \frac{E_a}{R}\left(\frac{1}{T} - \frac{1}{T_R}\right) \qquad (3.4)$$

where k_T is the rate constant at temperature (T, K), $k_{T,R}$ is the rate constant at the reference temperature (T_R=298 K), E_a is the activation energy, and R is the universal gas constant (Langmuir, 1997), to predict how rates will slow with decreasing temperatures. Activation energies from five studies (Jonckbloedt, 1998; Oelkers, 2001; Rosso and Rimstidt, 2000; Van Herk et al., 1989; Wogelius and Walther, 1992) were averaged to obtain an activation energy of 63 kJ/mol. Figure 3.2 shows that olivine grain lifetimes increase by about ten times if the temperature is reduced from 298 K to the freezing point of pure water (273 K). The freezing point of acidic sulfate solutions, which have been postulated for Mars, could be as much as 70°C lower (Knoll et al., 2005; Knoll and Grotzinger, 2006). If we chose either the smallest activation energy of 42 kJ/mol (Rosso and Rimstidt, 2000) or the largest activation energy of 79.5 kJ/mol (Wogelius and Walther, 1992), it would either decrease the lifetime by 16 times or increase the lifetime by 10 times respectively.

The shrinking particle model (Lasaga, 1998) shows that each order of magnitude increase in grain size increases grain lifetime by one order of magnitude. Typical olivine crystals on Earth are a few millimeters in diameter. Some Martian meteorites have olivine grains ranging in size from 50 μm to 2 mm (Barrat et al., 2002; Wang et al., 2004). We chose 1 mm as our reference grain size; however, larger grains would have proportionally longer lifetimes (Figure 3.2).

If the liquid water on Mars were stationary, lack of mixing could slow down the transport of H^+ to the olivine surface and thus slow the dissolution rate. Preliminary studies show that transport limitation could slow olivine dissolution in unstirred settings by as much 2.5 times (Figure 3.2) (Rimstidt et al., 1996).

Numerous studies have shown that laboratory dissolution rates are two to three orders of magnitude faster than field rates (Velbel, 1986; Velbel, 1993; White and Brantley, 2003). Similarly, sedimentary grain lifetimes are up to three orders of magnitude longer than lifetimes predicted from laboratory rate measurements (Kowalewski and Rimstidt, 2003). Some possible reasons for this discrepancy include uncontrolled or unaccounted effects on reactive surface area, energetically reactive sites, chemical affinity, temperature, dislocation densities, coatings, hydrodynamics, and grain aging (Velbel, 1986; Velbel, 1993; White and Brantley, 2003). Many of these effects have already been considered in this paper. None of these factors alone seem to account for the entire observed difference between laboratory and field rates. Although there is not a widely accepted explanation for this lab/field difference, we postulate that similar processes acting on the Martian surface will create a similar discrepancy, which would increase grain lifetimes by 100 to 1000 times (Figure 3.2). Because we have already considered some of these effects in Figure 2, we propose that a lab/field discrepancy correction of about two orders of magnitude would be appropriate.

How can we use Figure 3.2 to constrain the lifetime of olivine, and therefore, the duration of liquid water on Mars? The rate effects in Figure 3.2 are multiplicative; therefore, because the y-axis is a log scale, the scale bars shown in Figure 3.2 can simply be added onto each other to estimate a total lifetime. As discussed in the Introduction, we cannot completely constrain the pH of a solution in contact with olivine on the Martian surface. However, our model allows a lifetime prediction for any pH value. For example, if we wish to consider the fate of olivine in locations that now contain jarosite, the pH is constrained to the range of 2.5 to 4.5. If we consider a 1 mm forsterite diameter grain at 298 K and pH 3.5, its reference lifetime would be approximately 140 years. Assuming that the discrepancy between laboratory and field rates under these conditions is approximately two orders of magnitude, the lifetime could increase to 14,000 years. If the temperature were 273 K rather than 298 K, the lifetime could be about ten times

longer, making it 140,000 years. Unstirred conditions would increase the lifetime by no more than 2.5 times (0.5 log units) to 350,000 years. Similarly, if we assume that the olivine-rich basalts have been in contact with water in a setting similar to Iceland (Stefansson and Gislason, 2001), a 1 mm diameter forsterite grain at 273 K at pH 7.5 and unstirred conditions would have a lifetime of up to 30 million years, assuming a two order of magnitude discrepancy between laboratory and field rates.

Validating this mineral lifetime diagram by comparing its predictions with olivine lifetimes on Earth is difficult because of the lack of quantitative lifetime information for field conditions. However, Kowalewski and Rimstidt (2003) used an entirely different approach to estimate that the lifetime of 1 mm diameter olivine grains in soils with a pH near 5.5 is around 3.9 million years. For comparison, our olivine lifetime diagram predicts a lifetime for 1 mm olivine grains at pH 5.5 and at 10°C of 1.5 million years. This suggests that our diagram gives estimates that are in the correct order of magnitude.

Many other scenarios are possible, and reasonable estimates of olivine lifetimes must be constrained by a more complete knowledge of the surface conditions over Martian history. For example, if we assume relatively dilute solutions then the minimum temperature for the existence of liquid water will be slightly below 0°C. If we assume briny conditions, which allow aqueous solutions to exist at much lower temperatures (which would result in a much longer lifetime), the activity of water would be lower, perhaps too low to be tolerated by organisms (Knoll and Grotzinger, 2006). Regardless of what physiochemical conditions that we postulate for early Martian history, we can now propose a scenario and ask, “Is it reasonable to expect that life could have originated in this time frame?”

3.5 REFERENCES

Bandfield, J.L., Hamilton, V.E., and Christensen, P.R. (2000) A Global View of Martian Surface Compositions from MGS-TES. Science, 287, 1626-1630.

Barrat, J.A., Jambon, A., Bohn, M., Gillet, P., Sautter, V., Gopel, C., Lesourd, M., and Keller, F. (2002) The picritic shergottite north west Africa 1068 (NWA 1068 or "Louise Michel"). Luner and Planetary Science Conference XXXIII, abstract #1538.

Bibring, J.-P., Langevin, Y., Gendrin, A., Gondet, B., Poulet, F., Berthe, M., Soufflot, A., Arvidson, R., Mangold, N., Mustard, J., Drossart, P., and team, t.O. (2005) Mars Surface Diversity as Revealed by the Omega/Mars Express Observations. Science, 307, 1576-1581.

Blum, A.E., and Lasaga, A.C. (1988) Role of surface speciation in the low-temperature dissolution of minerals. Nature, 331, 431-433.

Carr, M.H. (1996) Water on Mars. 229 p. Oxford University press, New York, New York.

Christensen, P.R., Bandfield, J.L., Clark, R.N., Edgett, K.S., Hamilton, V.E., Hoefen, T., Kieffer, H.H., Kuzmin, R.O., Lane, M.D., Malin, M.C., Morris, R.V., Pearl, J.C., Pearson, R., Roush, T.L., Ruff, S.W., and Smith, M.D. (2000) Detection of crystalline hematite mineralization on Mars by the Thermal Emission Spectrometer: Evidence for near-surface water. Journal of Geophysical Research, 105(E4), 9623-9642.

Christensen, P.R., Wyatt, M.B., Glotch, T.D., Rogers, A.D., Anwar, S., Arvidson, R.E., Bandfield, J.L., Blaney, D.L., Budney, C., Calvin, W.M., Fallacaro, A., Fergason, R.L., Gorelick, N., Graff, T.G., Hamilton, V.E., Hayes, A.G., Johnson, J.R., Knudson, A.T., McSween Jr., H.Y., Mehall, G.L., Mehall, L.K., Moersch, J.E., Morris, R.V., Smith, M.D., Squyres, S.W., Ruff, S.W., and Wolff, M.J. (2004) Mineralogy at Meridiani Planun from the Mini-TES Experiment on the Opportunity Rover. Science, 306, 1733-1739.

Clark, B.C., Morris, R.V., McLennan, S.M., Gellert, R., Jolliff, B.L., Knoll, A.H., Squyres, S.W., Lowenstein, T.K., Ming, D.W., Tosca, N.J., Yen, A., Christensen, P.R., Gorevan, S., Bruckner, J., Calvin, W., Dreibus, G., Farrand, W., Klingelhofer, G., Waenke, H., Zipfel, J., Berthe, M., Grotzinger, J., McSween, H.Y., and Rieder, R. (2005) Chemistry and mineralogy of outcrops at Meridiani Planum. Earth and Planetary Science Letters, 240, 73-94.

Golubev, S.V., Pokrovsky, O.S., and Schott, J. (2005) Experimental determination of the effect of dissolved CO_2 on the dissolution kinetics of Mg and Ca silicates at 25 C. Chemical Geology(217), 227-238.

Grandstaff, D.E. (1986) The dissolution rate of forsteritic olivine from Hawaiian beach sand. In S.M. Colman, and D.P. Dethier, Eds. Rates of Chemical Weathering of Rocks and Minerals, p. 41-59. Academic Press, Orlando, Florida.

Hamilton, V.E., and Christensen, P.C. (2005) Evidence for extensive olivine-rich bedrock in Nili Fossae, Mars. Geology, 33(6), 433-436.

Jonckbloedt, R.C.L. (1998) Olivine dissolution in sulfuric acid at elevated temperatures-implications for the olivine process, an alternative waste acid neutralizing process. Journal of Geochemical Exploration, 62, 337-346.

Klingelhofer, G., Morris, R.V., Bernhardt, B., Schroder, C., Rodionov, D.S., de Souza Jr., P.A., Yen, A., Gellert, R., Evlanov, E.N., Zubkov, B., Foh, J., Bonnes, U., Kankeleit, E., Gutlich, P., Ming, D.W., Renz, F., Wdowiak, T., Squyres, S.W., and Arvidson, R.E. (2004) Jarosite and Hematite at Meridiani Planum from Opportunity's Mossbauer Spectrometer. Science, 306, 1740-1745.

Knoll, A.H., Carr, M., Clark, B., DesMarais, D.J., Farmer, J.D., Fischer, W.W., Grotzinger, J.P., McLennan, S.M., Malin, M., Schroder, C., Squyres, S., Tosca, N.J., and Wdowiak, T. (2005) An astrobiological perspective on Meridiani Planum. Earth and Planetary Science Letters, 240, 179-189.

Knoll, A.H., and Grotzinger, J. (2006) Water on Mars and the Prospect of Martian Life. Elements, 2, 169-173.

Koeppen, W.C., and Hamilton, V.E. (2006) The distribution and composition of olivine on Mars. Luner and Planetary Science Conference XXXVII, abstract #1964.

Kowalewski, M., and Rimstidt, J.D. (2003) Average lifetime and age spectra of detrital grains: Toward a unifying theory of sedimentary grains. Journal of Geology, 111.

Kuebler, K.E., Wang, A., Haskin, L.A., and Joliff, B.L. (2003) A study of olivine alteration to iddingsite using Raman spectroscopy. Luner and Planetary Science Conference XXXIV, abstract #2086.

Langmuir, D. (1997) Aqueous Environmental Geochemistry. Prentice-Hall, Inc., Upper Saddle River, New Jersey.

Lasaga, A.C. (1998) Kinetic Theory in the Earth Sciences 728 p. Princeton University Press Princeton, New Jersey.

Leshin, L.A., and Vicenzi, E. (2006) Aqueous Processes Recorded by Martian Meteorites: Analyzing Martian Water on Earth. Elements, 2(3), 157-162.

Luce, R.W., Bartlett, R.W., and Parks, G.W. (1972) Dissolution kinetics of magnesium silicates. Geochimica et Cosmochimica Acta, 36, 35-50.

Madden, M.E.E., Bodnar, R.J., and Rimstidt, J.D. (2004) Jarosite as an indicator of water-limited chemical weathering on Mars. Nature, 431, 821-823.

McSween Jr., H.Y., Grove, T.L., and Wyatt, M.B. (2003) Constraints on the composition and petrogenesis of the Martian crust Journal of Geophysical Research, 108, E12, 5135, doi:10.1029/2003JE002175.

Mustard, J.F., Poulet, F., Gendrin, A., Bibring, J.-P., Langevin, Y., Gondet, B., Mangold, N., Bellucci, G., and Altieri, F. (2005) Olivine and Pyroxene Diversity in the Crust of Mars. Science, 307, 1594-1597.

Oelkers, E.H. (2001) An experimental study of forsterite dissolution rates as a function of temperature and aqueous Mg and Si concentrations. Chemical Geology, 175, 485-494.

Pokrovsky, O.S., and Schott, J. (2000a) Forsterite surface composition in aqueous solutions: A combined potentiometric, electrokinetic, and spectroscopic approach. Geochimica et Cosmochimica Acta, 64(19), 3299-3312.

-. (2000b) Kinetics and mechanism of forsterite dissolution at 25 C and pH from 1 to 12. Geochimica et Cosmochimica Acta, 64(19), 3313-3325.

Rimstidt, J.D., Rosso, J.J., Weissbart, E.J., Hatfield, J., and Skinner, K.L. (1996) Factors affecting mineral dissolution rate measurements. Geological Society of America 28th Annual Meeting, 28, p. 145, Denver, Colorado.

Rogers, A.D., Christensen, P.C., and Bandfield, J.L. (2005) Compositional heterogeneity of the ancient Martian crust: Analysis of Ares Vallis bedrock with THEMIS and TES data. Journal of Geophysical Research, Vol. 110, E05010, doi:10.1029/2005JE002399.

Rosso, J.J., and Rimstidt, J.D. (2000) A high resolution study of forsterite dissolution rates. Geochimica et Cosmochimica Acta, 64, 797-811.

Shuster, D.L., and Weiss, B.P. (2005) Martian Surface Paleotemperatures from Thermochronology of Meteorites. Science, 309, 594-597.

Siegel, D.I., and Pfannkuch, H.O. (1984) Silicate mineral dissolution at pH 4 and near standard temperature and pressure. Geochimica et Cosmochimica Acta, 48, 197-201.

Smith, M.D., Wolff, M.J., Lemmon, M.T., Spanovich, N., Banfield, D., Budney, C.J., Clancy, R.T., Ghosh, A., Landis, G.A., Smith, P., Whitney, B., Christensen, P.R., and Squyres, S.W. (2004) First Atmospheric Science Results from the Mars Exploration Rovers Mini-TES. Science, 306, 1750-1753.

Squyres, S.W., Grotzinger, J.P., Arvidson, R.E., Bell III, J.F., Calvin, W., Christensen, P.R., Clark, B.C., Crisp, J.A., Farrand, W.H., Herkenhoff, K.E., Johnson, J.R., Klingelhofer, G., Knoll, A.H., McLennan, S.M., McSween Jr., H.Y., Morris, R.V., Rice Jr., J.W., Rieder, R., and Soderblom, L.A. (2004) In Situ Evidence for an Ancient Aqueous Environment at Meridiani Planum, Mars. Science, 306, 1709-1714.

Squyres, S.W., and Knoll, A.H. (2005) Sedimentary Geology at Meridiani Planum, Mars. Earth and Planetary Science Letters, 240(1), 1-190.

Squyres, S.W., Knoll, A.H., Arvidson, R.E., Clark, B.C., Grotzinger, J.P., Jolliff, B.L., McLennan, S.M., Tosca, N., Bell III, J.F., Calvin, W.M., Farrand, W.H., Glotch, T.D., Golombek, M.P., Herkenhoff, K.E., Johnson, J.R., Klingelhofer, G., McSween, H.Y., and Yen, A.S. (2006) Two Years at Meridiani Planum: Results from the Opportunity Rover. Science, 313, 1403-1407.

Stefansson, A., and Gislason, S.R. (2001) Chemical Weathering of Basalts, Southwest Iceland: Effect of Rock Crystallinity and Secondary Minerals on Chemical Fluxes to the Ocean. American Journal of Science, 301, 513-556.

Stopar, J.D., Taylor, G.J., Hamiliton, V.E., and Browning, L. (2006) Kinetic model of olivine dissolution and extent of aqueous alteration on Mars. Geochimica et Cosmochimica Acta, in press.

Taylor, J.R. (1982) An Introduction to Error Analysis: The Study of Uncertainities in Physical Measurements. 270 p. University Science Books, Mill Valley, CA.

Van Herk, J., Pietersen, H.S., and Schuiling, R.D. (1989) Neutralization of industrial waste acids with olivine- The dissolution of forsteritic olivine at 40-70°C. Chemical Geology, 76, 341-352.

Velbel, M.A. (1986) Influence of surface area, surface characteristics, and solution composition on feldspar weathering rates. In J.A. Davis, and K.F. Hayes, Eds. ACS Symposium Series No. 323, *Geochemical Processes at Mineral Surfaces*, p. 615-634.

-. (1993) Constancy of siliciate-mineral weathering-rate ratios between natural and experimental weathering: implications for hydrologic control of differences in absolute rates. Chemical Geology, 105, 89-99.
Wang, A., Kubler, K., Jolliff, B., and Haskin, L.A. (2004) Mineralogy of a Martian meteorite as determined by Raman spectroscopy. Journal of Raman Spectroscopy, 35, 504-514.
Weissbart, E.J., and Rimstidt, J.D. (2000) Wollastonite: Incongruent dissolution and leached layer formation. Geochimica et Cosmochimica Acta, 64, 4007-4016.
Westrich, H.R., Cygan, R.T., Casey, W.H., Zemitis, C., and Arnold, G.W. (1993) The dissolution kinetics of mixed-cation orthosilicate minerals. American Journal of Science, 293(November 1993), 869-893.
White, A.F., and Brantley, S.L. (2003) The effect of time on the weathering of silicate minerals: why do weathering rates differ in the laboratory and field? Chemical Geology, 202, 479-506.
Wilson, M.J. (2004) Weathering of the primary rock forming minerals: processes, products, and rates. Clay Minerals, 39, 233-266.
Wogelius, R.A., and Walther, J.V. (1991) Olivine dissolution at 25C: Effects of pH, CO2, and organic acids. Geochimica et Cosmochimica Acta, 55(4), 943-954.
-. (1992) Olivine dissolution kinetics at near-surface conditions. Chemical Geology, 97, 101-112.
Yen, A.S., Gellert, R., Schroder, C., Morris, R.V., Bell III, J.F., Knudson, A.T., Clark, B.C., Ming, D.W., Crisp, J.A., Arvidson, R.E., Blaney, D.L., Bruckner, J., Christensen, P.R., DesMarais, D.J., De Souza Jr., P.A., Economou, T.E., Ghosh, A., Hahn, B.C., Herkenhoff, K.E., Haskin, L.A., Hurowitz, J.A., Joliff, B.L., Johnson, J.R., Klingelhofer, G., Madsen, M.B., McLennan, S.M., McSween Jr., H.Y., Richter, L., Rieder, R., Rodionov, D., Soderblom, L., Squyres, S.W., Tosca, N.J., Wang, A., Wyatt, M., and Zipfel, J. (2005) An integrated view of the chemistry and mineralogy of martian soils. Nature, 436, 49-54.

CHAPTER 4: FORSTERITE DISSOLUTION RATE: THE EFFECT OF IONIC STRENGTH, AQUEOUS MAGNESIUM, AQUEOUS SULFATE, ACTIVITY OF WATER, PH, TEMPERATURE, AND SURFACE AREA

4.1 ABSTRACT

Eighty-two batch reactor experiments from 1 < pH < 4 in magnesium sulfate, sodium sulfate, magnesium nitrate solutions, and potassium nitrate solutions show that ionic strength up to 12 m, log m_{Mg} up to 4 m, and log m_{SO4} up to 3 m have no effect on forsterite dissolution rates. However, decreasing the water activity slows forsterite dissolution rates by a small amount. The effect of decreasing dissolution rates with decreasing a_{H2O} is consistent with the idea that water acts as a ligand that participates in the dissolution process.

Forsterite dissolution rate data from 14 previously published studies were combined with results from our experiments to produce 572 data that were analyzed using multiple linear regression to produce rate laws in terms of both BET and geometric surface areas. For pH < 5.05

$$r_{BET} = 1.00 \times 10^{5} \left(e^{\frac{-68550}{RT}} \right) a_{H^+}^{0.48} \qquad \text{or} \qquad r_{geo} = 1.10 \times 10^{6} \left(e^{\frac{-69715}{RT}} \right) a_{H^+}^{0.50}$$

and for pH > 5.05

$$r_{BET} = 32.36 \left(e^{\frac{-55084}{RT}} \right) a_{H^+}^{0.22} \qquad \text{or} \qquad r_{geo} = 759 \left(e^{\frac{-58924}{RT}} \right) a_{H^+}^{0.24}$$

The change in n_{H+} from 0.48 to 0.22 at pH 5.05 appears to reflect a change in the reaction mechanism. This change is near the pH at which the surface composition changes from being Mg-enriched to Si-enriched. Rate models based on BET and geometric surface areas fit the data equally well; however, rates predicted using geometric surface areas

were about five times faster than those predicted using BET surface areas on a mol/$m_2$sec basis. It is important to recognize that geometric surface areas should be used in models based on grain geometry such as the shrinking particle model and our mineral lifetime diagram.

4.2 INTRODUCTION

Table of Notation 4

a_i	activity of species i
A	pre-exponential factor
A_{BET}	BET surface area (m^2/g)
A_{geo}	geometric surface area (m^2/g)
d	grain diameter (m)
E_a	activation energy (kJ/mol)
I	ionic strength (molal)
k	rate constant
m	molality (m)
M	mass of solution at sample time (g)
M_0	initial mass of solution (g)
M_{fo}	mass of forsterite grains (g)
$m_{i,c}$	corrected concentration for species i (molal)
m_i	concentration of species i (molal)
n	number of data
n_i	reaction order of species i
ρ	density (g/m^2)
R	gas constant (8.314 $kJK^{-1}mol^{-1}$)
r'	apparent rate (molal/sec)
r	total rate of olivine destruction (mol/m^2sec)
T	temperature (K)
v	number of ions
W_a	molecular weight of water
$\sigma_{\bar{x}}$	standard error of the mean
σ	standard deviation of the sample
ϕ	osmotic coefficient

4.2.1 Forsterite as a model silicate mineral

Chemical weathering of silicate minerals is a vital earth surface geochemical process. Silicate minerals make up 92 percent of Earth's crust and are sufficiently

reactive that their dissolution controls the chemistry of soils, groundwaters, surface waters, and the atmosphere, which means that we can only understand earth surface geochemistry within the framework of our understanding of the silicate mineral dissolution process.

Olivine provides an excellent model system to test ideas about silicate dissolution. Olivine is an orthosilicate, which has no Si-O-Si bonds, so its dissolution mechanism is relatively simple compared to other silicate minerals where slow breaking of Si-O-Si bonds causes development of complex leached layers. Of the olivine minerals, most previous studies have reported dissolution rates for forsterite (Mg_2SiO_4) as a function of *pH,* temperature, organic ligands, etc., giving us a large database that can be summarized into a comprehensive rate law.

4.2.2 Importance of large data sets

Although the published dissolution rate data for forsterite dissolution are extensive, each study was designed to test the effect of one, or at most a few, variables on the rate. These studies provide an excellent foundation for building a more comprehensive rate model. However, the relatively small number of data in each study limits the reliability of derived values of E_a and n_{H+} in the rate laws. For example, reported values of activation energy and reaction orders for H^+ from these studies vary widely (Table 4.1). In small data sets, the effect of each datum is much greater than in a large data set, so that spurious data or data with large random errors can significantly distort estimates of regression coefficients. This is because the standard error of these estimated values, σ_p, is related to the standard deviation of the measured rates, σ_r, by the expression

$$\sigma_p = \frac{\sigma_r}{\sqrt{n}} \qquad (4.1)$$

where n is the number of observations (WAINER, 2007). Because dissolution rate measurements generally show significant scatter (we estimate ±0.3 log units for a typical standard deviation), the standard errors of derived E_a and n_{H+} based on only a few data are generally quite large. In order to decrease the standard error, the sample size must be increased. This can be done by pooling data from many studies to form a very large data

set with a large number of data. Of course, regression models assume only random error and do not reflect the accuracy of the model.

We have compiled 572 published rate data for forsterite dissolution rates from all available published studies (Table 4.1, Appendix 4.2). In addition to those data, experiments described in this paper contribute 83 data to this pooled set. We used this large pooled data set to develop a rate law for forsterite dissolution as a function of *pH*, temperature, and ionic strengths at *pH* 1-12.

Large data sets allow investigation of some fundamental problems that are difficult to test with directed experimental designs. The problem of "reactive surface area" is a good example. Although there is widespread agreement that silicate mineral dissolution reaction rates are proportional to the interfacial area between the solid and solution, there are problems with determining the proportionality constant, k (mol/m^{2}sec), because both the surface area and surface reactivity change with extent of reaction (i.e. time) (GAUTIER et al., 2001; GRANDSTAFF, 1978). The changing reactivity has been attributed to changing "reactive surface area" but this term does not actually explain what causes the reactivity to change. This problem is further complicated by the fractal nature of dissolving mineral surfaces which makes the BET-measured surface area not only different from adsorbate gas to adsorbate gas but also different from the surface area estimated from particle size (geometric surface area) (BRANTLEY and MELLOTT, 2000). Because many geochemical models, e.g. the shrinking particle model or the mineral lifetime diagram, use geometric surface area, we need to understand how these surface area measurements relate and what they mean regarding mineral reactivity.

Table 4.1. Summary of experimental conditions for previous forsterite dissolution studies used in this paper. Values for nH+ were calculated for pH < 8. Information marked NA was not analyzed. A_{BET} for this study and (OLSEN and RIMSTIDT, in review) were calculated using an empirical equation from (BRANTLEY and MELLOTT, 2000).

Reference	X_{Fo}	d,µm	A_{geo}, m^2/g	A_{BET}, m^2/g	Exp Type	n	RPV	pH	n_{H+}	T,°C	E_a, kJ/ mole
BAILEY (1976)	92	105-149	0.010	NA	BR	14	Mg, Si	4		25-65	50.2
BLUM and LASAGA (1988)	93	290-410	0.005	0.029		18	Mg, Si	1.8-11.4		25	
CHEN and BRANTLEY (2000)	91	75-150	0.017	0.034	pH-stat	16	Mg, Si	2-5	0.70	65	125
GOLUBEV et al. (2005)	100 91	50-100 50-100	0.025 0.025	0.107 0.059	MFR	32	Mg, Si	2-11.5		25	
GRANDSTAFF (1986)	82	74-149	0.017	0.93	pH-stat	29	Mg, Si	3-5	1.00	1-49	38.1
HÄNCHEN et al.(2006)	91	90-180	0.014	0.0797	MFR	44	Mg, Si	2-12.5	0.46	90-150	52.9
LUCE et al.(1972a)	91	74-149	0.017	0.0445	BR	6	Mg, Si	1.7-9.6		25	
OELKERS (2001)	89	50-100	0.025	0.0808	MFR	26	Mg, Si	2		25-65	63.8
OLSEN and RIMSTIDT (in review)	92	250-350	0.006	0.0528	BR	36	Si	1-5	0.46	25	
OLSEN and RIMSTIDT (this study)	92	250-350	0.006	0.0528	BR	47	Si	1-5	0.52	25	
POKROVSKY and SCHOTT (2000b)	91	50-100	0.025	0.0808	MFR	106	Mg, Si	1-11	0.50	25	
ROSSO and RIMSTIDT (2000)	92	250-350	0.006	0.0356	MFR	253	Mg, Si	1.8-4	0.50	25-45	42.6
SIEGEL and PFANNKUCH (1984)		38-42	0.046	1.3	BR	1	Mg, Si	4		22	
VAN HERK et al.(1989)	92	105-125	0.016	0.63	pH-stat	12	Mg, Si	1-3		40-70	30
WOGELIUS and WALTHER (1991b)	100 91	250-420 149-250		0.0307 0.0598	BR, MFR	34	Mg, Si	3.1-12.2	0.54	25	
WOGELIUS and WALTHER (1992)	96	250-420		0.0307	BR, MFR		Mg, Si	1.8-9.8		65	79.5

4.2.3 Effect of salinity on rate

Although most natural waters have a relatively low ionic strength, minerals are often exposed to saline to hypersaline conditions in arid settings. Surprisingly, there is very little information about the effect of salinity on mineral dissolution rates (GLEDHILL and MORSE, 2004; VOGELSBERGER et al., 1999). One particular environment of interest is weathering on Mars, where highly concentrated brines have been proposed. Additionally, the dissolution of olivine in high ionic strength solutions can occur in many industrial applications. Olivine has been proposed as a mineral that could be used to sequester carbon dioxide by reacting with CO_2 to form magnesite. Also, olivine can be used to neutralize waste acids from industrial processes (SCHUILING et al., 1986; VAN HERK et al., 1989). These waste acid solutions could contain high concentrations of dissolved salts that might affect the dissolution rate. Salinity might affect dissolution rates in two ways: by increasing the ionic strength of the solution, which might change the activity coefficient of the activated complex, or by decreasing the activity of water in the solution, which might reduce its participation in the activated complex.

Studies of the effect of salinity on dissolution rates have not always differentiated the effect of ions that participate in the activated complex from the effect of non-participatory ions. Several previous studies have showed a direct effect of some cations on silica dissolution rates. Among studies of the effects of salts with ions that participate directly in the dissolution reaction, ICENHOWER and DOVE (2000) showed that quartz dissolution rates increase by a factor of 21 times in 0.05 m NaCl solutions, but that dissolution rates become roughly constant at concentrations above about 0.10 m NaCl. MOGOLLON et al. (2000) found that Na^+, K^+, Mg^{2+}, and Ca^{2+} have no effect on boehmite dissolution rate, while monovalent anions decrease dissolution rate and sulfate increases the dissolution rate. STILLINGS and BRANTLEY (1995) showed that dissolution rates of feldspar powders of compositions ranging from An_0 to An_{76} decreased by 1.5 to 7 times in solutions containing NaCl and $(CH_3)NCl$. VOGELSBERGER et al. (1999) showed that for $0.001 < I < 0.1$, increasing ionic strength increases silica dissolution rates at 40° C, but this probably reflects the direct participation of cations in the activated complex as documented by ICENHOWER and DOVE (2000). Only one study (GLEDHILL and MORSE,

2004) examined the effect of high salinity brines on mineral dissolution where there is no evidence that ions participated in the reaction; they found that calcite dissolution rates were not significantly affected by ionic strength up to 4.4 m.

4.3 METHODS

4.3.1 Salinity experiments

4.3.1.1 Materials

We used forsteritic (Fo92) olivine from Aimcor Mine, Green Mountain, NC, USA, for all experiments. For a detailed description of this material, see ROSSO and RIMSTIDT (2000). The olivine was crushed and sieved and the 45-60 mesh size (250-350 μm) was retained. Because the olivine grains were coated with a small amount of talc, they were pretreated by sonicating in 1 m HNO_3 10 times for 1 minute each time, followed by soaking in 6 m HNO_3 overnight to remove as much talc as possible prior to the experiments. In addition to removing the talc, this pretreatment provided a silica-rich surface on which to conduct our experiments, which meant that initial dissolution was stoichiometric. For a detailed discussion of this pretreatment method see (OLSEN and RIMSTIDT, in review). Because grains of this size are near the limit for reliable BET surface area analysis, we chose to normalize our reaction rates using a surface area of 0.0528 m^2/g based on the empirical equation from BRANTLEY and MELLOTT (2000), which is comparable to surface areas for grains of this diameter in other olivine studies.

4.3.1.2 Experimental methods

Forty-seven batch reactor experiments were run over a pH range of 2 to 4 in magnesium sulfate, sodium sulfate, and magnesium nitrate solutions. Additionally, thirty-five experiments had previously been run over the *pH* range of 1 to 4 in potassium nitrate solutions (OLSEN and RIMSTIDT, in review). Each experiment consisted of 5 or 10 grams of forsterite and 100 mL of solution in a 250 mL Erlenmeyer flask immersed in a shaker bath set at 25ºC. Solutions were made using magnesium and sodium sulfate and magnesium and potassium nitrate to adjust the ionic strength. Sulfuric acid and nitric

acid were used to adjust the pH. Ionic strengths ranged from 0.27 m to 11.98 m. Approximately 6 mL of solution was collected every 20 minutes over the 2 hour duration of each experiment. For some experiments, samples were taken every 30 minutes for 3 hours in order to obtain a larger Si concentration for analysis. Because magnesium sulfate and magnesium nitrate solutions contained high concentrations of magnesium, magnesium release data were not collected and only silica release rates were used to determine rates. Silica concentrations were determined using the molybdate blue colorimetric method (GOVETT, 1961).

4.3.1.3 Correction for sample withdrawal

Because approximately 6 mL of solution was sampled every twenty minutes over the course of each experiment, it was necessary to correct for the changing surface area to mass ratio so that the data could be analyzed as an ideal batch reactor experiment. To find the corrected concentration, we summed the change in concentration over each time interval multiplied by the mass of solution present at the time of sampling and then divided this product by the mass of solution present at the beginning of the experiment.

$$m_{i,c} = \frac{\sum_{i=1}^{n} \Delta m(i) M(i)}{M_0} \quad (4.2)$$

This approach was used in OLSEN and RIMSTIDT (in review). This adjusted the sample concentration downward by 2 to 25 percent.

4.3.1.4 Initial rate method

Six concentration versus time data were collected for silica from each experiment. Data were analyzed using the initial rate method where the concentration versus time data were fit by linear regression and the apparent rate (r', molal/sec) was taken as the slope of the regression line. The apparent rate was converted to the rate of forsterite destruction using the relationship:

$$r = \frac{r' M}{A}. \quad (4.3)$$

These rates were used in subsequent regression models.

4.3.1.5 Calculation of a_w

Water activity was calculated using the equation

$$\ln a_w = -\frac{vmW_A}{1000}\phi \qquad (4.4)$$

(ROBINSON and STOKES, 2002). Osmotic coefficients were taken from empirical data for each solution chemistry from ROBINSON and STOKES (2002).

4.3.2 Pooled data set

4.3.2.1 Data selection and analysis procedures

Rate data were compiled from 14 published olivine dissolution studies (Table 4.1) to create a pooled data set. All data from previous studies are compiled in Appendix 4.2. Rate data for salinity experiments that had an a_{H2O} above 0.90 were also included in this data set. All dissolution rates were converted to have units of mol/m^{2}sec. Mg release rates were corrected for forsterite composition by dividing the rate by twice the mole fraction of forsterite. When both Si and Mg release rates were reported, those data were averaged. Data from (VAN HERK et al., 1989) were reanalyzed using a shrinking particle model taken from (BURKIN, 2001), which allowed us to obtain a dissolution rate for particles that dissolved completely over the course of an experiment. This pooled data set covers the pH range of approximately 1 to 12.

Data were analyzed using the JMP statistical software program version 5.1.2, produced by the SAS Institute Inc., of Cary, North Carolina. We chose a *p*-value of less than 0.05 as the cut off for deciding that a regression coefficient is not statistically different from zero (OTT and LONGNECKER, 2001).

During the fitting process, Chauvenet's criterion was used to eliminate extreme outliers from the pooled data set. Chauvenet's criterion identifies outliers by calculating the number of points that would be expected to fall outside of a given number of standard deviations; if more data points than would be expected from random error fall outside of this range, they are rejected as likely caused by experimental blunders (TAYLOR, 1982).

4.3.2.2 Different reaction mechanisms

For data collected at 25°C, there is a break in the slope of the log *r* versus *pH* graph. This appears to be due to a change in reaction mechanism. To account for this, the low pH and high pH data were divided and analyzed separately. In order to determine more precisely where to locate the break in slope, we separated the 25°C data into low pH and high pH data sets at 0.5 pH unit intervals over the range of 3.5 and 8.5. Each data set was fit by linear regression to the expression $\log r = \log k + n \log a_{H^+}$ and the resulting lines were plotted to determine where they intersected. Figure 3.2 shows that if we separated the data into two subsets anywhere between pH 4.5 and pH 7.5 the resulting regression lines intersected between pH 4.4 and pH 5.6. For this reason, we used an average of these intersection points to choose a separation point of pH 5.05. Subsequently, the low pH and high pH data sets were each fit to the equation

$$\log r = \log A + \frac{E_a}{2.303R}\left(\frac{1}{T}\right) + \log a_{H^+} \qquad (4.5)$$

using multiple linear regression.

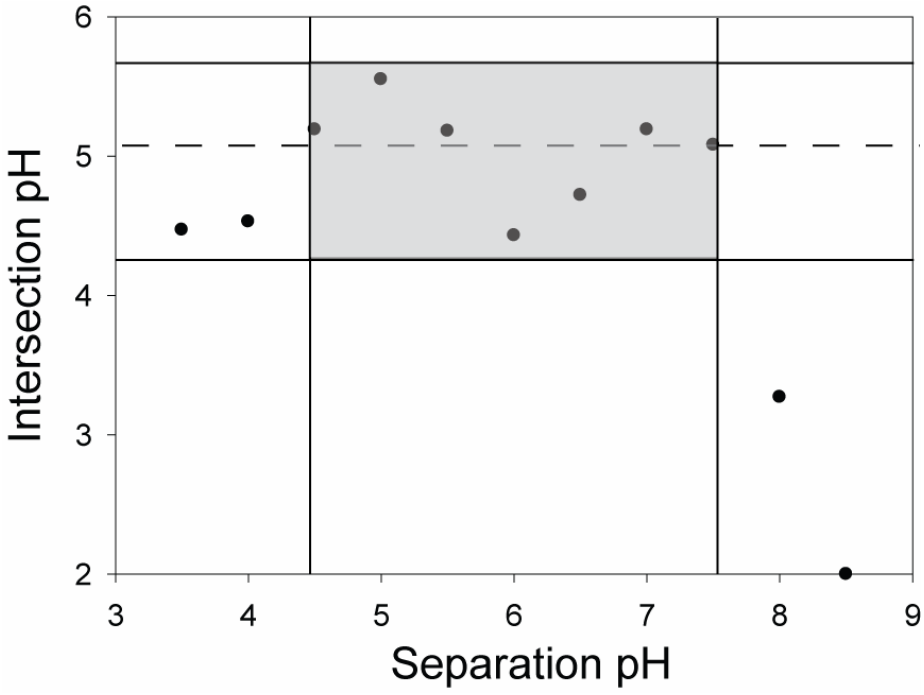

Figure 4.1. Relationship between the point of intersection of low and high pH regression models and the pH chosen to separate data set.

4.3.2.3 BET versus geometric comparison

One goal of this study was to decide whether a calculated geometric surface area based on grain diameter can more accurately describe the effect of surface area on rates than measured BET surface area. See BRANTLEY and MELLOTT (2000) for a discussion of this issue. We tested this using a subset of our pooled data set for which we had both BET surface area and grain size information. Geometric surfaces areas were calculated using the equation

$$A_{geo} = \frac{6}{\rho d} \qquad (4.6)$$

A range of grain sizes was used in each experiment, so an average geometric surface area was calculated. The area-averaged diameter, which is not the same as the arithmetic mean of the same size range, is given by

$$d_e = \frac{d_{\max} - d_{\min}}{\ln\left(\frac{d_{\max}}{d_{\min}}\right)} \qquad (4.7)$$

where d_e is the area-averaged diameter, d_{max} is the maximum grain diameter, and d_{min} is the minimum grain diameter (TESTER et al., 1994). Reported rates based on BET surface area were recast to the rates based on geometric surface area using the equation

$$r_{geo} = r_{BET}\left(\frac{A_{geo}}{A_{BET}}\right). \qquad (4.8)$$

We were not able to use some data sets listed in Table 4.1 because the grain size was not reported (WOGELIUS and WALTHER, 1991b; WOGELIUS and WALTHER, 1992) or because the data were analyzed using a shrinking particle model which is based solely on geometric surface areas (BAILEY, 1976; VAN HERK et al., 1989). However, data from these sources were used in subsequent regressions. A total of 534 data was used in this surface area comparison.

4.4 RESULTS

4.4.1 Salinity experiments

The results of all dissolution rate experiments in salt solutions are tabulated in Appendix 4.1 along with the solution chemistry and the variables (pH, $I^{0.5}$, a_{H2O}) that were used in the regression models.

4.4.1.1 Effect of ionic strength

We chose to use $I^{0.5}$ as the regression variable because there is a theoretical basis for a relationship between rate and $I^{0.5}$ for solution species (LAIDER, 1987; WILLIAMSON and RIMSTIDT, 1993). This approach was used previously in OLSEN and RIMSTIDT (in review). However, it has not been tested for reactions occurring on mineral surfaces. Regressing r versus I or log I produced similar regression models to $I^{0.5}$ and did not produce a better fit than $I^{0.5}$ in any of the regression models. Additionally, $I^{0.5}$ satisfies the mathematical requirement that as ionic strength declines to zero, $10^{I^{0.5}}$ becomes one.

The rate data for each salt (KNO_3, $Mg(NO_3)_2$, Na_2SO_4, and $MgSO_4$) was regressed separately using the model $\log r = \log a + bI^{0.5} + c \log pH$ in order to determine if the effect of ionic strength is different in different salt solutions. Then the data were pooled and regressed together using the same model. One datum with a negative rate was eliminated (Experiment MN9). We believe this negative rate was due to carry over of forsterite grains into the sample bottle which made the initial sample concentration higher than subsequent samples. Results of all regression models are included in Table 4.2.

Table 4.2. Results of regression models for ionic strength data sets used to test hypotheses about the effect of I, salt type, m_{Mg} and m_{SO4} on dissolution rates. Bold font represents p-values that are not statistically significant.

Data set R^2 n		Regression coefficient (std error)	*p*-value
$MgSO_4$	Intercept	-6.09(0.14)	<0.001
0.95	pH	-0.70(0.04)	<0.001
21	$I^{0.5}$	-0.10(0.03)	0.009
Na_2SO_4	Intercept	-6.51(0.12)	<0.001
0.98	pH	-0.53(0.03)	<0.001
9	$I^{0.5}$	-0.1(0.06)	**0.13**
$Mg(NO_3)_2$	Intercept	-7.31(0.30)	<0.001
0.61	pH	-0.38(0.08)	<0.001
17	$I^{0.5}$	**-0.1(0.06)**	**0.14**
KNO_3	Intercept	-7.09(0.07)	<0.001
0.96	pH	-0.48(0.02)	<0.001
35	**$I^{0.5}$**	0.12(0.05)	0.02
Combined data	Intercept	-6.82(0.08)	<0.001
0.87	pH	-0.52(0.02)	<0.001
82	log a_{H2O}	3.52(0.89)	<0.001
	$I^{0.5}$	0.01(0.03)	**0.66**
Combined data	Intercept	-6.81(0.07)	<0.001
0.87	pH	-0.52(0.02)	<0.001
82	log a_{H2O}	3.26(0.65)	<0.001
Magnesium	Intercept	-6.67(0.16)	<0.001
0.8	pH	-0.57(0.05)	<0.001
38	log a_{H2O}	3.56(1.11)	0.003
	log m_{Mg}	**0.05(0.10)**	**0.64**
Sulfate	Intercept	-6.32(0.12)	<0.001
0.94	pH	-0.64(0.03)	<0.001
30	log a_{H2O}	6.41(3.91)	0.11
	log m_{SO4}	**-0.07(0.10)**	**0.52**

These regression models showed that $I^{0.5}$ is not a significant predictor of log r in Na_2SO_4 and $Mg(NO_3)_2$ solutions. Regressions of $MgSO_4$ and KNO_3 solutions show that

that $I^{0.5}$ is a statistically significant predictor ($p < 0.05$) of *log r* in these cases, but the effect was very small (regression coefficients of -0.10 and +0.12 respectively).

4.4.1.2 Effect of a_{H2O}

Inspection of our data showed that changing salinity had essentially no effect on dissolution rates at low concentrations but did affect the rates at high concentrations. This suggests that although the rates are not strongly affected by *I*, they are affected by the reduced activity of water in briny solutions. Therefore, we regressed the combined data set against log a_{H2O} in order to determine if slowing of the reaction rate at high salinities was due to less H_2O being available to react with the mineral. Water activity was calculated from osmotic coefficients given in ROBINSON and STOKES (2002). This regression model (first "Combined data" row in Table 4.2) shows that when log a_{H2O}, $I^{0.5}$, and *pH* are included in a regression model, $I^{0.5}$ is no longer a significant predictor of rate ($p = 0.66$) but *log* a_{H2O} is. As a result of $I^{0.5}$ not being statistically significant it was dropped from a subsequent model, and a regression of *pH* and log a_{H2O} against log *r* for all 82 data produced (second "Combined data" row in Table 4.2)

$$\log r = -6.81(0.07) - 0.52(0.02)pH + 3.26(0.65)\log a_{H_2O} \qquad (4.9)$$

where the number in parenthesis is the standard error of the regression coefficient.

4.4.1.3 Effect of Mg^{2+}

POKROVSKY and SCHOTT (2000b) and ROSSO and RIMSTIDT (2000) reported that low concentrations of aqueous Mg had no effect on forsterite dissolution rates. This is not surprising because forsterite dissolution at low *pH* is very far from equilibrium (OLSEN and RIMSTIDT, in review). Our data allowed us to test the effect of very high concentrations of aqueous Mg (up to 4 m) on forsterite dissolution rates. Because m_{Mg} and $I^{0.5}$ are highly correlated in our experiments, we were unable to determine the effect of aqueous Mg in our preliminary regression models that included $I^{0.5}$. However, because the preliminary models showed that ionic strength does not affect forsterite dissolution rates, we eliminated it from subsequent models and regressed log *r* against *pH,* log a_w, and log m_{Mg}. This regression model included only experiments that were conducted in solutions that contained magnesium at the beginning of the experiment. This model

showed that log m_{Mg} is not a significant predictor (p = 0.64) of forsterite dissolution rate at concentrations up to 4 m (Table 4.2).

4.4.1.4 Effect of SO_4^{2-}

We were able to test the effect of sulfate on forsterite dissolution rates. Sulfate is one of the most common anions in natural waters. Additionally, it is likely that olivine on Mars has interacted with high salinity sulfate solutions and sulfate may have affected its weathering rate and lifetime (ARVINDSON et al., 2005). Sulfate concentration and ionic strength are strongly correlated in our data set (Table 4.2), but because our preliminary regression models showed that ionic strength does not significantly affect forsterite dissolution rates, we were able to regress all 30 experiments conducted in sulfate solutions versus pH, log a_w, and log m_{SO4}. That regression model shows that log m_{SO4} is not a significant predictor of rate (p = 0.52) when controlling for pH and log a_{H2O} (Table 4.2).

4.4.2 Analysis of the pooled data set

The pooled data set, based on data from sources listed in Table 4.1 and selected from the salinity data set, was used to test the relative merits of using Ageo in rate laws rather than ABET and to create very robust rate laws that take advantage of all published data.

4.4.2.1 A_{BET} versus A_{geo}

Regressions of both log r_{BET} and log r_{geo} versus pH and $1/T$ show similar results (Table 4.3). Both models have nearly identical R^2 values indicating that one model does not necessarily fit the data better than the other. In order to test whether or not the regression coefficients for the log r_{BET} and the log r_{geo} model are statistically different, we used the variances of the regression coefficients for pH and 1/T to calculate confidence intervals around the estimates from each model using the T-distribution. This test showed that the difference between the regression coefficients for both pH (p = 0.49 at pH < 5.05 and p = 0.99 at pH > 5.05) and $1/T$ (p = 0.57 at pH < 5.05 and p = 0.20 at pH > 5.05) in the two models are not significantly different than zero.

Table 4.3: Results of regressions for surface area comparison data set.

Data set R^2 n		Regression coefficient (std error)	*p*-value
BET low pH	Intercept	4.98(0.21)	<0.001
0.90	pH	-0.48(0.01)	<0.001
440	1/T	-3584(64)	<0.001
Geo low pH	Intercept	5.60(0.21)	<0.001
0.90	pH	-0.49(0.01)	<0.001
445	1/T	-3532(64)	<0.001
BET high pH	Intercept	1.43(0.51)	0.007
0.87	pH	-0.22(0.03)	<0.001
85	1/T	-2876(181)	<0.001
Geo high pH	Intercept	3.01(0.50)	<0.001
0.89	pH	-0.22(0.03)	<0.001
85	1/T	-3200(175)	<0.001

4.4.2.2 Regression results for pooled data set

Because of the conclusion that regressions based on A_{geo} and A_{BET} fit the data equally well, we created regression models for all data form the sources listed in Table 4.1. As stated earlier, either A_{geo} and A_{BET} was unavailable for some data sets so the number of data included in the A_{geo} and A_{BET} are different. Multiple linear regressions of log r versus pH and $1/T$ were performed for rates calculated using both BET and geometric surface areas to produce the regression models

$$\log r_{BET} = 5.00(0.21) - 0.48(0.01)pH - 3589(63)\frac{1}{T} \qquad (R^2=0.90,\ n = 444) \qquad (4.10)$$

$$\log r_{geo} = 6.04(0.22) - 0.50(0.01)pH - 3650(68)\frac{1}{T} \qquad (R^2=0.89,\ n = 460) \qquad (4.11)$$

at pH < 5.05 and

$$\log r_{BET} = 1.51(0.45) - 0.22(0.02)pH - 2884(158)\frac{1}{T} \qquad (R^2=0.89,\ n = 96) \qquad (4.12)$$

$$\log r_{geo} = 2.88(0.44) - 0.24(0.02)pH - 3085(155)\frac{1}{T} \qquad (R^2=0.92,\ n = 84) \qquad (4.13)$$

at pH > 5.05. Figures 4.2 and 4.3 show the leverage plots for these two models.

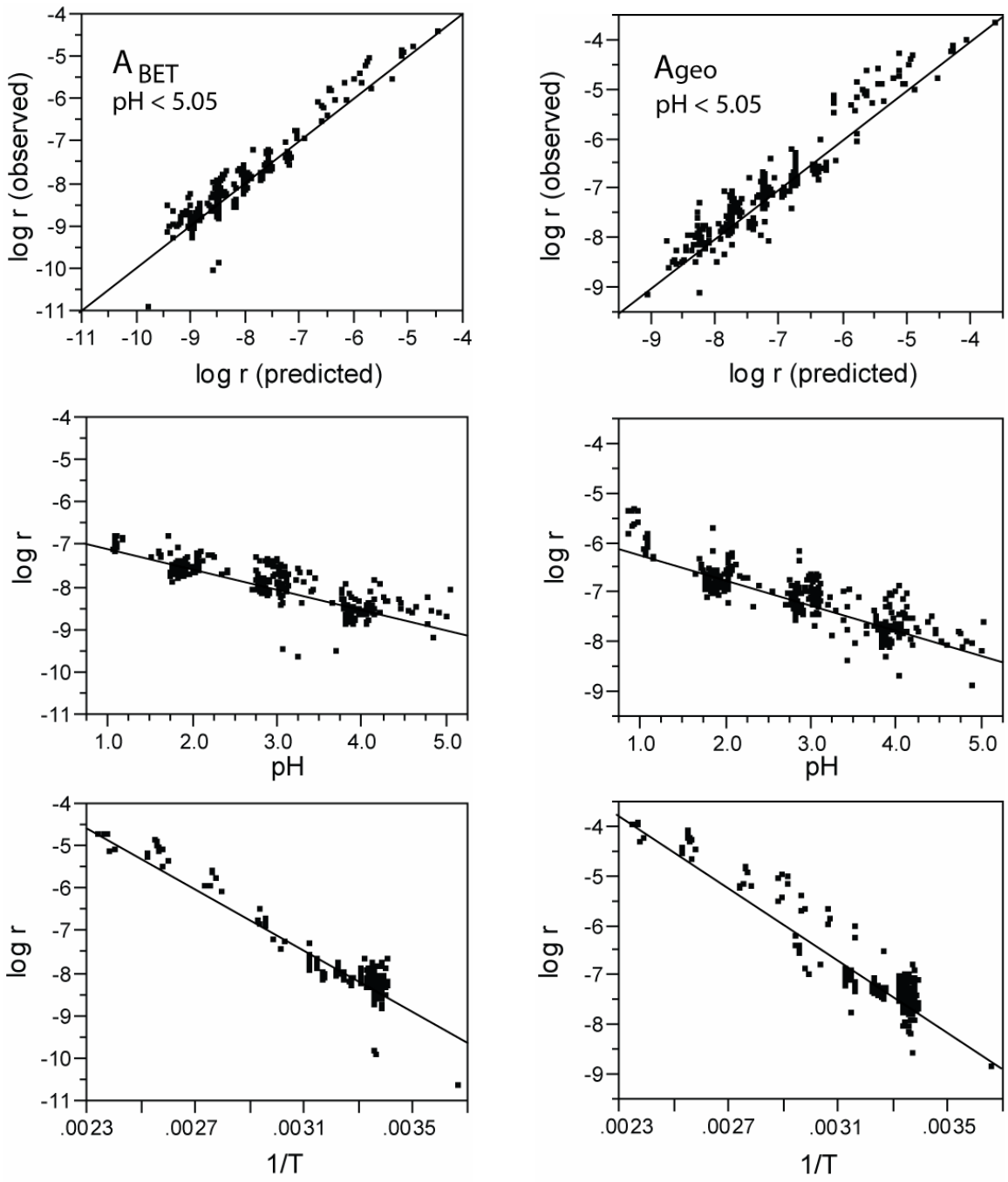

Figure 4.2. Results of the multiple linear regression model for rates for pH < 5.05 calculated from BET (left) and geometric (right) surface areas. The top graph shows predicted log *r* versus observed log *r*; The middle graph shows the effect of pH on log *r*; The bottom graph shows the effect of 1/*T* on log *r*. R^2, *n*, and *p*-values are included in Table 4.3.

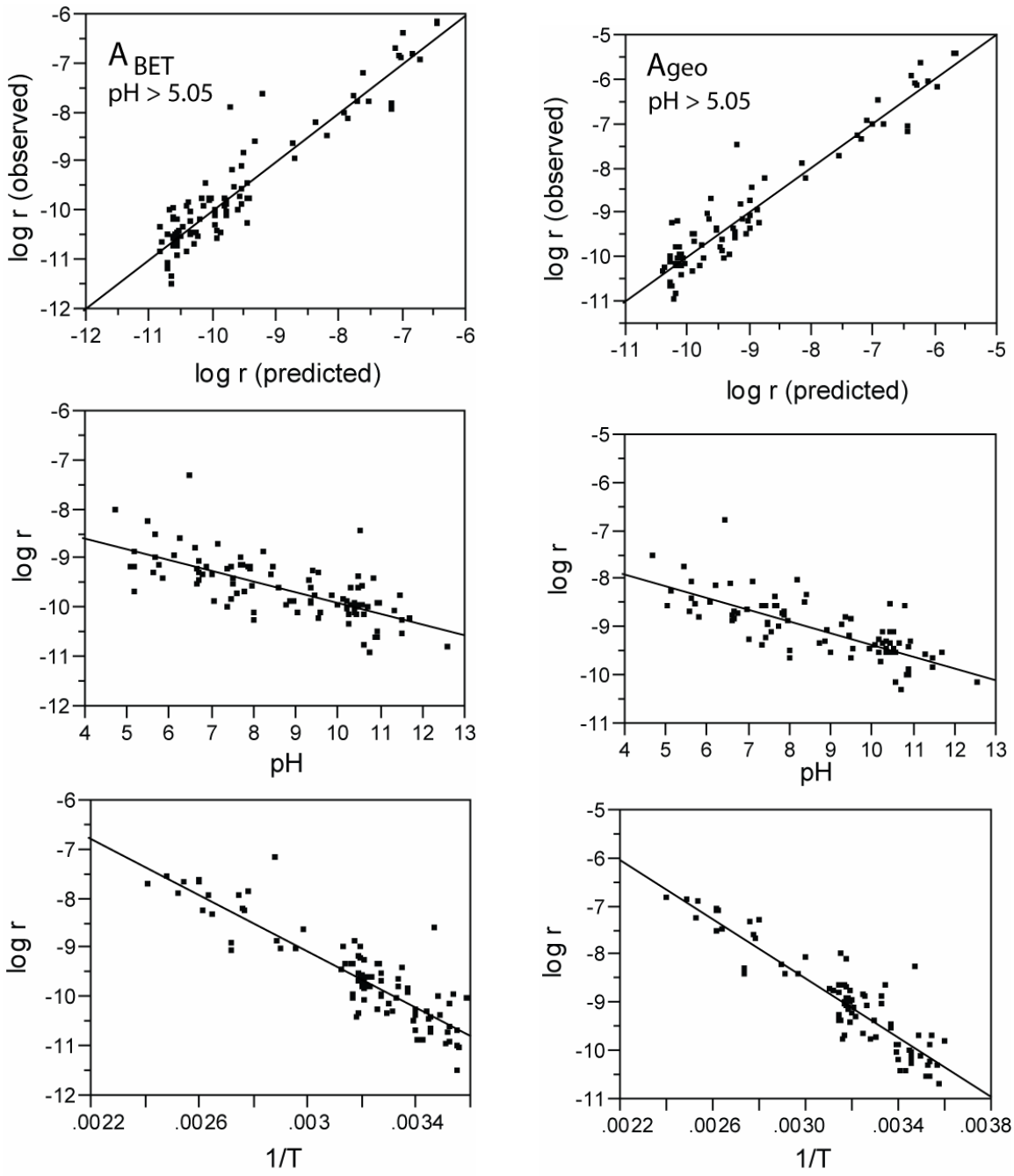

Figure 4.3. Results of the multiple linear regression model for rates calculated for pH > 5.05 from BET (left) and geometric (right) surface areas. The top graph shows predicted log *r* versus observed log *r*; The middle graph shows the effect of pH on log *r*; The bottom graph shows the effect of *1/T* on log *r*. R^2, *n*, and *p*-values are included in Table 4.3.

4.5 DISCUSSION AND CONCLUSIONS

4.5.1 Salinity

4.5.1.1 Effect of ionic strength, Mg^{2+} (aq), SO_4^{2-} (aq), and a_{H2O}

Previous studies have reported contradictory results regarding the effect of ionic strength on mineral dissolution kinetics. Our results (Table 4.2) show that ionic strength has no effect on forsterite dissolution at 25°C for $I \leq 12$ m. We interpret this to mean that the activity coefficient of the activated complex is unaffected by ions in solution. This could mean that the activated complex is unchanged or it could mean that the activated complex acts more like it is part of the solid that a part of the solution.

However, at high salinity, the rate decreases because of lower activity of water. It is important to note that the relationships between salt concentration and I and salt concentration and a_{H2O} are not the same (Figure 4.4). This effect is very small and will have little practical effect in most geologic environments. However, it does have important mechanistic implications. The reaction order of 3.26 (Table 4.2) for water suggests that multiple water molecules participate in the bond-breaking reaction for the rate-determining step. This result is consistent with less water being available to act as a ligand in the activated complex (OLSEN and RIMSTIDT, in review).

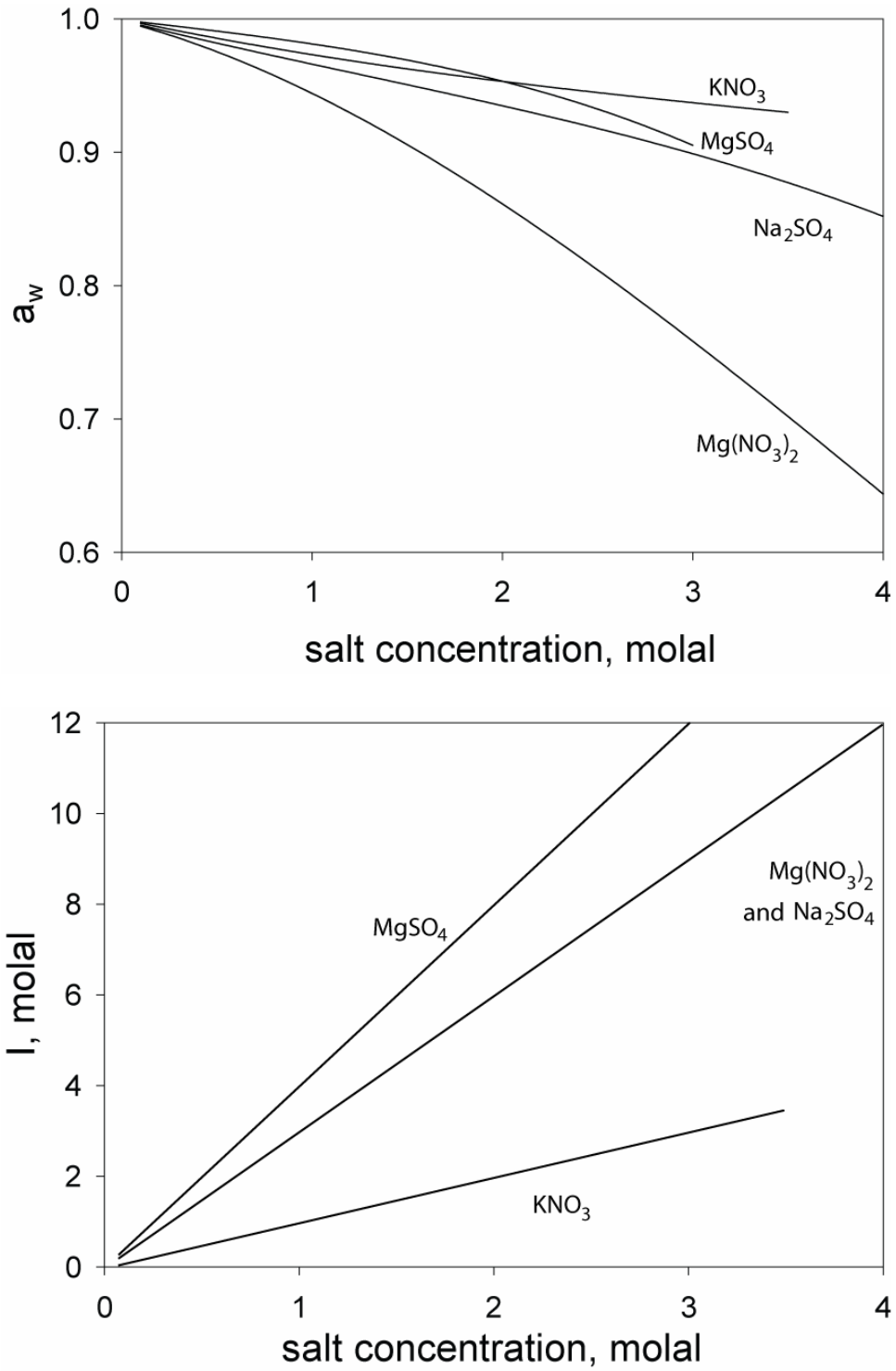

Figure 4.4. Relationship between salt concentration and a_{H2O} (top) and salt concentration and I (bottom) based on data from ROBINSON and STOKES (2002). Saturation concentration of $MgSO_4$ is approximately 3 m, Na_2SO_4 is approximately 4 m, $Mg(NO_3)_2$ is approximately 5 m, and KNO_3 is approximately 3.5 m.

Aqueous magnesium does affect on the dissolution rate of forsterite to m_{Mg} up to 4 m (Table 4.2). This is not surprising because the forsterite dissolution reaction is far from equilibrium. Even in our most Mg-rich experiments, $\Delta G_r = 10RT$, so all of our solutions were very undersaturated with respect to forsterite. Similarly, we found that aqueous sulfate up to 3 m does not have any effect on the dissolution rate of forsterite (Table 4.2).

4.5.1.2 Surface charge and dissolution rates

Several mineral dissolution models are based on the assumption that dissolution rates are controlled by the rate of ion transport through a double layer at the mineral surface. See BLESA et al. (1994) and GORICHEV and KIPRIYANOV (1984) for reviews of these models. These models assert that the dissolution rate is a function of surface potential as a reflection of the amount of work needed to transport the ions through the potential field adjacent to the mineral surface. Because surface potential is partly controlled by the ionic strength of the solution, these models would predict that the dissolution rate is a function of ionic strength. Our experiments clearly show that forsterite dissolution rates are not affected by changing ionic strength, and our results lead us to conclude that the fundamental assumption of the surface potential models is not valid for forsterite dissolution. This conclusion is consistent with the analysis of BLESA et al. (1994) who showed that ΔG for transferring an ion from the surface to the Stern plane is always below 30 kJ/mol for typical values of z and $\Delta\Psi$. However, the activation energy for forsterite dissolution at pH < 5.05 is around 69 kJ/mol (Table 4.2); therefore, the work needed for ion transport through the double layer is much less than the observed activation energy for forsterite dissolution. Our activation energy value along with the lack of salinity effect is more consistent with breaking chemical bonds in the mineral structure as the rate-determining step.

4.5.1.3 Geological and industrial relevance

High salinity solutions are routinely present in arid and hypersaline environments where they are known to cause physical disaggregation of rocks by a process known as salt weathering (DOEHNE, 2002; RIJNIERS et al., 2003; WINKLER and WILHEIM, 1970). Surprisingly little is known about the effect of salinity on chemical weathering. Our

results suggest that mineral dissolution rates in highly saline solutions may be slightly slower because of lower a_{H2O}. This is of particular interest with respect to the persistence of olivine grains on Mars, where the presence of jarosite (MADDEN et al., 2004) and magnesium sulfates (i.e. epsomite and kieserite (ARVINDSON et al., 2005)) is indicative of mineral precipitation from sulfate-bearing solutions. Our results suggest that very saline solutions might slow olivine dissolution rates slightly and thus slightly lengthen olivine lifetimes on Mars (OLSEN and RIMSTIDT, 2007).

High salinity solutions might also occur in mineral CO_2 sequestration process. Forsterite is often suggested as a mineral that could be reacted to trap CO_2 by the formation of magnesite (GIAMMAR et al., 2005). Forsterite is a good candidate for CO_2 sequestration because of its relatively quick dissolution rates and a relatively simple set of reactions that produce magnesium carbonate. To dissolve forsterite in large enough quantities to consume significant amounts of CO_2, high ionic strength solutions might be required. Our results suggest that high salinities of these solutions will have only a minor retardation effect on forsterite dissolution rates in sequestration processes.

SCHUILING et al. and VAN HERK et al. (1986; 1989) developed and patented a method to use olivine to neutralize waste acids produced by industrial processes. Waste acid streams are likely to contain significant concentrations of reaction byproducts, giving the solutions a high ionic strength. Our results show that at elevated salinities, the reduced activity of water can depress forsterite dissolution rates only slightly.

4.5.2 Pooled data set results

4.5.2.1 BET versus geometric surface area

We compared rates calculated using BET surface areas to rates calculated using geometric surface areas and found that, although the predicted r_{geo} in terms of mol/m^{2}sec are greater than the predicted r_{BET} by 5.6 times at *pH* 1 and 2.2 times at *pH* 12, the R^2 value and pH and 1000/T regression variables are not significantly different in either model, leading us to conclude that both approaches to normalizing rates to surface area adequately describe the dissolution rates.

Previous studies have pointed out problems with rates that are normalized to BET surface areas (BRANTLEY et al., 1986; GAUTIER et al., 2001; GRANDSTAFF, 1978). One

problem is that as minerals dissolve BET surface area increases but at the same time the highly reactive sites dissolve away so that r/A_{BET} declines. GRANDSTAFF (1978) showed that the surface area of forsterite grains increased by four times as dissolution rates decreased over the course of a 140 hour experiment. Another problem is that ratios of r_{BET} to r_{geo} are highly variable (Figure 4.5) because of inconsistencies in the BET measurements from time to time and laboratory to laboratory. Most BET surface areas are measured before grains are reacted, although some authors perform BET analysis after some sort of pre-treatment or even at the end of the experiment so that the reported r/A_{BET} can be quite different from experiment to experiment. This begs the question of whether BET surface area-based rates are of more value than surface area-based rates. For the data set considered here, we found that individual data sets based on BET rates are less comparable to each other because of inherent scatter in the BET measurements. A final consideration is that many of the potential uses of rate laws derived from these experiments involve models that are based on geometric surface areas. For example, see the mineral lifetime diagram at the end of this paper.

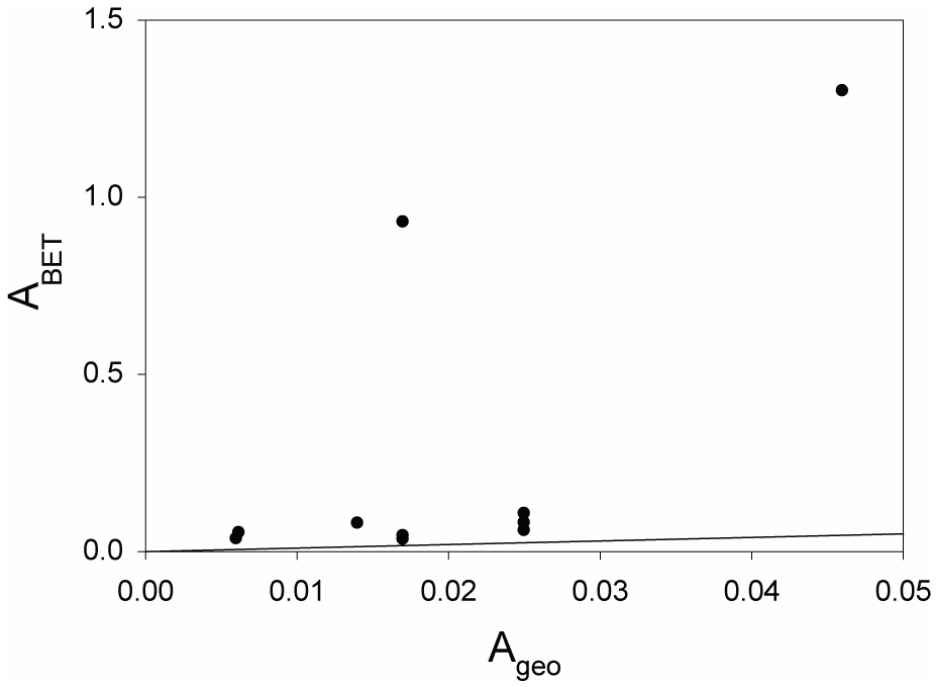

Figure 4.5. Ratio of geometric surface areas to surface areas measured using BET. Closed circles are A_{BET}/A_{geo} for studies in Table 4.1.

4.5.2.2 Rate law for pooled data set and implications for reaction mechanism

The regression model for the BET surface area rates from the pooled data set (Equations 4.10 and 4.12) can be transformed into the following rate laws

$$r_{BET} = 1.00 \times 10^{5} \left(e^{\frac{-68550}{RT}} \right) a_{H^+}^{0.48} \qquad [\text{pH} < 5.05] \quad (4.14)$$

$$r_{BET} = 32.36 \left(e^{\frac{-55084}{RT}} \right) a_{H^+}^{0.22} \qquad [\text{pH} > 5.05]. \quad (4.15)$$

Transformation of the regression models for the geometric surface area-based rates (Equations 4.11 and 4.13) produces the following rate laws

$$r_{geo} = 1.10 \times 10^{6} \left(e^{\frac{-69715}{RT}} \right) a_{H^+}^{0.50} \qquad [\text{pH} < 5.05] \quad (4.16)$$

$$r_{geo} = 759 \left(e^{\frac{-58924}{RT}} \right) a_{H^+}^{0.24} \qquad [\text{pH} > 5.05]. \quad (4.17)$$

As noted earlier, the rate laws calculated using BET and geometric surface areas have very similar reaction orders for H^+ and activation energies but the geometric surface area rate laws predict rates that are up to six times faster on a mol/m^{2}sec basis. Equations 4.14 and 4.15 predict rates that can be compared with the rates of dissolution of other minerals that are reported on a A_{BET} basis. Equations 4.16 and 4.17 should be used for models that relate dissolution rates to geometric surface areas such as shrinking particle models and the mineral lifetime model (OLSEN and RIMSTIDT, 2007).

The activation energies of 68.5 kJ/mole at pH < 5.05 (Equation 4.14) and 55.1 kJ/mole at pH > 5.05 (Equation 4.15), higher than the activation energies reported by most studies (Table 4.1, Figure 4.6). Most of these studies were conducted over rather narrow temperature ranges. By combining the data sets, we were able to evaluate the effect of temperature over a 150° temperature range, giving a value in which we have considerably more confidence. Our estimated activation energy values have standard errors ~2%. These high activation energy values are indicative of a bond breaking processes and are significantly higher than activation energies that are characteristic of transport-controlled dissolution (LASAGA, 1981). CASEY et al. (1993) reported that activation energy changes with pH for tephroite (Mn_2SiO_4) dissolution. We investigated

this possibility in the pooled data set by adding an interaction parameter that tested whether pH affects activation energy and found that the interaction term of pH and 1/T in that model was not significant ($p = 0.65$ at pH < 5.05 and $p = 0.74$ at pH > 5.05); therefore, we conclude that for forsterite dissolution E_a is not affected by changing *pH*.

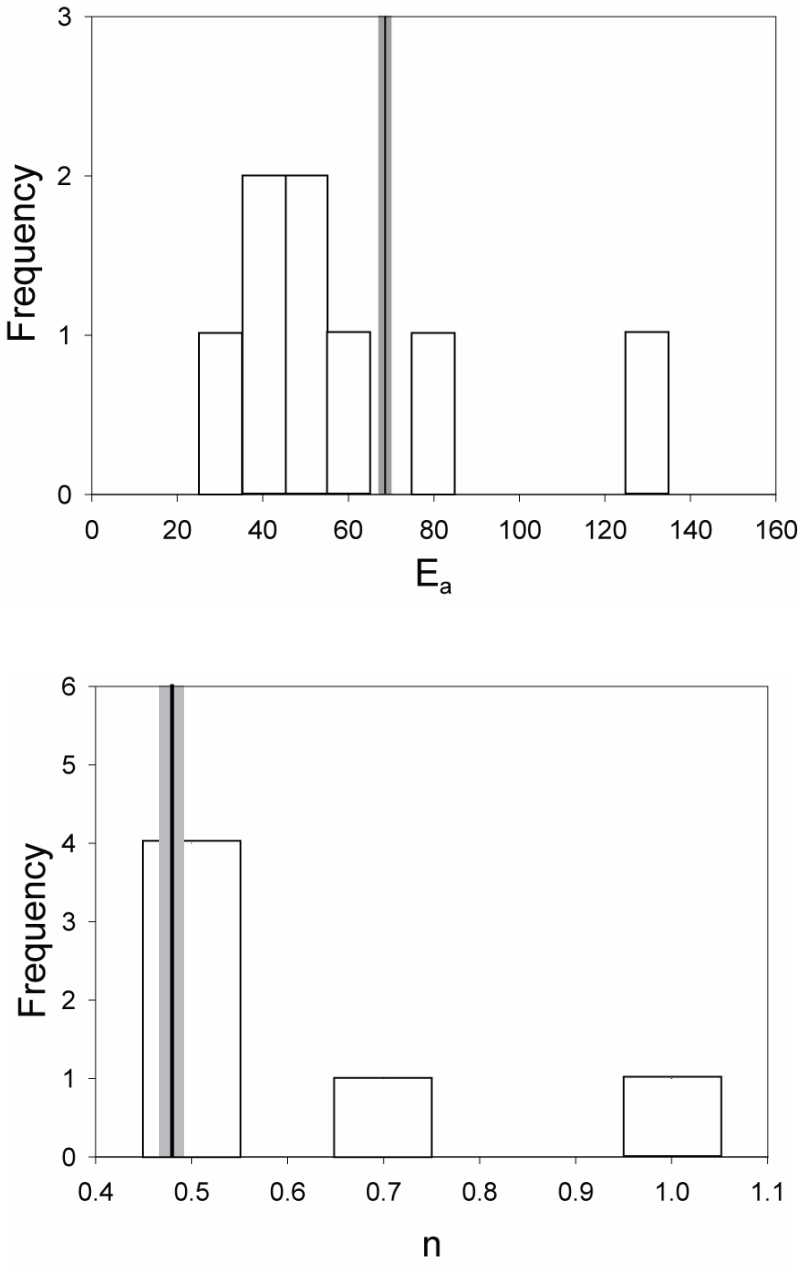

Figure 4.6. Frequency of E_a and n_{H+} calculated from studies in Table 4.1. Solid line is E_a or n calculated from the pooled data set; grey box is one standard error of E_a or n_{H+} calculated from pooled data set.

Figure 4.6 shows that n_{H+} for pH < 5.05 determined from the pooled data set (0.48 ± 0.1) agrees with n_{H+} values from most other studies, although two are much higher. Interestingly, a_{H+} still controls forsterite dissolution at pH > 5.05, although the reaction order declines from approximately 0.5 to 0.25. The changes in slope and activation energy are clearly indicative of a change in reaction mechanism around pH 5.05. Because a_{H+} is a factor in the rate law over the entire pH range, we conclude that H^+ participates in the activated complex over the entire pH range. This is consistent with the idea that a Lewis acid and a Lewis base must work in concert to cause bond breaking (LIU et al., 2006a; OLSEN and RIMSTIDT, in review). The effect of decreasing dissolution rates with decreasing a_{H2O} is consistent with the idea that water acts as a ligand (Lewis base) that participates in the dissolution process (LIU et al., 2006a; OLSEN and RIMSTIDT, in review). Because of the way the data were fit, low pH and high pH rate laws cannot be added together. However, we believe that these two mechanisms do overlap at intermediate pH. Interestingly, the change in reaction mechanism around pH 5.25 corresponds with the pH at which forsterite goes from preferentially releasing Mg to solution to preferentially releasing Si (see Figure 6 in POKROVSKY and SCHOTT (2000a)).

4.5.2.3 Factors that affect forsterite dissolution

The large amount of data evaluated in this paper provide a clearer idea of the factors that do and do not affect forsterite dissolution rates. We showed that aqueous magnesium up to 4 m, aqueous sulfate up to 3 m, and ionic strength up to 12 m do not affect forsterite dissolution rates. Decreasing the water activity slows forsterite dissolution rates by about 0.33 times for every 0.1 unit decrease in a_{H2O}. Because of the limited number of data and the relatively small effect expected for salinities of geologic or technological interest, this effect was not included in the rate laws developed from the pooled data set (Equations 4.14 - 4.17). Previous studies have shown that carbonate concentration (GOLUBEV et al., 2005; POKROVSKY and SCHOTT, 2000b; WOGELIUS and WALTHER, 1991b) and aqueous SiO_2 concentration (OELKERS, 2001; POKROVSKY and SCHOTT, 2000b) have either no or a very small effect on dissolution rates under most conditions. We were unable to further test these effects due to the limited amount of data. Temperature, pH, organic acids (GRANDSTAFF, 1986; OLSEN and RIMSTIDT, in

review; WOGELIUS and WALTHER, 1991b), mineral composition (WESTRICH et al., 1993), grain size, hydrodynamics (RIMSTIDT et al., 1996), and a lab/field discrepancy (VELBEL, 1986; VELBEL, 1993; WHITE and BRANTLEY, 2003) do affect forsterite dissolution rates.

4.5.2.4 Implications for mineral lifetime diagram

We developed a mineral lifetime diagram as a way to evaluate the persistence of olivine on Mars (OLSEN and RIMSTIDT, 2007). However, this diagram can also used to evaluate lifetimes on mineral grains in terrestrial environments. Based on the foregoing discussion, we have updated the diagram to include the effect of oxalic acid (OLSEN and RIMSTIDT, in review) and a_{H2O} on forsterite dissolution rates and reevaluated the grain lifetimes using our rate law based on geometric surface area rate law. The lifetime (t) of a dissolving spherical olivine grain is calculated using a shrinking particle model (LASAGA, 1998)

$$t = \frac{d}{2V_m r} \ . \quad (4.18)$$

This model is intrinsically based on the geometric surface area of the particle.

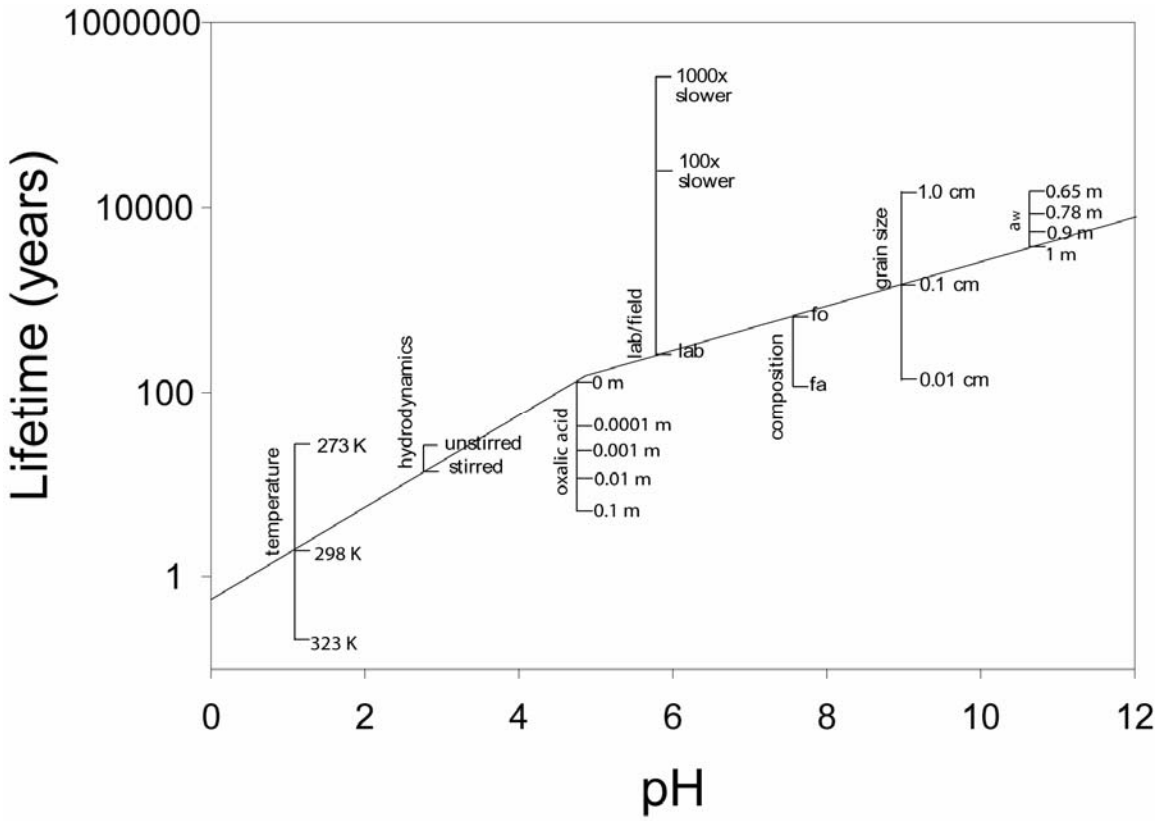

Figure 4.7. Olivine grain lifetime diagram. See OLSEN and RIMSTIDT (2007) for details about its construction and interpretation. Forsterite grain lifetimes are given as a function of pH for laboratory conditions at 298 K. Vertical scales show how changing variables increase (scales above graph) or decrease (scales below graph) olivine grain lifetimes. Scales have been placed at arbitrary pH values and can describe the effects of these variables at any pH.

4.6 REFERENCES

Amrhein, C. and Suarez, D. L., 1988. The use of a surface complexation model to describe the kinetics of ligand-promoted dissolution of Anorthite. *Geochimica et Cosmochimica Acta* **52**, 2785-2793.

Arvindson, R. E., Poulet, F., Bibring, J.-P., Wolff, M., Gendrin, A., Morris, R. V., Freeman, J. J., Langevin, Y., Mangold, N., and Bellucci, G., 2005. Spectral Reflectance an Morphologic Correlations in Eastern Terra Meridiani, Mars. *Science* **307**, 1591-1593.

Bailey, A., 1976. Effects of temperature on the reaction of silicates with aqueous solutions in the low temperature range. In: Cadek, J. and Paces, T. Eds.)*Proceed. Internat. Symp. on Water-Rock Interaction*. Geological Survey Prague, Prague.

Bandfield, J. L., Hamilton, V. E., and Christensen, P. R., 2000. A Global View of Martian Surface Compositions from MGS-TES. *Science* **287**, 1626-1630.

Barrat, J. A., Jambon, A., Bohn, M., Gillet, P., Sautter, V., Gopel, C., Lesourd, M., and Keller, F., 2002. The picritic shergottite north west Africa 1068 (NWA 1068 or "Louise Michel") *Luner and Planetary Science Conference XXXIII*.

Bennett, P. C., Melcer, M. E., Siegel, D. I., and Hassett, J. P., 1988. The dissolution of quartz in dilute aqueous solutions of organic acids at 25°C *Geochimica et Cosmochimica Acta* **52**, 1521-1530.

Bibring, J.-P., Langevin, Y., Gendrin, A., Gondet, B., Poulet, F., Berthe, M., Soufflot, A., Arvidson, R., Mangold, N., Mustard, J., Drossart, P., and team, t. O., 2005. Mars Surface Diversity as Revealed by the Omega/Mars Express Observations. *Science* **307**, 1576-1581.

Blesa, M. A., Morando, P. J., and Regazzoni, A. E., 1994. *Chemical Dissolution of Metal Oxides*. CRC Press, Boca Raton.

Blum, A. E. and Lasaga, A. C., 1988. Role of surface speciation in the low-temperature dissolution of minerals. *Nature* **331**, 431-433.

Blum, A. E. and Stillings, L. L., 1995. Feldspar Dissolution Kinetics. In: White, A. F. and Brantley, S. L. Eds.), *Chemical weathering rates of silicate minerals*. Mineralogical Society of America, Washington, D.C.

Brantley, S. L., Crane, S. R., Crerar, D. A., Hellmann, R., and Stallard, R., 1986. Dissolution at dislocation etch pits in quartz. *Geochimica et Cosmochimica Acta* **50**, 2349-2361.

Brantley, S. L. and Mellott, N. P., 2000. Surface area and porosity of primary silicate minerals. *American Mineralogist* **85**, 1767-1783.

Burkin, A. R., 2001. *Chemical Hydrometallurgy: Theory and Principles*. Imperial College Press, London.

Cama, J. and Ganor, J., 2006. The effects of organic acid on the dissolution of silicate minerals: A case study of oxalate catalysis of kaolinite dissolution. *Geochimica et Cosmochimica Acta* **70**, 2191-2209.

Carr, M. H., 1996. *Water on Mars*. Oxford University press, New York, New York.

Casey, W., Hochella, M., and Westrich, H., 1993. The surface chemistry of manganiferous silicate minerals as inferred from experiments on tephroite (Mn_2SiO_4). *Geochimica et Cosmochimica Acta* **57**, 785-593.

Casey, W. and Westrich, H., 1992. Control of dissolution rates of orthosilicate minerals by divalent metal-oxygen bonds. *Nature* **355**, 157-159.

Casey, W. H., 2001. A view of reactions at mineral surfaces from the aqueous phase. *Mineralogical Magazine* **65**, 323-337.

Casey, W. H. and Ludwig, C., 1996. The mechanism of dissolution of oxide minerals. *Nature* **381**, 506-509.

Chen, Y. and Brantley, S. L., 2000. Forsterite dissolution at 65°C and 2<pH<5. *Chem. Geol.* **165**, 267-281.

Christensen, P. R., Bandfield, J. L., Clark, R. N., Edgett, K. S., Hamilton, V. E., Hoefen, T., Kieffer, H. H., Kuzmin, R. O., Lane, M. D., Malin, M. C., Morris, R. V., Pearl, J. C., Pearson, R., Roush, T. L., Ruff, S. W., and Smith, M. D., 2000. Detection of crystalline hematite mineralization on Mars by the Thermal Emission Spectrometer: Evidence for near-surface water. *Journal of Geophysical Research* **105**, 9623-9642.

Christensen, P. R., Wyatt, M. B., Glotch, T. D., Rogers, A. D., Anwar, S., Arvidson, R. E., Bandfield, J. L., Blaney, D. L., Budney, C., Calvin, W. M., Fallacaro, A., Fergason, R. L., Gorelick, N., Graff, T. G., Hamilton, V. E., Hayes, A. G., Johnson, J. R., Knudson, A. T., McSween Jr., H. Y., Mehall, G. L., Mehall, L. K., Moersch, J. E., Morris, R. V., Smith, M. D., Squyres, S. W., Ruff, S. W., and Wolff, M. J., 2004. Mineralogy at Meridiani Planun from the Mini-TES Experiment on the Opportunity Rover. *Science* **306**, 1733-1739.

Clark, B. C., Morris, R. V., McLennan, S. M., Gellert, R., Jolliff, B. L., Knoll, A. H., Squyres, S. W., Lowenstein, T. K., Ming, D. W., Tosca, N. J., Yen, A., Christensen, P. R., Gorevan, S., Bruckner, J., Calvin, W., Dreibus, G., Farrand, W., Klingelhofer, G., Waenke, H., Zipfel, J., Berthe, M., Grotzinger, J., McSween, H. Y., and Rieder, R., 2005. Chemistry and mineralogy of outcrops at Meridiani Planum. *Earth and Planetary Science Letters* **240**, 73-94.

Doehne, E., 2002. Salt weathering: a selective review. In: Siegesmund, S., Weiss, T., and Vollbrecht, A. Eds.), *Natural Stone, Weathering Phenomena, Conservation Strategies, and Case Studies*. The Geological Society of London, London.

Drever, J. I. and Vance, G. F., 1994. Role of Soil Organic Acids in Mineral Weathering Processes. In: Pittman, E. D. and Lewan, M. D. Eds.), *Organic Acids in Geological Processes*. Springer-Verlag, New York.

Fox, T. R. and Comerford, N. B., 1990. Low-molecular-weight organic acids in selected forest soils of the southeastern USA. *Soil Science Society of America Journal* **54**, 1139-1144.

Franklin, S. P., Hajash, A. J., Dewers, T. A., and Tieh, T. T., 1994. The role of carboxylic acids in albite and quartz dissolutions: An experimental study under diagenetic conditions. *Geochimica et Cosmochimica Acta* **58**, 4259-4279.

Furrer, C. and Stumm, W., 1986. The coordination chemistry of weathering: I. Dissolution kinetics of gamma-Al2O3 and BeO. *Geochimica et Cosmochimica Acta* **50**, 1847-1860.

Gautier, J.-M., Oelkers, E. H., and Schott, J., 2001. Are quartz dissolution rates proportional to B.E.T. surface areas? *Geochimica et Cosmochimica Acta* **65**, 1059-1070.

Giammar, D. E., Bruant, R. G., and Peters, C. A., 2005. Forsterite dissolution and magnesite precipitation at conditions relevant for deep saline aquifer storage and sequestration of carbon dioxide. *Chemical Geology* **217**, 257-276.

Gledhill, D. K. and Morse, J. K., 2004. Dissolution kinetics of calcite in NaCl-$CaCl_2$-$MgCl_2$ Brines at 25°C and 1 bar pCO_2. *Aquatic Geochemistry* **10**, 171-190.

Golubev, S. V., Pokrovsky, O. S., and Schott, J., 2005. Experimental determination of the effect of dissolved CO_2 on the dissolution kinetics of Mg and Ca silicates at 25 C. *Chemical Geology*, 227-238.

Gorichev, I. G. and Kipriyanov, N. A., 1984. Regular kinetic features of the dissolution of metal oxides in acidic media. **53**, 1039-1061.

Govett, G. J. S., 1961. Critical factors in the colorimetric determination of silica. *Analytica Chimica Acta* **25**, 69-80.

Grandstaff, D. E., 1978. Changes in surface area and morphology and the mechanism of forsterite dissolution. *Geochimica et Cosmochimica Acta* **42**, 1899-1901.

Grandstaff, D. E., 1980. The dissolution rate of forsteritic olivine from Hawaiian beach sand. In: Grandstaff, D. E. (Ed.),*International Symposium on Water-Rock Interaction, 3rd*, Edmonton, Alberta.

Grandstaff, D. E., 1986. The dissolution rate of forsteritic olivine from Hawaiian beach sand. In: Colman, S. M. and Dethier, D. P. Eds.), *Rates of Chemical Weathering of Rocks and Minerals*. Academic Press, Orlando, Florida.

Hamilton, V. E. and Christensen, P. C., 2005. Evidence for extensive olivine-rich bedrock in Nili Fossae, Mars. *Geology* **33**, 433-436.

Hänchen, M., Prigiobbe, V., Storti, G., Seward, T. M., and Mazzotti, M., 2006. Dissolution kinetics of forsteritic olivine at 90-150°C including effects of presence of CO_2. *Geochimica et Cosmochimica Acta* **70**, 4403-4416.

Huang, W. H. and Kiang, W. C., 1972. Laboratory dissolution of plagioclase feldspars in water and organic acids at room temperature. **57**, 1849-1859.

Icenhower, J. P. and Dove, T. M., 2000. The dissolution kinetics of amorphous silica into sodium chloride solutions: Effects of temperature and ionic strength. *Geochimica et Cosmochimica Acta* **64**, 4193-4203.

Jonckbloedt, R. C. L., 1998. Olivine dissolution in sulfuric acid at elevated temperatures-implications for the olivine process, an alternative waste acid neutralizing process. *Journal of Geochemical Exploration* **62**, 337-346.

Kettler, R. M., Wesolowski, D. J., and Palmer, D. A., 1998. Dissociation Constants of Oxalic Acid in Aqueous Sodium Chloride and Sodium Trifluoromethanesulfonate Media to 175 C. *Journal of Chemical Engineering Data* **43**, 337-350.

Klingelhofer, G., Morris, R. V., Bernhardt, B., Schroder, C., Rodionov, D. S., de Souza Jr., P. A., Yen, A., Gellert, R., Evlanov, E. N., Zubkov, B., Foh, J., Bonnes, U., Kankeleit, E., Gutlich, P., Ming, D. W., Renz, F., Wdowiak, T., Squyres, S. W., and Arvidson, R. E., 2004. Jarosite and Hematite at Meridiani Planum from Opportunity's Mossbauer Spectrometer. *Science* **306**, 1740-1745.

Knoll, A. H., Carr, M., Clark, B., DesMarais, D. J., Farmer, J. D., Fischer, W. W., Grotzinger, J. P., McLennan, S. M., Malin, M., Schroder, C., Squyres, S., Tosca,

N. J., and Wdowiak, T., 2005. An astrobiological perspective on Meridiani Planum. *Earth and Planetary Science Letters* **240**, 179-189.
Knoll, A. H. and Grotzinger, J., 2006. Water on Mars and the Prospect of Martian Life. *Elements* **2**, 169-173.
Koeppen, W. C. and Hamilton, V. E., 2006. The distribution and composition of olivine on Mars *Luner and Planetary Science Conference XXXVII*.
Kowalewski, M. and Rimstidt, J. D., 2003. Average lifetime and age spectra of detrital grains: Toward a unifying theory of sedimentary grains. *Journal of Geology* **111**.
Kuebler, K. E., Wang, A., Haskin, L. A., and Joliff, B. L., 2003. A study of olivine alteration to iddingsite using Raman spectroscopy *Luner and Planetary Science Conference XXXIV*.
Laider, K. J., 1987. Theories of Reaction Rates. *Harper & Row, Publishers*, 80-99.
Langmuir, D., 1997. *Aqueous Environmental Geochemistry*. Prentice-Hall, Inc., Upper Saddle River, New Jersey.
Lasaga, A. C., 1981. Rate Laws of Chemical Reactions. In: Lasaga, A. C. and Kirkpatrick, R. J. Eds.), *Kinetics of Geochemical Processes*. Mineralogical Society of America.
Lasaga, A. C., 1998. *Kinetic Theory in the Earth Sciences* Princeton University Press Princeton, New Jersey.
Leshin, L. A. and Vicenzi, E., 2006. Aqueous Processes Recorded by Martian Meteorites: Analyzing Martian Water on Earth. *Elements* **2**, 157-162.
Liu, Y., Olsen, A. A., and Rimstidt, J. D., 2006a. Mechanism for the dissolution of olivine series minerals in acidic solutions. *American Mineralogist* **91**, 455-458.
Liu, Y., Olsen, A. A., and Rimstidt, J. D., 2006b. Mechanism for the dissolution of olivine series minerals in acidic solutions. *American Mineralogist* **91**, 455-458.
Luce, R. W., Bartlett, R. W., and Parks, G. W., 1972a. Dissolution kinetics of magnesium silicates. *Geochimica et Cosmochimica Acta* **36**, 35-50.
Luce, R. W., Bartlett, R. W., and Parks, G. W., 1972b. Dissolution kinetics of magnesium silicates. *Geochimica et Cosmochimica Acta* **36**, 35-50.
Madden, M. E. E., Bodnar, R. J., and Rimstidt, J. D., 2004. Jarosite as an indicator of water-limited chemical weathering on Mars. *Nature* **431**, 821-823.
Manley, E. P. and Evans, L. J., 1986. Dissolution of feldspars by low-molecular-weight aliphatic and aromatic acids. *Soil Science*, 106-112.
Mast, A. M. and Drever, J. I., 1987. The effect of oxalate on the dissolution rates of oligoclase and tremolite. *Geochimica et Cosmochimica Acta* **51**, 2559-2568.
McSween Jr., H. Y., Grove, T. L., and Wyatt, M. B., 2003. Constraints on the composition and petrogenesis of the Martian crust *Journal of Geophysical Research* **108, E12, 5135, doi:10.1029/2003JE002175**.
Mogollon, J. L., Perez-Duaz, A., and Lo Monaco, S., 2000. The effects of ion identity and ionic strength on the dissolution rate of gibbsitic bauxite. *Geochimica et Cosmochimica Acta* **64**, 781-795.
Mustard, J. F., Poulet, F., Gendrin, A., Bibring, J.-P., Langevin, Y., Gondet, B., Mangold, N., Bellucci, G., and Altieri, F., 2005. Olivine and Pyroxene Diversity in the Crust of Mars. *Science* **307**, 1594-1597.

Nagy, K., Blum, A., and Lasaga, A., 1991. Dissolution and precipitation kinetics of kaolinite at 80C and pH 3: the dependance on solution saturation state. *American Journal of Science* **291**, 649-686.

Oelkers, E. H., 2001. An experimental study of forsterite dissolution rates as a function of temperature and aqueous Mg and Si concentrations. *Chemical Geology* **175**, 485-494.

Olsen, A. A. and Rimstidt, J. D., 2007. Using a mineral lifetime diagram to evaluate the persistence of olivine on Mars. *American Mineralogist* **92**.

Olsen, A. A. and Rimstidt, J. D., in review. Oxalate-promoted forsterite dissolution at low pH. *Geochimica et Cosmochimica Acta*.

Ott, R. L. and Longnecker, M., 2001. An Introduction to Statistical Methods and Data Analysis. Duxbury, Pacific Grove, California.

Pokrovsky, O. S. and Schott, J., 2000a. Forsterite surface composition in aqueous solutions: A combined potentiometric, electrokinetic, and spectroscopic approach. *Geochimica et Cosmochimica Acta* **64**, 3299-3312.

Pokrovsky, O. S. and Schott, J., 2000b. Kinetics and mechanism of forsterite dissolution at 25 C and pH from 1 to 12. *Geochimica et Cosmochimica Acta* **64**, 3313-3325.

Poulson, S. R., Drever, J. I., and Stillings, L. L., 1997. Aqueous Si-oxalate complexing, oxalate adsorption onto quartz, and the effect of oxalate upon quartz dissolution rates. *Chemical Geology* **140**, 1-7.

Rijniers, L. A., Huinink, H. P., Pel, L., and Kopinga, K., 2003. Salt crystallization in porous materials and its implication for stone decay*EUROMAT 2003, Symposium P2- Materials and Conservation of Cultural Heritage, EPFL-Lausanne*.

Rimstidt, J. D., Rosso, J. J., Weissbart, E. J., Hatfield, J., and Skinner, K. L., 1996. Factors affecting mineral dissolution rate measurements*Geological Society of America 28th Annual Meeting*, Denver, Colorado.

Robinson, R. A. and Stokes, R. H., 2002. *Electrolyte Solutions*. Dover Publications, New York.

Rogers, A. D., Christensen, P. C., and Bandfield, J. L., 2005. Compositional heterogeneity of the ancient Martian crust: Analysis of Ares Vallis bedrock with THEMIS and TES data. *Journal of Geophysical Research* **Vol. 110, E05010, doi:10.1029/2005JE002399**.

Rosso, J. J. and Rimstidt, J. D., 2000. A high resolution study of forsterite dissolution rates. *Geochimica et Cosmochimica Acta* **64**, 797-811.

Sanemasa, I., Yoshida, M., and Ozawa, T., 1972. The dissolution of olivine in aqueous solutions of inorganic acids. *Bulletin of the Chemical Society of Japan* **45**, 1741-1746.

Schott, J., Berner, R. A., and Sjoberg, E. L., 1981. Mechanism of pyroxene and amphibole weathering- I. Experimental studies of iron-free minerals. *Geochimica et Cosmochimica Acta* **45**, 2123-2135.

Schuiling, R. D., van Herk, J., and Pietersen, H. S., 1986. A potential process for neutralisation of industrial wastes by reaction with olivine. *Geologie en Mijnbouw* **65**, 243-246.

Seyama, H., Soma, M., and Tanaka, A., 1996. Surface characterization of acid-leached olivines by X-ray photoelectron spectroscopy. *Chemical Geology* **129**, 209-216.

Shuster, D. L. and Weiss, B. P., 2005. Martian Surface Paleotemperatures from Thermochronology of Meteorites. *Science* **309**, 594-597.

Siegel, D. I. and Pfannkuch, H. O., 1984. Silicate mineral dissolution at pH 4 and near standard temperature and pressure. *Geochimica et Cosmochimica Acta* **48**, 197-201.

Smith, M. D., Wolff, M. J., Lemmon, M. T., Spanovich, N., Banfield, D., Budney, C. J., Clancy, R. T., Ghosh, A., Landis, G. A., Smith, P., Whitney, B., Christensen, P. R., and Squyres, S. W., 2004. First Atmospheric Science Results from the Mars Exploration Rovers Mini-TES. *Science* **306**, 1750-1753.

Squyres, S. W., Grotzinger, J. P., Arvidson, R. E., Bell III, J. F., Calvin, W., Christensen, P. R., Clark, B. C., Crisp, J. A., Farrand, W. H., Herkenhoff, K. E., Johnson, J. R., Klingelhofer, G., Knoll, A. H., McLennan, S. M., McSween Jr., H. Y., Morris, R. V., Rice Jr., J. W., Rieder, R., and Soderblom, L. A., 2004. In Situ Evidence for an Ancient Aqueous Environment at Meridiani Planum, Mars. *Science* **306**, 1709-1714.

Squyres, S. W. and Knoll, A. H., 2005. Sedimentary Geology at Meridiani Planum, Mars. *Earth and Planetary Science Letters* **240**, 1-190.

Squyres, S. W., Knoll, A. H., Arvidson, R. E., Clark, B. C., Grotzinger, J. P., Jolliff, B. L., McLennan, S. M., Tosca, N., Bell III, J. F., Calvin, W. M., Farrand, W. H., Glotch, T. D., Golombek, M. P., Herkenhoff, K. E., Johnson, J. R., Klingelhofer, G., McSween, H. Y., and Yen, A. S., 2006. Two Years at Meridiani Planum: Results from the Opportunity Rover. *Science* **313**, 1403-1407.

Stefansson, A. and Gislason, S. R., 2001. Chemical Weathering of Basalts, Southwest Iceland: Effect of Rock Crystallinity and Secondary Minerals on Chemical Fluxes to the Ocean. *American Journal of Science* **301**, 513-556.

Stillings, L. L. and Brantley, S. L., 1995. Feldspar dissolution at 25°C and pH 3: Reaction stoichiometry and the effect of cations. *Geochimica et Cosmochimica Acta* **59**, 1483-1496.

Stillings, L. L., Drever, J. I., Brantley, S. L., Sun, Y., and Oxburgh, R., 1996. Rates of feldspar dissolution at pH 3-7 with 0-8 mM oxalic acid. *Chemical Geology* **132**, 79-89.

Stopar, J. D., Taylor, G. J., Hamiliton, V. E., and Browning, L., 2006. Kinetic model of olivine dissolution and extent of aqueous alteration on Mars. *Geochimica et Cosmochimica Acta* **in press**.

Stumm, W. and Wollast, R., 1990. Coordination of chemistry of weathering: kinetics of the surface-controlled dissolution of oxide minerals. *Reviews of Geophysics* **28**, 53-69.

Taylor, J. R., 1982. *An Introduction to Error Analysis: The Study of Uncertainities in Physical Measurements*. University Science Books, Mill Valley, CA.

Tester, J. W., Worley, W. G., Robinson, B. A., Grigsby, C. O., and Feerer, J. L., 1994. Correlating quartz dissolution kinetics in pure water from 25 to 625°C. *Geochimica et Cosmochimica Acta* **58**, 2407-2420.

Van Herk, J., Pietersen, H. S., and Schuiling, R. D., 1989. Neutralization of industrial waste acids with olivine- The dissolution of forsteritic olivine at 40-70°C. *Chemical Geology* **76**, 341-352.

Velbel, M. A., 1986. Influence of surface area, surface characteristics, and solution composition on feldspar weathering rates. In: Davis, J. A. and Hayes, K. F. Eds.), *ACS Symposium Series No. 323, Geochemical Processes at Mineral Surfaces*.

Velbel, M. A., 1993. Constancy of siliciate-mineral weathering-rate ratios between natural and experimental weathering: implications for hydrologic control of differences in absolute rates. *Chemical Geology* **105**, 89-99.

Vogelsberger, W., Lobbus, M., Sonnefeld, J., and Seidel, A., 1999. The influence of ionic strength on the dissolution process of silica. *Colloids and Surfaces* **159**, 311-319.

Wainer, H., 2007. The Most Dangerous Equation. *American Scientist* **May-June**, 249-256.

Wang, A., Kubler, K., Jolliff, B., and Haskin, L. A., 2004. Mineralogy of a Martian meteorite as determined by Raman spectroscopy. *Journal of Raman Spectroscopy* **35**, 504-514.

Weissbart, E. J. and Rimstidt, J. D., 2000. Wollastonite: Incongruent dissolution and leached layer formation. *Geochimica et Cosmochimica Acta* **64**, 4007-4016.

Welch, S. A. and Ullman, W. J., 1993. The effect of organic acids on plagioclase dissolution rates and stoichiometry. *Geochimica et Cosmochimica Acta* **57**, 2725-2736.

Welch, S. A. and Ullman, W. J., 1996. Feldspar dissolution in acidic and organic solutions: Compositional and pH dependence of dissolution rate. *Geochimica et Cosmochimica Acta* **60**, 2939-2948.

Westrich, H. R., Cygan, R. T., Casey, W. H., Zemitis, C., and Arnold, G. W., 1993. The dissolution kinetics of mixed-cation orthosilicate minerals. *American Journal of Science* **293**, 869-893.

White, A. F. and Brantley, S. L., 1995. *Chemical weathering rates of silicate minerals*. Mineralogical Society of America, Washington, D.C.

White, A. F. and Brantley, S. L., 2003. The effect of time on the weathering of silicate minerals: why do weathering rates differ in the laboratory and field? *Chemical Geology* **202**, 479-506.

Williamson, M. A. and Rimstidt, J. D., 1993. The rate of decomposition of the ferric-thiosulfate complex in acidic aqueous solutions. *Geochimica et Cosmochimica Acta* **57**, 3555-3561.

Wilson, M. J., 2004. Weathering of the primary rock forming minerals: processes, products, and rates. *Clay Minerals* **39**, 233-266.

Winkler, E. M. and Wilheim, E. J., 1970. Salt Burst by Hydration Pressures in Architectural Stone in Urban Atmosphere. *Geological Society of America Bulletin* **81**, 567-572.

Wogelius, R. and Walther, J., 1991a. Olivine dissolution at 25C: Effects of pH, CO2, and organic acids. *Geochimica et Cosmochimica Acta* **55**, 943-954.

Wogelius, R. A. and Walther, J. V., 1991b. Olivine dissolution at 25C: Effects of pH, CO2, and organic acids. *Geochimica et Cosmochimica Acta* **55**, 943-954.

Wogelius, R. A. and Walther, J. V., 1992. Olivine dissolution kinetics at near-surface conditions. *Chemical Geology* **97**, 101-112.

Yen, A. S., Gellert, R., Schroder, C., Morris, R. V., Bell III, J. F., Knudson, A. T., Clark, B. C., Ming, D. W., Crisp, J. A., Arvidson, R. E., Blaney, D. L., Bruckner, J., Christensen, P. R., DesMarais, D. J., De Souza Jr., P. A., Economou, T. E.,

Ghosh, A., Hahn, B. C., Herkenhoff, K. E., Haskin, L. A., Hurowitz, J. A., Joliff, B. L., Johnson, J. R., Klingelhofer, G., Madsen, M. B., McLennan, S. M., McSween Jr., H. Y., Richter, L., Rieder, R., Rodionov, D., Soderblom, L., Squyres, S. W., Tosca, N. J., Wang, A., Wyatt, M., and Zipfel, J., 2005. An integrated view of the chemistry and mineralogy of martian soils. *Nature* **436**, 49-54.

APPENDIX 4.1:

Silica release rates for all experiments from this paper and from (OLSEN and RIMSTIDT, in review) in mol/m^2sec. All rates were standardized to a surface area of 0.0528 m^2/g. Samples with asterisks were originally published in (OLSEN and RIMSTIDT, in review).

Exp.	pH	m_K	m_{Na}	m_{Mg}	m_{SO4}	m_{NO3}	log r_{Si}	$I^{0.5}$
M1R	2.00	0	0	0.10	0.12	0	-7.69	0.66
M2R	2.00	0	0	0.29	0.32	0	-7.72	1.11
M3R	2.00	0	0	0.97	1.00	0	-7.81	1.99
M4R	2.00	0	0	2.94	2.96	0	-8.03	3.43
M5R	3.03	0	0	0.10	0.10	0	-8.15	0.64
M6R	2.96	0	0	0.30	0.30	0	-8.03	1.10
M7R	2.98	0	0	1.00	1.00	0	-8.19	2.00
M8R	2.99	0	0	2.99	3.00	0	-8.67	3.46
MII1	3.95	0	0	0.10	0.10	0	-9.05	0.63
MII2	4.01	0	0	0.30	0.30	0	-9.03	1.09
MII3	3.96	0	0	1.00	1.00	0	-9.05	2.00
MII4	4.00	0	0	2.99	2.99	0	-9.08	3.46
MS11	2.04	0	0	1.47	1.47	0	-7.61	2.43
MS12	4.01	0	0	1.48	1.48	0	-9.07	2.43
MS13	3.07	0	0	1.47	1.47	0	-8.43	2.43
MS14	3.03	0	0	1.92	1.93	0	-8.44	2.77
MS15	3.99	0	0	1.98	1.98	0	-9.27	2.81
MS16	2.02	0	0	1.97	1.99	0	-7.65	2.81
MS17	3.99	0	0	2.45	2.45	0	-9.30	3.13
MS18	3.01	0	0	2.45	2.45	0	-8.38	3.13
MS19	1.99	0	0	2.46	2.48	0	-7.66	3.14
N1	2.01	0	0.20	0.00	0.12	0	-7.66	0.59
N2	2.03	0	0.59	0.00	0.32	0	-7.70	0.96
N3	2.07	0	1.92	0.00	1.00	0	-7.83	1.72
N4	2.96	0	0.20	0.00	0.10	0	-8.10	0.55
N5	3.04	0	0.58	0.00	0.29	0	-8.08	0.94
N6	2.92	0	1.84	0.00	0.93	0	-8.15	1.67
N7	4.09	0	0.20	0.00	0.10	0	-8.71	0.55
N8	4.07	0	0.60	0.00	0.30	0	-8.86	0.95
N9	4.03	0	1.99	0.00	1.00	0	-8.80	1.73
MN1	2.01	0	0	1.94	0	3.89	-8.20	2.41
MN2	2.96	0	0	1.96	0	3.92	-9.05	2.43
MN3	4.02	0	0	1.99	0	3.98	-8.83	2.44
MN4	2.03	0	0	2.97	0	5.94	-8.21	2.99
MN5	3.03	0	0	2.99	0	5.97	-8.65	2.99
MN6	3.94	0	0	2.99	0	5.97	-8.63	2.99
MN7	1.99	0	0	3.90	0	7.81	-8.62	3.42
MN8	3.04	0	0	3.92	0	7.84	-9.22	3.43
MN11	4.00	0	0	0.24	0	0.49	-8.85	0.86
MN12	2.99	0	0	0.24	0	0.48	-8.84	0.85
MN13	2.03	0	0	0.23	0	0.49	-7.95	0.84
MN14	3.02	0	0	0.55	0	1.10	-8.80	1.29

Exp.	pH	m_K	m_{Na}	m_{Mg}	m_{SO4}	m_{NO3}	log *r*	$I^{0.5}$
MN15	2.02	0	0	0.53	0	1.10	-7.98	1.27
MN16	4.03	0	0	0.55	0	1.10	-9.23	1.28
MN17	4.04	0	0	0.09	0	0.18	-8.85	0.52
MN18	3.02	0	0	0.09	0	0.19	-8.64	0.52
MN19	2.01	0	0	0.08	0	0.23	-8.04	0.54
SB 96*	2.97	0.10	0	0	0	0.10	-8.61	0.32
SB 97*	3.02	0.30	0	0	0	0.30	-8.47	0.55
SB 98*	3.02	0.59	0	0	0	0.59	-8.47	0.77
SB 99*	2.99	0.89	0	0	0	0.89	-8.45	0.94
SB 100*	2.98	1.18	0	0	0	1.19	-8.40	1.09
SB 101*	2.95	1.48	0	0	0	1.48	-8.30	1.22
SB 102*	2.94	1.78	0	0	0	1.78	-8.37	1.33
SB 103*	2.97	2.07	0	0	0	2.07	-8.50	1.44
SB 104*	3.05	2.37	0	0	0	2.37	-8.55	1.54
SB105*	1.96	0.10	0	0	0	0.10	-8.02	0.32
SB106*	1.95	0.30	0	0	0	0.30	-8.02	0.55
SB107*	1.96	0.59	0	0	0	0.59	-7.97	0.77
SB108*	2.00	0.89	0	0	0	0.89	-8.00	0.95
SB109*	2.01	1.19	0	0	0	1.19	-7.98	1.09
SB110*	2.01	1.48	0	0	0	1.48	-7.94	1.22
SB111*	2.00	1.78	0	0	0	1.78	-7.95	1.34
SB112*	2.01	2.08	0	0	0	2.08	-7.89	1.44
SB113*	2.00	2.37	0	0	0	2.37	-7.91	1.54
SB114*	3.83	0.10	0	0	0	0.10	-8.70	0.31
SB115*	3.91	0.30	0	0	0	0.30	-8.79	0.54
SB116*	4.05	0.59	0	0	0	0.59	-8.94	0.77
SB117*	3.92	0.89	0	0	0	0.89	-8.94	0.94
SB118*	3.87	1.19	0	0	0	1.19	-8.71	1.09
SB119*	3.91	1.48	0	0	0	1.48	-9.08	1.22
SB121*	4.10	2.08	0	0	0	2.08	-8.94	1.44
SB122*	4.04	2.37	0	0	0	2.37	-8.56	1.54
SB123*	1.00	0.10	0	0	0	0.10	-7.54	0.39
SB124*	1.02	0.29	0	0	0	0.30	-7.58	0.59
SB125*	1.05	0.59	0	0	0	0.59	-7.50	0.80
SB126*	1.05	0.88	0	0	0	0.89	-7.41	0.96
SB127*	1.04	1.18	0	0	0	1.18	-7.38	1.11
SB128*	1.02	1.47	0	0	0	1.48	-7.28	1.23
SB129*	1.04	1.77	0	0	0	1.77	-7.31	1.35
SB130*	1.05	2.07	0	0	0	2.07	-7.22	1.45
SB131*	1.04	2.36	0	0	0	2.36	-7.46	1.55

APPENDIX 4.2:

Magnesium and silica release data used in the pooled data set. Release rates are given in mol/m^{2}sec. Mg release rates were corrected for forsterite composition by dividing the rate by twice the mole fraction of forsterite times two.

pH	log $r_{Mg, BET}$	log $r_{Mg, GEO}$	log $r_{Si, BET}$	log $r_{Si, GEO}$	T (°C)
		BAILEY (1976)			
4	NA	-7.32	NA	-7.33	25
4	NA	-7.07	NA	NA	35
4	NA	-6.79	NA	-6.82	45
4	NA	-6.42	NA	NA	55
4	NA	-6.26	NA	-6.22	65
		BLUM and LASAGA (1988)			
1.8	-7.79	NA	-7.84	NA	25
2.35	-8.05	NA	-8.07	NA	25
2.89	-8.17	NA	-8.2	NA	25
3.04	-8.13	NA	-8.13	NA	25
3.38	-8.5	NA	-8.49	NA	25
3.7	-8.61	NA	-8.57	NA	25
4.08	-8.29	NA	-8.21	NA	25
4.38	-8.72	NA	-8.71	NA	25
4.41	-8.75	NA	-9.33	NA	25
4.73	-9.44	NA	-9.19	NA	25
5.53	-11.65	NA	-11.81	NA	25
7.24	-11.89	NA	-12.14	NA	25
8.78	-10.07	NA	-9.22	NA	25
8.93	-10.09	NA	-9.8	NA	25
8.97	-10.02	NA	-9.62	NA	25
9.46	-10.54	NA	-10.45	NA	25
11.02	-9.91	NA	-10.01	NA	25
11.35	-10.25	NA	-9.84	NA	25
		CHEN and BRANTLEY (2000)			
2	-6.35	-6.05	-6.09	-5.79	65
2.95	-7.02	-6.71	-6.76	-6.46	65
2.95	-7.08	-6.78	-6.83	-6.53	65
2.95	-7.12	-6.81	-6.85	-6.55	65
2.95	-7.06	-6.76	-6.82	-6.51	65
2.95	-6.97	-6.67	-6.68	-6.38	65
4	-7.85	-7.55	-7.6	-7.3	65
5	-8.4	-8.1	-8.19	-7.89	65
		GOLUBEV et al. (2005)			
1.98	-8.3	-7.92	-7.92	-7.54	25
2.28	-8.36	-7.98	-7.98	-7.6	25
3.05	-8.47	-8.09	-8.19	-7.81	25
3.71	-8.72	-8.34	-8.37	-7.99	25
3.8	-8.79	-8.41	-8.48	-8.1	25

4.16	-8.53	-8.15	-8.26	-7.88	25
4.72	-8.83	-8.45	-8.55	-8.17	25
5.25	-8.77	-8.39	-8.49	-8.11	25
6	-9.02	-8.64	-8.72	-8.34	25
6.2	-9.21	-8.83	-9.07	-8.69	25
6.66	-9.86	-9.48	-9.39	-9.01	25
6.8	-9.42	-9.04	-9.07	-8.69	25
7.2	-10.18	-9.8	-9.64	-9.26	25
8.06	-10.38	-10	-9.82	-9.44	25
8.4	-9.86	-9.48	-9.71	-9.33	25
8.45	-9.97	-9.59	-9.69	-9.31	25
8.46	-9.96	-9.58	-9.71	-9.33	25
8.46	-9.84	-9.46	-9.71	-9.33	25
9.85	-10.09	-9.71	-9.99	-9.61	25
9.95	-10.07	-9.69	-9.74	-9.36	25
10.05	-10.13	-9.75	-9.76	-9.38	25
10.5	-10.85	-10.47	-10.37	-9.99	25
10.65	-11.15	-10.77	-10.19	-9.81	25
10.75	-11.22	-10.84	-10.38	-10	25
10.85	-10.35	-9.97	-10.07	-9.69	25
10.9	-11.18	-10.8	-10.37	-9.99	25
11	-10.39	-10.01	-10.06	-9.68	25
11.03	-11.21	-10.83	-10.35	-9.97	25
11.1	-10.41	-10.03	-10.03	-9.65	25
11.1	-11.19	-10.81	-10.3	-9.92	25
11.45	-11.17	-10.79	-10.26	-9.88	25
11.85	-11.7	-11.32	-10.38	-10	25
		GRANDSTAFF (1978)			
3	-9.93	-8.18	-9.88	-8.13	25
3.2	-10.08	-8.33	-10.1	-8.35	25
3.48	-10.24	-8.49	-10.28	-8.53	25
4	-10.87	-9.12	-10.91	-9.16	25
4.5	-11.5	-9.75	-11.53	-9.78	25
5	-12.06	-10.31	-12.06	-10.31	25
3.48	-10.87	-9.14	-10.95	-9.22	1
3.48	-9.82	-8.09	-9.85	-8.12	46
		HÄNCHEN et al. (2006)			
2	NA	NA	-4.95	-4.2	120
2.01	NA	NA	-5.66	-4.91	90
2.01	NA	NA	-4.89	-4.13	120
2.02	NA	NA	-5.66	-4.91	90
2.02	NA	NA	-4.99	-4.24	120
2.02	NA	NA	-4.43	-3.67	150
2.92	NA	NA	-4.78	-4.03	150
3.02	NA	NA	-6.06	-5.31	90
3.18	NA	NA	-5.82	-5.07	90
3.25	NA	NA	-5.84	-5.09	90
3.27	NA	NA	-5.8	-5.04	90
3.29	NA	NA	-5.07	-4.32	120
3.34	NA	NA	-5.15	-4.4	120

3.34	NA	NA	-4.94	-4.19	150
3.39	NA	NA	-5.26	-4.51	120
3.39	NA	NA	-5	-4.25	150
3.66	NA	NA	-6.1	-5.35	90
3.66	NA	NA	-5.41	-4.66	120
3.79	NA	NA	-5.54	-4.79	150
3.84	NA	NA	-5.54	-4.79	120
4.17	NA	NA	-6.04	-5.28	120
4.2	NA	NA	-5.66	-4.91	120
4.53	NA	NA	-5.77	-5.02	150
4.58	NA	NA	-6.77	-6.02	90
5.03	NA	NA	-6.22	-5.47	120
5.13	NA	NA	-6.2	-5.45	150
5.14	NA	NA	-6.4	-5.65	120
5.17	NA	NA	-6.19	-5.44	150
5.25	NA	NA	-7.23	-6.47	90
5.37	NA	NA	-6.91	-6.16	120
5.48	NA	NA	-6.88	-6.13	120
5.67	NA	NA	-7.79	-7.04	90
5.69	NA	NA	-6.7	-5.95	120
6.03	NA	NA	-7.82	-7.07	120
6.03	NA	NA	-7.96	-7.21	120
6.32	NA	NA	-6.94	-6.19	150
6.45	NA	NA	-8.13	-7.38	90
6.64	NA	NA	-8.03	-7.28	90
6.9	NA	NA	-6.82	-6.07	150
7.59	NA	NA	-7.8	-7.04	120
8.69	NA	NA	-7.68	-6.93	120
10.18	NA	NA	-8.98	-8.23	90
10.37	NA	NA	-8.66	-7.91	90
10.59	NA	NA	-8.5	-7.75	120
		LUCE et al. (1972a)			
1.66	-7.06	-6.62	-7.6	-7.17	25
3.18	-7.86	-7.42	-8.25	-7.81	25
4.99	-8.25	-7.81	-9.37	-8.93	25
7.02	-7.65	-7.22	-8.82	-8.38	25
9.58	-8.04	-7.61	-10.51	-10.08	25
		OELKERS (2001)			
2	-7.63	-7.11	-7.81	-7.29	25
2	-7.86	-7.35	-7.98	-7.46	25
2	-7.88	-7.36	-7.99	-7.47	25
2	-7.84	-7.32	-7.89	-7.37	25
2	-7.85	-7.33	-7.9	-7.38	25
2	-7.88	-7.36	-7.92	-7.4	25
2	-7.84	-7.32	-7.87	-7.35	25
2	-7.85	-7.33	-7.88	-7.36	25
2	-7.78	-7.26	-7.81	-7.29	25
2	-7.73	-7.21	-7.75	-7.23	25
2	-7.9	-7.38	-7.92	-7.4	25
2	-7.9	-7.38	-7.91	-7.4	25

2	-7.89	-7.37	-7.89	-7.37	25
2	-7.91	-7.4	-7.91	-7.39	25
2	-7.9	-7.39	-7.9	-7.38	25
2	-7.93	-7.41	-7.93	-7.41	25
2	-7.87	-7.35	-7.87	-7.35	25
2	-7.86	-7.34	-7.85	-7.33	25
2	-7.92	-7.4	-7.91	-7.39	25
2	-7.93	-7.41	-7.92	-7.4	25
2	-7.95	-7.43	-7.93	-7.41	25
2	-7.91	-7.39	-7.89	-7.37	25
2	NA	NA	-7.03	-6.53	45
2	NA	NA	-6.57	-6.07	65
2	NA	NA	-6.97	-6.47	55
2	NA	NA	-7.58	-7.07	35
		POKROVSKY and SCHOTT (2000b)			
1.03	-7.22	-6.7	-7.23	-6.72	25
1.11	-7.31	-6.79	-7.33	-6.82	25
1.12	-7.29	-6.77	-7.28	-6.77	25
2.13	-7.66	-7.14	-7.7	-7.19	25
2.18	-7.69	-7.17	-7.71	-7.2	25
2.21	-7.71	-7.19	-7.72	-7.21	25
2.7	NA	NA	-7.73	-7.22	25
2.74	NA	NA	-7.83	-7.32	25
2.81	NA	NA	-7.82	-7.31	25
2.82	NA	NA	-7.89	-7.38	25
2.85	-8.3	-7.78	-8.3	-7.79	25
2.88	NA	NA	-7.9	-7.39	25
2.89	NA	NA	-7.96	-7.45	25
2.99	NA	NA	-7.93	-7.42	25
3.03	NA	NA	-7.97	-7.46	25
3.05	NA	NA	-8.18	-7.67	25
3.05	NA	NA	-8.28	-7.77	25
3.08	NA	NA	-8.14	-7.63	25
3.16	NA	NA	-8.25	-7.74	25
3.26	NA	NA	-8.34	-7.83	25
3.34	-8.55	-8.03	-8.55	-8.04	25
3.6	-8.81	-8.29	-8.8	-8.29	25
4.15	-9.06	-8.54	-9.03	-8.52	25
4.2	NA	NA	-8.69	-8.18	25
4.22	NA	NA	-8.78	-8.27	25
4.41	NA	NA	-8.8	-8.29	25
4.49	NA	NA	-8.98	-8.47	25
4.55	NA	NA	-9.03	-8.52	25
4.77	NA	NA	-8.98	-8.47	25
4.85	NA	NA	-9.02	-8.51	25
4.95	NA	NA	-9.15	-8.64	25
5.61	-9.78	-9.26	-9.79	-9.28	25
5.7	-9.45	-8.93	-9.49	-8.98	25
6.13	-9.87	-9.35	-9.92	-9.41	25
6.18	-9.61	-9.09	-9.6	-9.09	25

6.28	-9.74	-9.22	-9.72	-9.21	25
6.39	-10	-9.48	-10.04	-9.53	25
7.19	-10.11	-9.59	-10.11	-9.6	25
7.21	-10.06	-9.54	-10.04	-9.53	25
7.25	-9.91	-9.39	-9.88	-9.37	25
7.33	-9.91	-9.39	-9.93	-9.42	25
7.6	-10.46	-9.94	-10.47	-9.96	25
7.9	-10.6	-10.08	-10.57	-10.06	25
7.98	-10.45	-9.93	-10.39	-9.88	25
8.02	-10.14	-9.62	-10.13	-9.62	25
8.13	-10.28	-9.76	-10.33	-9.82	25
9.3	-10.64	-10.12	-10.49	-9.98	25
9.58	-11.04	-10.52	-10.54	-10.03	25
10.08	-10.9	-10.38	-10.79	-10.28	25
10.76	-10.63	-10.11	-10.38	-9.87	25
10.78	-10.95	-10.43	-10.95	-10.44	25
10.85	-11.03	-10.51	-10.31	-9.8	25
10.9	-10.59	-10.07	-10.44	-9.93	25
10.9	-10.69	-10.17	-10.69	-10.18	25
10.95	-11	-10.48	-10.6	-10.09	25
11.01	-10.55	-10.03	-10.57	-10.06	25
11.13	-10.76	-10.24	-10.71	-10.2	25
11.14	-11.38	-10.86	NA	NA	25
11.26	-11.51	-10.99	NA	NA	25
11.42	-11.21	-10.69	-11.18	-10.67	25
11.45	-11.02	-10.5	-11.19	-10.68	25
11.46	-11.18	-10.66	-11.25	-10.74	25
11.5	-10.29	-9.77	-11.02	-10.51	25
12.06	-10.86	-10.34	-10.85	-10.34	25
		ROSSO and RIMSTIDT (2000)			
1.73	-7.94	-7.17	-7.91	-7.15	25
1.75	-7.89	-7.13	-7.87	-7.11	25
1.76	-7.63	-6.86	-7.68	-6.91	35
1.76	-7.66	-6.90	-7.72	-6.96	35
1.77	-7.87	-7.11	-7.86	-7.10	25
1.77	-7.57	-6.81	-7.58	-6.82	35
1.77	-7.67	-6.91	-7.66	-6.90	35
1.78	-7.81	-7.05	-7.81	-7.05	25
1.78	-7.87	-7.11	-7.86	-7.10	25
1.78	-7.92	-7.16	-7.90	-7.14	25
1.78	-7.61	-6.85	-7.59	-6.83	35
1.78	-7.61	-6.84	-7.65	-6.89	35
1.78	-7.69	-6.93	-7.67	-6.91	35
1.78	-7.65	-6.89	-7.70	-6.94	35
1.79	-7.85	-7.09	-7.84	-7.07	25
1.79	-7.87	-7.11	-7.88	-7.12	25
1.79	-7.55	-6.79	-7.58	-6.82	35
1.80	-7.68	-6.92	-7.67	-6.91	35
1.80	-7.41	-6.65	-7.38	-6.62	45

1.81	-7.87	-7.11	-7.83	-7.07	25
1.81	-7.87	-7.11	-7.81	-7.05	25
1.81	-7.85	-7.09	-7.84	-7.08	25
1.81	-7.62	-6.86	-7.65	-6.89	35
1.81	-7.66	-6.90	-7.66	-6.90	35
1.81	-7.69	-6.93	-7.71	-6.94	35
1.81	-7.45	-6.69	-7.49	-6.73	45
1.81	-7.41	-6.65	-7.38	-6.62	45
1.81	-7.41	-6.65	-7.37	-6.61	45
1.82	-7.86	-7.10	-7.79	-7.03	25
1.82	-7.85	-7.09	-7.85	-7.09	25
1.82	-7.89	-7.13	-7.83	-7.07	25
1.82	-7.42	-6.65	-7.42	-6.66	45
1.82	-7.40	-6.64	-7.40	-6.64	45
1.82	-7.37	-6.61	-7.38	-6.62	45
1.82	-7.39	-6.63	-7.40	-6.64	45
1.83	-7.71	-6.95	-7.69	-6.93	35
1.83	-7.42	-6.66	-7.40	-6.64	45
1.83	-7.41	-6.65	-7.39	-6.63	45
1.83	-7.46	-6.70	-7.46	-6.70	45
1.83	-7.34	-6.58	-7.32	-6.56	45
1.83	-8.00	-7.24	-7.40	-6.64	45
1.84	-7.73	-6.97	-7.71	-6.95	35
1.84	-7.42	-6.66	-7.40	-6.64	45
1.85	-7.96	-7.20	-7.91	-7.15	25
1.85	-7.88	-7.12	-7.81	-7.05	25
1.85	-7.96	-7.20	-7.89	-7.13	25
1.86	-7.89	-7.13	-7.89	-7.13	25
1.86	-7.80	-7.04	-7.76	-7.00	25
1.86	-7.95	-7.19	-7.85	-7.09	25
1.86	-7.98	-7.22	-7.86	-7.10	25
1.86	-7.95	-7.19	-7.86	-7.10	25
1.86	-7.93	-7.17	-7.87	-7.11	25
1.86	-7.92	-7.16	-7.87	-7.11	25
1.87	-7.99	-7.23	-7.88	-7.12	25
1.88	-7.73	-6.97	-7.72	-6.96	35
1.88	-7.73	-6.96	-7.72	-6.96	35
1.88	-7.64	-6.88	NA	NA	35
1.88	-7.64	-6.88	-7.68	-6.92	35
1.88	-7.53	-6.77	-7.48	-6.72	45
1.89	-7.63	-6.87	-7.64	-6.88	35
1.89	-7.69	-6.93	-7.71	-6.95	35
1.89	-7.65	-6.88	-7.72	-6.96	35
1.89	-7.73	-6.97	-7.69	-6.93	35
1.89	-7.52	-6.76	-7.52	-6.76	45
1.90	-7.69	-6.93	-7.75	-6.99	35
1.90	-7.69	-6.93	-7.76	-7.00	35
1.90	-7.58	-6.82	-7.57	-6.80	35

1.90	-7.67	-6.91	-7.30	-6.54	35
1.90	-7.65	-6.89	-7.66	-6.90	35
1.90	-7.69	-6.93	-7.69	-6.93	35
1.90	-7.43	-6.67	-7.42	-6.65	45
1.91	-7.61	-6.85	-7.59	-6.83	35
1.91	-7.61	-6.85	-7.63	-6.86	35
1.91	-7.57	-6.81	-7.64	-6.88	35
1.91	-7.58	-6.82	-7.59	-6.83	35
1.91	-7.74	-6.98	-7.65	-6.89	35
1.91	-7.73	-6.97	-7.67	-6.91	35
1.91	-7.67	-6.91	-7.62	-6.86	35
1.91	-7.50	-6.74	-7.47	-6.71	45
1.91	-7.42	-6.66	-7.43	-6.67	45
1.91	-7.41	-6.65	-7.41	-6.65	45
1.92	-7.65	-6.89	-7.68	-6.92	35
1.92	-7.72	-6.96	-7.70	-6.94	35
1.92	-7.52	-6.76	-7.48	-6.72	45
1.92	-7.54	-6.78	-7.49	-6.73	45
1.92	-7.39	-6.63	-7.38	-6.62	45
1.92	-7.37	-6.61	-7.36	-6.60	45
1.92	-7.43	-6.67	-7.42	-6.66	45
1.93	-7.66	-6.90	-7.69	-6.93	35
1.93	-7.71	-6.95	-7.74	-6.98	35
1.93	-7.71	-6.95	-7.73	-6.97	35
1.93	-7.45	-6.69	-7.42	-6.66	45
1.93	-7.45	-6.69	-7.42	-6.66	45
1.93	-7.50	-6.74	-7.46	-6.70	45
1.93	-7.32	-6.56	-7.34	-6.58	45
1.93	-7.33	-6.57	-7.24	-6.48	45
1.93	-7.31	-6.55	-7.30	-6.54	45
1.93	-7.35	-6.59	-7.35	-6.59	45
1.93	-7.39	-6.63	-7.38	-6.62	45
1.94	-7.59	-6.83	NA	NA	35
1.94	-7.51	-6.75	-7.47	-6.71	45
1.95	-7.44	-6.68	-7.44	-6.68	45
1.95	-7.45	-6.69	-7.44	-6.68	45
1.95	-7.52	-6.76	-7.45	-6.69	45
2.02	-7.44	-6.68	-7.42	-6.66	45
2.69	-8.30	-7.54	-8.24	-7.48	25
2.72	-8.13	-7.37	-8.14	-7.38	35
2.74	-8.31	-7.54	-8.22	-7.46	25
2.77	-8.25	-7.49	-8.21	-7.45	25
2.77	-8.23	-7.47	-8.27	-7.51	25
2.77	-8.30	-7.54	-8.25	-7.49	25
2.77	-8.28	-7.52	-8.28	-7.52	25
2.77	-8.30	-7.53	-8.27	-7.51	25
2.77	-8.29	-7.53	-8.27	-7.51	25
2.77	-8.29	-7.53	-8.25	-7.49	25

2.77	-8.31	-7.55	-8.27	-7.51	25
2.77	-8.30	-7.54	-8.21	-7.45	25
2.77	-8.33	-7.57	-8.36	-7.60	25
2.77	-8.03	-7.27	-8.02	-7.25	35
2.77	-8.12	-7.36	-8.15	-7.39	35
2.78	-8.30	-7.54	-8.26	-7.50	25
2.78	-8.29	-7.53	-8.27	-7.51	25
2.78	-8.28	-7.52	-8.25	-7.49	25
2.78	-8.28	-7.52	-8.24	-7.48	25
2.78	-8.32	-7.56	-8.29	-7.53	25
2.78	-8.05	-7.29	-8.02	-7.25	35
2.78	-8.02	-7.26	-8.01	-7.25	35
2.78	-8.09	-7.33	-8.10	-7.34	35
2.79	-8.28	-7.52	-8.26	-7.50	25
2.79	-8.12	-7.36	-8.10	-7.34	35
2.79	-8.10	-7.34	-8.09	-7.33	35
2.79	-8.15	-7.39	-8.16	-7.40	35
2.79	-8.16	-7.40	-8.21	-7.44	35
2.80	-8.07	-7.31	-8.02	-7.26	35
2.81	-8.09	-7.33	-8.06	-7.30	35
2.81	-8.12	-7.36	-8.13	-7.37	35
2.82	-8.12	-7.36	-8.16	-7.40	35
2.82	-8.09	-7.33	-8.04	-7.28	35
2.82	-8.11	-7.35	-8.12	-7.36	35
2.83	-8.14	-7.38	-8.15	-7.39	35
2.83	-8.14	-7.38	-8.13	-7.37	35
2.83	-8.09	-7.33	-8.11	-7.35	35
2.83	-8.11	-7.35	-8.10	-7.34	35
2.84	-8.18	-7.42	-8.25	-7.49	35
2.84	-8.06	-7.30	-8.13	-7.37	35
2.84	-8.09	-7.33	-8.14	-7.38	35
2.84	-8.10	-7.34	-8.09	-7.33	35
2.84	-8.05	-7.29	-8.04	-7.28	35
2.84	-8.04	-7.28	-8.06	-7.30	35
2.85	-8.34	-7.58	-8.21	-7.45	25
2.85	-8.33	-7.57	-8.24	-7.48	25
2.88	-7.87	-7.11	-7.83	-7.07	45
2.88	-7.94	-7.18	-7.89	-7.13	45
2.88	-7.82	-7.06	-7.82	-7.05	45
2.88	-7.84	-7.08	-7.85	-7.09	45
2.89	-7.94	-7.18	-7.87	-7.11	45
2.89	-7.94	-7.18	-7.84	-7.08	45
2.89	-7.85	-7.09	-7.84	-7.08	45
2.89	-7.86	-7.10	-7.88	-7.12	45
2.89	-7.84	-7.08	-7.78	-7.02	45
2.90	-7.84	-7.08	-7.81	-7.05	45
2.91	-7.87	-7.11	-7.84	-7.08	45
2.91	-7.88	-7.12	-7.86	-7.10	45

2.91	-7.79	-7.03	-7.78	-7.02	45
2.91	-7.90	-7.14	-7.77	-7.01	45
2.91	-7.88	-7.12	-7.77	-7.01	45
2.92	-7.85	-7.09	-7.82	-7.06	45
2.92	-7.81	-7.05	-7.76	-7.00	45
2.92	-7.83	-7.07	-7.80	-7.04	45
2.92	-7.84	-7.08	-7.78	-7.02	45
2.92	-7.82	-7.06	-7.74	-6.98	45
2.92	-7.85	-7.09	-7.79	-7.03	45
2.93	-7.82	-7.05	-7.79	-7.02	45
2.93	-7.89	-7.13	-7.84	-7.08	45
2.93	-7.78	-7.02	-7.74	-6.98	45
2.93	-7.78	-7.02	-7.74	-6.98	45
2.93	-7.85	-7.09	-7.81	-7.05	45
2.93	-7.83	-7.07	-7.80	-7.03	45
2.93	-7.90	-7.14	-7.87	-7.11	45
2.93	-7.82	-7.06	-7.76	-7.00	45
2.95	-7.97	-7.20	-7.95	-7.19	45
2.95	-7.93	-7.17	-7.89	-7.13	45
2.96	-8.37	-7.61	-8.29	-7.53	25
2.96	-8.37	-7.61	-8.31	-7.55	25
2.96	-7.92	-7.16	-7.89	-7.13	45
2.96	-7.91	-7.15	-7.84	-7.07	45
3.72	-8.95	-8.19	-8.82	-8.06	25
3.72	-8.81	-8.05	-8.68	-7.92	25
3.73	-8.80	-8.04	-8.65	-7.88	25
3.73	-8.88	-8.12	NA	NA	25
3.73	-8.85	-8.09	NA	NA	25
3.73	-8.87	-8.11	NA	NA	25
3.73	-8.87	-8.11	NA	NA	25
3.73	-8.90	-8.14	NA	NA	25
3.73	-8.91	-8.15	NA	NA	25
3.74	-8.90	-8.14	NA	NA	25
3.74	-8.92	-8.16	NA	NA	25
3.77	-8.96	-8.20	-8.83	-8.07	25
3.80	-8.64	-7.88	-8.58	-7.82	35
3.82	-8.63	-7.87	-8.61	-7.85	35
3.83	-8.70	-7.94	-8.67	-7.91	35
3.84	-8.59	-7.83	-8.51	-7.75	35
3.85	-8.71	-7.95	-8.67	-7.90	35
3.85	-8.68	-7.92	NA	NA	35
3.86	-8.72	-7.96	NA	NA	35
3.86	-8.69	-7.93	NA	NA	35
3.86	-8.69	-7.93	NA	NA	35
3.86	-8.66	-7.90	NA	NA	35
3.87	-8.74	-7.98	-8.74	-7.98	35
3.87	-8.72	-7.96	NA	NA	35
3.87	-8.68	-7.92	NA	NA	35

3.87	-8.41	-7.65	-8.48	-7.72	45
3.88	-8.59	-7.83	-8.56	-7.80	35
3.88	-8.67	-7.91	NA	NA	35
3.88	-8.39	-7.63	-8.44	-7.68	45
3.88	-8.67	-7.90	-8.56	-7.80	45
3.88	-8.60	-7.84	-8.44	-7.68	45
3.89	-8.61	-7.85	-8.56	-7.80	45
3.89	-8.58	-7.82	-8.52	-7.75	45
3.89	-8.40	-7.64	-8.49	-7.73	45
3.89	-8.56	-7.79	-8.42	-7.66	45
3.90	-8.62	-7.86	-8.63	-7.87	35
3.90	-8.62	-7.86	-8.57	-7.80	35
3.90	-8.63	-7.86	-8.60	-7.84	35
3.90	-8.62	-7.86	-8.61	-7.85	35
3.90	-8.60	-7.84	-8.53	-7.77	35
3.90	-8.59	-7.83	-8.42	-7.66	45
3.90	-8.59	-7.83	-8.47	-7.71	45
3.91	-8.68	-7.91	-8.65	-7.89	35
3.91	-8.58	-7.82	-8.57	-7.81	35
3.92	-8.54	-7.78	-8.47	-7.71	45
3.93	-8.54	-7.78	-8.52	-7.76	45
3.94	-8.65	-7.88	-8.54	-7.78	45
3.94	-8.64	-7.88	-8.46	-7.70	45
3.96	-8.52	-7.76	-8.47	-7.71	45
3.96	-8.52	-7.76	-8.45	-7.69	45
3.96	-8.54	-7.78	-8.47	-7.71	45
3.96	-8.58	-7.81	-8.58	-7.82	45
3.96	-8.57	-7.81	-8.53	-7.77	45
3.97	-8.63	-7.87	-8.59	-7.83	35
3.97	-8.60	-7.84	-8.58	-7.82	45
3.97	-8.58	-7.82	-8.45	-7.69	45
3.97	-8.59	-7.83	-8.61	-7.85	45
3.97	-8.59	-7.83	-8.56	-7.80	45
3.98	-8.63	-7.87	-8.59	-7.83	35
3.98	-8.63	-7.87	-8.63	-7.87	35
3.98	-8.65	-7.88	-8.64	-7.88	35
3.98	-8.58	-7.82	-8.49	-7.72	45
3.98	-8.59	-7.83	-8.43	-7.67	45
4.01	-8.67	-7.91	-8.64	-7.88	35
4.04	-8.66	-7.89	-8.61	-7.85	35
4.10	-8.66	-7.90	-8.67	-7.90	35
4.12	-8.68	-7.91	-8.67	-7.91	35
		SIEGEL and PFANNKUCH (1984)			
4.1	-10.65	-9.2	-11.49	-10.04	25
		VAN HERK et al. (1989)			
1	NA	NA	NA	-5.26	40
1	NA	NA	NA	-5.5	40

1	NA	NA	NA	-4.89	50
1	NA	NA	NA	-5.2	50
1	NA	NA	NA	-4.62	60
1	NA	NA	NA	-4.93	60
1	NA	NA	NA	-4.3	70
1	NA	NA	NA	-4.76	70
2	NA	NA	NA	-4.66	70
2	NA	NA	NA	-5.13	70
3	NA	NA	NA	-5.13	70
3	NA	NA	NA	-5.3	70
		WOGELIUS and WALTHER (1991b)			
2	-7.99	NA	-8.15	NA	25
3	-8.79	NA	-8.83	NA	25
4.1	-9.07	NA	-9.1	NA	25
5.7	-9.78	NA	NA	NA	25
5.7	-10.34	NA	-10.21	NA	25
7.4	-9.8	NA	-9.77	NA	25
9.1	-10.54	NA	-10.03	NA	25
9.9	-10.46	NA	NA	NA	25
9.9	-10.58	NA	-10.47	NA	25
9.9	-10.38	NA	-10.1	NA	25
10.4	-10.74	NA	-10.14	NA	25
10.8	-11.27	NA	-10.52	NA	25
12	-10.36	NA	NA	NA	25
		WOGELIUS and WALTHER (1992)			
1.8	-6.61	NA	-6.29	NA	65
6	-8.36	NA	-8.13	NA	65
9.8	-7.64	NA	NA	NA	65